UCLA
UCLA Electronic Theses and Dissertations

Title
Characteristics of Electronic Cigarette Aerosol and Its Impact on Indoor Air Quality

Permalink
https://escholarship.org/uc/item/4mz826qt

Author
Li, Liqiao

Publication Date
2021

Peer reviewed|Thesis/dissertation

eScholarship.org Powered by the California Digital Library
University of California

UNIVERSITY OF CALIFORNIA

LOS ANGELES

Characteristics of Electronic Cigarette Aerosol and Its Impact on Indoor Air Quality

A dissertation submitted in partial satisfaction of

the requirements for the degree

Doctor of Environmental Health Sciences

by

Liqiao Li

2021

© Copyright by

Liqiao Li

2021

ABSTRACT OF THE DISSERTATION

Characteristics of Electronic Cigarette Aerosol

and Its Impact on Indoor Air Quality

by

Liqiao Li

Doctor of Environmental Health Sciences

University of California, Los Angeles, 2021

Professor Yifang Zhu, Chair

In recent years, electronic cigarettes (e-cigs) have gained increasing popularity among adolescents and young adults while emerging data raise concerns about their health effects. Essentially different from conventional tobacco cigarettes (t-cigs), e-cigs produce an aerosol via vaporization of the e-liquid, which is typically made of propylene glycol (PG), vegetable glycerin (VG), nicotine, water, and flavoring compounds. E-cig aerosols mainly consisting of liquid droplets were found highly dynamic and volatile. However, knowledge on the transport and transformation of e-cig aerosols and the related exposure is still limited. This dissertation investigated the characteristics of e-cig aerosols and evaluated the impacts of e-cig use on indoor

air quality focusing on the effects of e-liquid and environmental factors. This work is subdivided into the following seven chapters: an overview (Chapter 1), a literature review (Chapter 2), three chapters of original research (Chapters 3-5), the conclusions of the work (Chapter 6).

We first conducted a literature review to summarize the effects of e-cigs on indoor particulate matter (PM) pollution, chemical compositions of e-cig aerosols, and associated respiratory and cardiovascular effects. Many studies have reported high levels of ultrafine particles (UFPs, particles with an aerodynamic diameter $\leq$ 100 nm) and $PM_{2.5}$ (particles with an aerodynamic diameter $\leq$ 2.5 μm) due to e-cig use (i.e., vaping) indoors, which were comparable to t-cig smoke. Although the concentrations of toxic chemical compounds in e-cig aerosols are generally lower than those in t-cig smoke, a substantial amount of vaporized PG, VG, nicotine, and hazardous substances, such as aldehydes and heavy metals, has been reported. Evidence confirms that e-cig use impairs indoor air quality and poses bystanders for risk of secondhand exposure.

To explore the effects of e-liquid compositions on the e-cig aerosols, we investigated how PG/VG ratio and nicotine content affect e-cig aerosol emissions and dynamics. We found that adding nicotine to the e-liquid altered the particle emission factors. For nicotine-free e-liquids, increasing the PG/VG ratio resulted in increased particle loss rates measured by particle number concentration (PNC) and $PM_{2.5}$. This pattern was not observed with nicotine in the e-liquids. The particle loss rates, however, were significantly different with and without nicotine.

In real-world settings, we assessed the impacts of e-cig use on indoor air quality in vape shops and their neighboring indoor spaces in multiunit buildings. The mean (SD) PNC and $PM_{2.5}$ concentration in the studied vape shops were 2.8×10^4 (2.3×10^4) particles/cm^3 and 276 (546) $\mu g/m^3$. Out of the six studied pairs, PNCs in five vape shops and $PM_{2.5}$ in two vape shops were significantly correlated with those in their neighboring businesses. Nicotine was detected in the

air of all the studied vape shops [mean (SD) 2.59 (1.02) μg/m^3] and neighboring businesses [mean (SD) 0.17 (0.13) μg/m^3]. We also identified major factors such as dilution, ventilation, and vaping density (puffs/h/100m^3) that influenced the behaviors of exhaled e-cig aerosols, and evaluated the transport of exhaled e-cig particles from the vape shop to its outdoor environment.

Compared to mainstream e-cig aerosols measured in laboratory chamber studies, larger particle sizes (mode ~ 250 nm) were observed at the end of vaping in vape shops. We developed a ventilated artificial lung system to better understand how the human lung environment alters the inhaled e-cig aerosols. We used this system to assess the effects of breathing, temperature, and relative humidity (RH) on characteristics of inhaled e-cig aerosols in the last Chapter. Increasing the respiratory rate (from 10 to 15 BPM) and breath volume (from 480 to 720 ml) resulted in enhanced particle decay rates from 32 to 80 h^{-1} in the ambient room environment. The decay rates under all breathing patterns increased by ~ 11 – 20% when changing the temperature and RH from ambient room to simulated lung conditions. The warm and humid lung environment resulted in hygroscopic growth of inhaled particles that significantly enhanced the presence of supermicron (> 1 μm) e-cig particles.

Overall, the use of e-cigs that leads to high levels of $PM_{2.5,}$ UFPs, and gas-phase nicotine degrade the indoor air quality, raising concerns regarding secondhand exposure to e-cig aerosols. E-cig aerosols that are highly dynamic in the environment, especially small particles, can travel farther away and penetrate into neighboring indoor spaces. The characteristics of e-cig aerosols and related exposures can be affected by a wide range of factors including, but not limited to, e-liquid compositions, air exchange rate, ventilation, dilution, vaping density (puffs/h/100m^3), distance, inhalation and exhalation process in the human lung, and environmental conditions with varying temperature and humidity. These data can guide exposure assessment and mitigation strategies.

The dissertation of Liqiao Li is approved.

Shane Que Hee

Irwin H. (Mel) Suffet

Aydogan Ozcan

Yifang Zhu, Committee Chair

University of California, Los Angeles

2021

TABLE OF CONTENTS

LIST OF FIGURES ..... **X**

LIST OF TABLES ..... **XV**

ACKNOWLEDGEMENTS ..... **XVI**

VITA ..... **XVII**

1. OVERVIEW **1**

2. EFFECTS OF ELECTRONIC CIGARETTES ON INDOOR AIR QUALITY AND HEALTH **5**

2.1. Abstract **5**

2.2. Introduction **5**

2.3. The literature search **7**

2.4. Impacts of e-cig on indoor air quality **8**

2.4.1. Indoor Particle Concentrations 8

2.4.2. Factors Affecting Indoor Particle Concentrations 10

2.5. Chemical compositions of e-cig aerosols **13**

2.6. Health effects of e-cig aerosols **16**

2.6.1. Respiratory Effects 17

2.6.2. Cardiovascular Effects 19

2.7. Conclusions and future perspectives 24

3. EFFECTS OF PROPYLENE GLYCOL, VEGETABLE GLYCERIN, AND NICOTINE ON EMISSIONS AND DYNAMICS OF ELECTRONIC CIGARETTE AEROSOLS 26

3.1. Abstract 26

3.2. Introduction 27

3.3. Materials and methods 29

3.4. Results and discussion 36

3.4.1. Particle emission 36

3.4.2. Decay of PNC and $PM_{2.5}$ 37

3.4.3. Particle loss rate 39

3.4.4. Particle size distribution 44

3.5. Conclusions 45

4. IMPACTS OF ELECTRONIC CIGARETTES USAGE ON AIR QUALITY OF VAPE SHOPS AND THEIR NEARBY AREAS 47

4.1. Abstract 47

4.2. Introduction 48

4.3. Materials and methods 51

4.3.1. Study sites 51

4.3.2. Sampling protocol 53

4.3.3. Measurement of particle number, $PM_{2.5}$, and particle size distribution 54

4.3.4. Measurement of airborne nicotine concentrations 55

4.3.5. Quality control/quality assurance for data collection and analysis 56

4.3.6. Data analysis 56

4.4. Results and discussion 57

4.4.1. E-cig related air pollutants in the vape shops and neighboring businesses 57

4.4.2. Predictors of air pollutants concentrations inside vape shops 61

4.4.3. Impacts of EEV emissions from vape shops on nearby areas 63

4.4.4. Effects of vape shop door open and close on particle transport 67

4.5. Conclusions 75

5. DEVELOPMENT OF A VENTILATED ARTIFICIAL LUNG SYSTEM FOR CHARACTERIZING THE PHYSICOCHEMICAL PROPERTIES OF INHALED E-CIGARETTE AEROSOLS 77

5.1. Abstract 77

5.2. Introduction 78

5.3. Materials and methods 80

5.3.1. Development of the ventilated artificial lung system 80

5.3.2. Aerosol characterization and data analysis 82

5.4. Results and discussion 86

5.4.1. Effects of ventilation and lung chamber conditions on the e-cig particle concentration and decay 86

5.4.2. Particle size distribution..... 89

5.5. Conclusions..... 93

6. CONCLUSIONS..... 95

APPENDIX..... 98

Supplementary materials for Chapter 2..... 98

Supplementary materials for Chapter 3..... 102

Supplementary materials for Chapter 4..... 107

7. REFERENCES..... 113

LIST OF FIGURES

Figure 1.1. Different generations of electronic cigarettes. 1

Figure 2.1. Schematic process from electronic cigarette emissions, to secondhand exposures, and to potential health effects. 7

Figure 2.2. Average concentrations of (a) $PM_{2.5}$ mass concentration and (b) particle number concentration (PNC) from 11 studies on e-cigs and 16 studies on t-cigs in various indoor environments (i.e., laboratory settings and real-world public indoor spaces) by region. Abbreviation: ND = not detectable. 10

Figure 2.3. Chemical compositions of e-cig aerosols including (a) mainstream aerosols (μg/puff) from 37 studies and (b) secondhand aerosols ($\mu g/m^3$) from 11 studies. Concentrations of t-cig-emitted chemicals are presented in ranges (red line) as a reference group. All the data included are background-subtracted values, when applicable. "> LOQ%" indicates the percentage of available data points above the limit of quantification (LOQ). Abbreviations: VOCs=volatile organic compounds; TSNAs=tobacco-specific nitrosamines; NNK=4-(methylnitrosamino)-1-(3-pyridyl)-1-butanone; NNN=N'-Nitrosonornicotine. 16

Figure 3.1. A schematic diagram of the aerosol generation and sampling system. 30

Figure 3.2. Overall particle size distributions (dN/dLogDp) of DEHS and e-cig aerosols at the start of the decay cycle (t = 0). The plotted data are the means of all measurements conducted with each type of e-liquid mixture evaluated in this study. The plotted data also compare the initial particle size distribution of e-cig aerosols with and without nicotine. 32

Figure 3.3. Decay curves for PNC and $PM_{2.5}$ shown in (a) $C_t/C_{t=0}$, and (b) ln ($C_t/C_{t=0}$). The plotted data were collected with the e-liquid mixture having a PG/VG ratio of 30/70 without nicotine. 35

Figure 3.4. Averaged normalized concentration ($C_t/C_{t=0}$) decay curves for PNC (a and b) and $PM_{2.5}$ (c and d). The plotted data provide the means of six repeated measurements without nicotine (0.0%; a and c) and with nicotine (2.4%; b and d) in comparison to DEHS aerosols. ... 39

Figure 3.5. Particle loss rates as measured by (a) PNC and (b) $PM_{2.5}$ at different PG/VG ratios with 0.0% and 2.4% nicotine compared with DEHS. Statistically significant differences are noted with * ($p < 0.001$, Student's t-test). 43

Figure 3.6. Averaged particle size distributions (dN/dLogDp) for e-liquid mixtures (i.e., PG/VG =0/100, 50/50, and 100/0) without nicotine (0.0%; a, b, and c) and with nicotine (2.4%; d, e, and f). The vertical axes represent particle size on a logarithmic scale, the horizontal axes represent elapsed time in hours from the start of sampling, and the color scale represents particle number concentration at a certain time and diameter. Linear interpolation is used to fill the data gap between the SMPS and APS output (289 nm- 540 nm)..... 45

Figure 4.1. The schematic diagram of sampling types and sampling locations in a representative pair of vape shop and its neighboring business. 54

Figure 4.2. Box plots summarizing (a) PNC and (b) $PM_{2.5}$ mass concentrations measured during all sampling sessions for the six pairs of vape shops and neighboring businesses A-F by vaping density. The solid line in each box represents the median value, and the dash line in each box represents the mean value. 59

Figure 4.3. Relationships between hourly averaged PNC and $PM_{2.5}$ and vaping density (puffs/h/100 m^3) when the shop door was closed for vape shops A-F and I with particle samplings. 61

Figure 4.4. Relationships between the 24-h time-weighted average (TWA) nicotine concentration and air exchange rate (AER) in all the studied vape shops.... 62

Figure 4.5. Temporal profile of PNC and $PM_{2.5}$ in vape shop C and neighboring business C (a and b) as well as the particle size distributions in vape shop C for both low emission and high emission periods (c and d). 65

Figure 4.6. Temporal profile of (a) PNC in vape shop B and its neighboring business B as well as particle size distributions in (b) vape shop B and (c) neighboring business B during overlapping business hours on a day with ventilation changes. Note: The door of vape shop was closed during 13:30-14:30 and the door was open during 14:30-18:00. 69

Figure 4.7. Effects of door open and close on the particle transport from vape shop B to the outdoor environment (i.e., sampling location 3: ~1-3 m away from the front door of vape shop B)..... 71

Figure 4.8. Effects of door opening and closing on the particle transport from vape shop A to the outdoor environment (i.e., sampling location 3: ~1-3 m away from the front door of vape shop A). 72

Figure 4.9. I/O ratios for (a) PNC and (b) $PM_{2.5}$ in vape shops A and B with the effects of door opening and closing. The Mann-Whitney U test was used to compare the I/O ratios during door closed vs. door open..... 73

Figure 4.10. (a) PNC and (b) $PM_{2.5}$ at indoor sampling locations 1 (inside vape shop) as well as outdoor sampling locations 3 (outside ~1-3 m away from the vape shop door) and 4 (outside ~ 6-8 m away from the vape shop door) for vape shop I. The solid line in each box represents the median value, and the dash line in each box represents the mean value. 75

Figure 5.1. (a) Schematic diagrams of the ventilated artificial lung system with aerosol generation and lung chamber particle sampling methods; (b) The time series of PNC during a 4-puff vaping cycle and decay period as well as pressure changes due to continuous breathing at 10

BPM and 480 ml/breath; (c) Images recorded immediately after the 4th puff (t = 0 min) for the lung model with the effects of ventilation and environmental conditions. 86

Figure 5.2. The temporal profiles of the dilution-corrected PNC during the 4-puff vaping cycle and decay period under different experimental conditions: (a) ventilator on and off (ambient room environment), (b) varying breathing patterns (ambient room environment), and (c) ambient room vs. lung environmental conditions [10 breaths per min (BPM), 480 ml/breath]. The calculated particle decay rates under all experimental conditions are presented in panel (d). Error bars show the standard deviation of the mean. Please note different scale on Y-axis. 89

Figure 5.3. Average particle number distributions (dN/dLogDp) at t = 0, 5, and 10 min during the decay under the three environmental conditions (i.e., dry, room, and lung environments) with ventilator on (a – c) and off (d – f). The vertical axes represent particle size on a logarithmic scale, the horizontal axes represent elapsed time in minutes during the decay, and the color scale represents particle number concentration at a certain time and diameter. 90

Figure 5.4. Average particle mass distributions (dM/dLogDp) at t = 0, 5, and 10 min during the decay under the three environmental conditions (i.e., dry, room, and lung environments) with ventilator on (a – c) and off (d – f). The vertical axes represent particle size on a logarithmic scale, the horizontal axes represent elapsed time in minutes during the decay, and the color scale represents PM mass concentration at a certain time and diameter. 93

Figure A-1. Correlations between 10-min averaged PNCs in vape shops and neighboring businesses A-F. Linear regression equations and lines are provided. 109

Figure A-2. Correlations between 10-min averaged $PM_{2.5}$ in vape shops and neighboring businesses A-F. Linear regression equations and lines are provided. 110

Figure A-3. Correlations between 10-min averaged PNC inside and outside vape shops A-F. Linear regression equations and lines are provided. 111

Figure A-4. Correlations between 10-min averaged $PM_{2.5}$ inside and outside vape shops A-F. Linear regression equations and lines are provided. 112

LIST OF TABLES

Table 2.1. Summary of studies on the health effects in humans of active electronic cigarette use and passive exposure to secondhand electronic cigarette aerosols. Studies with the same design are shown in chronological order based on publication date. 20

Table 3.1. The mean (standard deviation) of emission factor (S_p), initial concentrations ($C_{t=0}$), and the time (t_{50}) taken to achieve 50% of $C_{t=0}$ for each e-liquid mixture and DEHS aerosols evaluated in the study 37

Table 4.1. Characteristics and nicotine concentrations of the nine studied vape shops and their neighboring businesses. 52

Table 4.2. Linear regression analysis relating the 10-min averaged PNC and $PM_{2.5}$ in neighboring businesses and outdoors (sampling location 3) to those in vape shops for pairs A-F. 66

Table 5.1. Summary of experimental conditions. 86

Table A-1. Summary of $PM_{2.5}$ and PNC levels, background concentration, emission protocol, room size, and air exchange rate for studies in Figure 2.2. 98

Table A-2. Summary of studies on particle size distribution of e-cigarette (e-cig) aerosols. 102

Table A-3. Properties of chemical compounds used in this study at 20 ºC and 1 atm. 104

Table A-4. A summary of log-linear regression analyses on log-normalized PNC and $PM_{2.5}$. . 105

Table A-5. Ventilation and sampling details of the nine studied vape shops and their neighboring businesses. 107

Table A-6. The mean (SD) PNC and $PM_{2.5}$ concentrations in the vape shops, neighboring businesses, and outdoor area (sampling location 3) for the six pairs A-F. 108

Table A-7. The median (IQR) PNC and $PM_{2.5}$ concentrations in the vape shops, neighboring businesses, and outdoor area (sampling location 3) for the six pairs A-F. 108

ACKNOWLEDGEMENTS

It is a genuine pleasure to express my sincere appreciation and gratitude to my advisor, Dr. Yifang Zhu, for all her support, guidance, and encouragement throughout my Ph.D. studies. She has provided invaluable advice to sharpen my thinking and brought my research work to a higher level. She is not only an academic mentor but also a role model in both my career and personal life.

I would like to thank my doctoral committee members, Dr. Shane Que Hee, Dr. Mel Suffet, and Dr. Aydogan Ozcan, for providing their technical support and insightful feedback during my Ph.D. program. I am also grateful to all my collaborators for their constructive and stimulating ideas. Special thanks to Dr. Michael D. Roth for his help and guidance throughout our collaboration work.

I thank Dr. Yan Lin, Charlene Nguyen, Dr. Eon S. Lee, and Dr. Haoxuan Chen, and all my fellow colleagues at UCLA for their contribution and help in all the time of this dissertation work. Working with them has been very enjoyable and I have learned a lot from them.

In addition, I want to express my deepest gratitude and love to my parents for their dedication and the many years of support that have enabled me to learn and grow throughout the years. I would also like to thank my boyfriend, Binwang Luo, for his love, encouragement, and support during the past few years. Thanks for emotionally and intellectually helping me in both work and life.

This work is supported by the Tobacco-Related Disease Research Program (TRDRP) (Contract #T30DT1007, 26IR-0002, 23XT-0001, and T29IR0480), National Heart, Lung and Blood Institute (NHLBI, R01HL139379-01A1), and UCLA Center for Occupational and Environmental Health.

VITA

Education

2017 – present	Ph.D. candidate in Environmental Health Sciences, UCLA
2015 – 2017	M.S. in Environmental Health Sciences, UCLA
2011 – 2015	B.S. in Environmental Engineering, Beijing Jiaotong University

Selected Publications

1. **Liqiao Li** and Yifang Zhu. (accepted) "Vaping and Secondhand Exposure" in Handbook of Indoor Air Quality, Edited by Yinping Zhang, Philip K. Hopke, and Corinne Mandin. 2021, Springer Nature.
2. **Liqiao Li**, Charlene Nguyen, Yan Lin, Yuening Guo, Nour Abou Fadel, Yifang Zhu. "Impacts of electronic cigarettes usage on air quality of vape shops and their nearby areas" 2021, ***Science of the Total Environment***.
3. **Liqiao Li**, Muchuan Niu, Yifang Zhu. "Assessing the effectiveness of using various face coverings to mitigate the transport of airborne particles produced by coughing indoors" 2020, ***Aerosol Science & Technology***.
4. **Liqiao Li**, Eon S. Lee, Charlene Nguyen, Yifang Zhu. "Effects of propylene glycol, vegetable glycerin, and nicotine on emissions and dynamics of electronic cigarette aerosols" 2020, ***Aerosol Science & Technology***.
5. **Liqiao Li**, Yan Lin, Tian Xia, and Yifang Zhu. "Effects of Electronic Cigarettes on Indoor Air Quality and Health." 2020, ***Annual Reviews of Public Health***, Vol 41.
6. Yi Luo*, Yichen Wu*, **Liqiao Li***, Yuening Guo, Ege Cetintas, Yifang Zhu, and Aydogan Ozcan. "Dynamic imaging and characterization of volatile aerosols in e-cigarette emissions using deep learning-based holographic microscopy" 2021, ***ACS Sensors*** (*indicates equal contribution).
7. Tiancong Ma, Xiang Wang, **Liqiao Li**, Bingbing Sun, Yifang Zhu, Tian Xia. "Electronic cigarette aerosols induce oxidative stress dependent cell death and NF-κB mediated acute lung inflammation in mice." 2020, ***Archives of Toxicology***.
8. Charlene Nguyen, **Liqiao Li**, Chanbopha Amy Sen, Emilio Ronquillo, and Yifang Zhu. "Fine and ultrafine particles concentrations in vape shops." 2019, ***Atmospheric Environment***, Vol 211

Selected Presentations

1. **Liqiao Li**, Haoxuan Chen, Airi Harui, Michael D. Roth, and Yifang Zhu. "Development of a ventilated artificial lung model for characterizing the physicochemical properties of inhaled e-cigarette aerosols." 39th American Association for Aerosol Research (AAAR) Annual Conference, Expected October 2021 (oral)
2. **Liqiao Li**. "Assessing the effectiveness of using various face coverings to mitigate transport of airborne particles produced by coughing indoors." AAAR Lecture Series, March 2021 (oral)

3. **Liqiao Li**, Charlene Nguyen, Yan Lin, Yuening Guo, and Yifang Zhu. "Impacts of electronic cigarettes usage on indoor air quality of vape shop and nearby business." Indoor Air 2020 (Virtual), COEX, Seoul, Korea, November 2020 (oral)
4. **Liqiao Li**, Muchuan Niu, and Yifang Zhu. "Assessing the effectiveness of using face coverings to mitigate the transport of particles generated from coughing." 38th AAAR Annual Conference, October 2020 (oral)
5. **Liqiao Li**, Charlene Nguyen, Yan Lin, and Yifang Zhu. "Impacts of e-cigarettes usage on the air quality of vape shop and its nearby areas." 10th International Aerosol Conference, St. Louis, Missouri, USA, September 2018 (oral and poster)

Fellowships & Awards

1. Award supported by Sheldon K. Friedlander Memorial Fund for Promoting Aerosols as an Enabling Discipline, AAAR Lecture Series (March 2021)
2. Predoctoral Fellowship Award, Tobacco-Related Disease Research Program (September 2019 – September 2021)
3. Environmental Health Sciences Opportunity Award, UCLA (2018-2019)
4. Graduate Student Fellowship, Department of Environmental Health Sciences, UCLA (July 2017 – June 2021)
5. Tony Norton Memorial Fellowship, UCLA (May 2017)

1. OVERVIEW

Electronic cigarettes (e-cigs), also known as vaping devices, are battery-powered nicotine delivery systems widely used as alternatives to conventional tobacco cigarettes (t-cigs). Different from t-cigs which generate smoke by combustion of tobacco leaves, e-cigs generate aerosols by vaporizing e-liquids, which typically contain propylene glycol (PG), vegetable glycerin (VG), nicotine, and flavoring additives. Since e-cig was first invented in 2003, the devices have evolved quickly over time from the first-generation cigalike/disposable type, to the more advanced and customizable tank mod, to the recent pod-system such as JUUL (**Figure 1.1**) (Li and Zhu 2021). In the meantime, thousands of flavors such as tobacco, menthol, fruit, candy, and sweets added in e-liquids have been widely adopted by e-cig users (Ali et al. 2020).

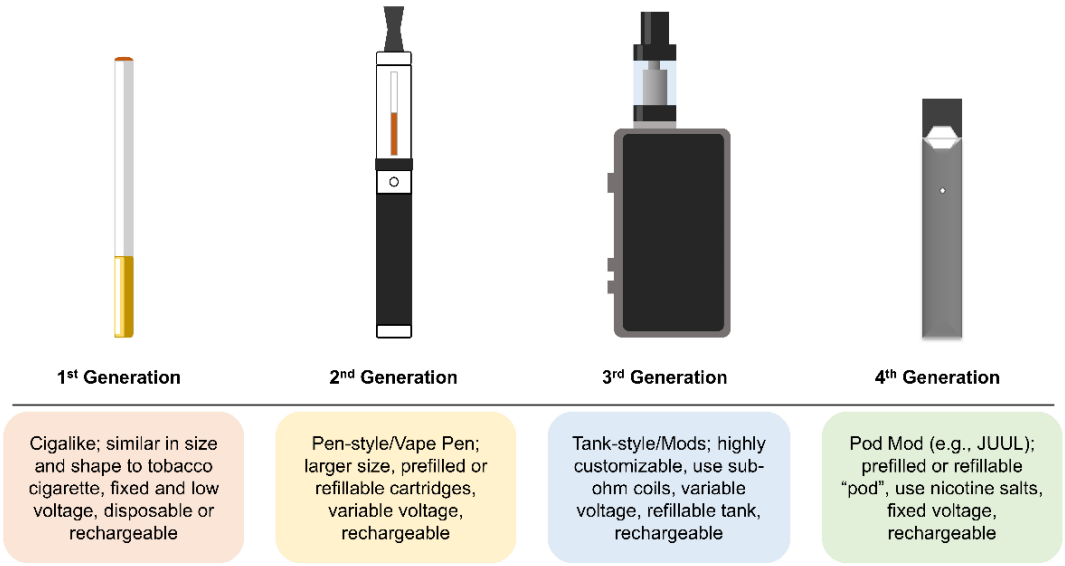


Figure 1.1. Different generations of electronic cigarettes.

The global e-cig market dominated by North America and Europe was valued at $15.04 billion in 2020, and it is expected to continue growing rapidly (Grand View Research 2021). Because of e-cig's appealing flavors, easy-to-use, and risk-free perceptions, the number of e-cig users has also increased markedly, especially among adolescents, despite the Food and Drug

Administration (FDA)'s prohibition of sales to persons under 18. In the United States, although the rates of t-cig use among youth have declined over years, the current e-cig use among middle and high school students substantially increased from 0.3 million in 2011 to 3.6 million in 2020 (CDC 2020b)**.** E-cigs are commonly represented as safer alternatives to t-cigs, yet the effectiveness of using e-cigs as an aid to smoking cessation is largely unknown. Meanwhile, the use of e-cigs has also increased greatly among never-smoking adolescents (Chen-Sankey et al. 2019). Although the use of e-cigs (i.e., vaping) has gained popularity worldwide (Yoong et al. 2018; Leventhal and Dai 2020), at present, limited is known about the health effects of exposure to e-cig aerosols. As of February 18, 2020, 2807 hospitalized cases and 68 deaths of e-cig or vaping product use-associated lung injury (EVALI) were reported in the United States (CDC 2020a). Despite the causes of the adverse health effects having not been yet clearly identified, exposure to e-cig aerosols has become an important public health concern.

Similar to t-cigs, high levels of ultrafine particles (UFPs, particles with an aerodynamic diameter $\leq$ 100 nm), which are approximately measured by the particle number concentration (PNC), and fine particulate matter ($PM_{2.5}$, particles with an aerodynamic diameter $\leq$ 2.5 μm) have been observed in e-cig emissions (Ingebrethsen et al. 2012; Fuoco et al. 2014; Li et al. 2020a; Zhao et al. 2016b). UFPs can penetrate deep into the lungs and circulatory system, potentially possessing greater toxicity to the human body than coarse particles (Franchini and Mannucci 2009). $PM_{2.5}$ has been linked to increased risks of adverse respiratory and cardiovascular diseases (Burnett et al. 2014; Anderson et al. 2012). Although a number of studies have reported that the potential toxicity of e-cig aerosols is lower than that of t-cig smoke (Romagna et al. 2013; McAuley et al. 2012; Ingebrethsen et al. 2012; Cheng 2014; Hecht et al. 2015), toxic compounds such as carbonyls, volatile organic compounds (VOCs), trace metals,

and nicotine-derived nitrosamines have been detected in e-cig aerosols (Sleiman et al. 2016; Ogunwale et al. 2017; Qu et al. 2019; Pankow et al. 2017; Li et al. 2020b).

E-cigs may not only pose health harms to active users but also bystanders. The majority of inhaled e-cig aerosols can be eventually exhaled, which may cause passive exposure to secondhand and even thirdhand vaping aerosols. The percentage of non-users who were exposed to secondhand e-cig aerosols in an indoor environment ranged from 4 to 30% in Europe (Amalia et al. 2020). In the United States, more than half of middle and high school students were exposed to secondhand e-cig aerosols (Gentzke et al. 2019). Exposure to secondhand e-cig aerosols in indoor environments is of particular concern because people typically spend more than 80% of their time indoors.

Essentially different from t-cig smoke, e-cig aerosols are highly dynamic since they contain a large amount of volatile or semi-volatile materials. Little is known about the e-cig aerosol dynamics and related intrinsic and environmental factors influencing the particle behavior after being inhaled and exhaled. Therefore, a better understanding of the characteristics of e-cig mainstream emissions, inhaled aerosols, and exhaled aerosols as sources of secondhand exposure indoors can provide valuable information to exposure assessment and related health effects. In Chapter 2, we conducted literature reviews and summarized the evidence on the effects of e-cigs on indoor air quality, chemical compositions of mainstream and secondhand e-cig aerosols, and associated respiratory and cardiovascular effects. In Chapter 3, we explored the e-liquid factors and investigated how the major components (i.e., PG, VG, and nicotine) affect e-cig aerosol emissions and dynamics under well-controlled experimental conditions. In Chapter 4, we assessed the impacts of e-cig use in vape shops located in multiunit buildings on the indoor air quality of neighboring indoor spaces. We also identified major factors that influence the

behaviors of exhaled e-cig aerosols and evaluated the transport of exhaled e-cig particles from the vape shop to its neighboring indoor spaces and outdoor environment. In Chapter 5, to understand how the human lung environment alters and transforms the inhaled e-cig aerosols into exhaled aerosols, we developed and evaluated a ventilated artificial lung system that simulated major aspects of the lung environment. This system allows us to assess e-cig aerosol characteristics controlling puffing, ventilation, retention, temperature, and humidification representing the human respiratory system. We investigated the effects of breathing, temperature, and relative humidity (RH) on the particle emission, decay rates, and size distribution to better understand how e-cig aerosols behave when inhaled into the human lung.

2. EFFECTS OF ELECTRONIC CIGARETTES ON INDOOR AIR QUALITY AND HEALTH

Published in Annual Review of Public Health [2020, Volume 41 (1), pp. 363 – 380]

DOI: 10.1146/annurev-publhealth-040119-094043

2.1. Abstract

With the rapid increase in electronic cigarette (e-cig) users worldwide, secondhand exposure to e-cig aerosols has become a serious public health concern. We summarize the evidence on the effects of e-cigs on indoor air quality, chemical compositions of mainstream and secondhand e-cig aerosols, and associated respiratory and cardiovascular effects. The use of e-cigs in indoor environments leads to high levels of fine and ultrafine particles similar to tobacco cigarettes (t-cigs). Concentrations of chemical compounds in e-cig aerosols are generally lower than those in t-cig smoke, but a substantial amount of vaporized propylene glycol, vegetable glycerin, nicotine, and toxic substances such as aldehydes and heavy metals have been reported. Exposures to mainstream e-cig aerosols have biologic effects, but only limited evidence showing adverse respiratory and cardiovascular effects in humans. Long-term studies are needed to better understand the dosimetry and health effects of exposures to secondhand e-cig aerosols.

2.2. Introduction

An electronic cigarette (e-cig) is a battery-powered nicotine delivery system widely used as an alternative to tobacco cigarettes (t-cig). Since 2011, the global e-cig market has grown rapidly and is projected to reach $48.9 billion by 2025, with more than 70% of the market in North America and Europe (Adroit Market Research 2018). The number of e-cig users has also increased markedly, especially among adolescents, despite the Food and Drug Administration's prohibition of sales to persons under the age of 18 (U.S. Department of Health and Human

Services 2016). In the United States, the total number of current e-cig users in middle and high schools increased from 0.3 million in 2011 to 3.6 million in 2018 (Cullen et al. 2018). Similar increases among adolescents have been observed in other countries, such as the United Kingdom, Canada, South Korea, New Zealand, Finland and Poland (Breland et al. 2017; Bauld et al. 2017). E-cigs are popular among adolescents likely because of their appealing flavors (Morean et al. 2018) and the newly introduced JUUL pods which use nicotine salts to deliver higher levels of nicotine (Huang et al. 2019; McKelvey et al. 2018).

For t-cigs, the combustion of tobacco leaves releases nicotine and substantial amounts of toxic by-products. In comparison, e-cigs deliver nicotine by vaporizing e-liquids, which typically use propylene glycol (PG) and vegetable glycerin (VG) as the suspension media for nicotine and various flavorings. E-cigs are marketed as a safer alternative to t-cigs because they are combustion-free, yet their use has also increased greatly among nonsmokers (McMillen et al. 2015). The impacts of e-cigs on population health remain largely unknown, but with increasing evidence on their biological effects from *in vitro* and *in vivo* studies (Dinakar and O'Connor 2016), the safety of e-cigs has become a serious public health concern.

Besides active e-cig users, bystanders could also be exposed to e-cig aerosols. It has been estimated that more than 70% of inhaled e-cig aerosols are eventually exhaled (Zhang et al. 2013) which may cause secondhand exposures. E-cigs are commonly used in many places, such as homes, cars, restaurants, bars, and workplaces (Giovenco et al. 2014) where vulnerable populations, such as children, adolescents, and pregnant women might be exposed (Wang et al. 2017; Drehmer et al. 2019). Secondhand exposure in indoor environments is of particular concern because people typically spend more than 80% of their time indoors (Jenkins et al. 1992), where emitted pollutants are not diluted as quickly or as extensively as outdoors. Yet, to

what extent such secondhand exposures affect human health is unclear. While a large number of health studies on t-cig secondhand smoke exist (Holcomb 1993), they cannot be extrapolated to e-cigs because the emission characteristics are different.

To provide a better understanding of the public health risks associated with secondhand exposures to e-cig aerosols, here we summarize the evidence for the impacts of e-cigs on indoor air quality and human health. The schematic process from e-cig emissions, to secondhand exposures, and to potential health effects is summarized in **Figure 2.1**.

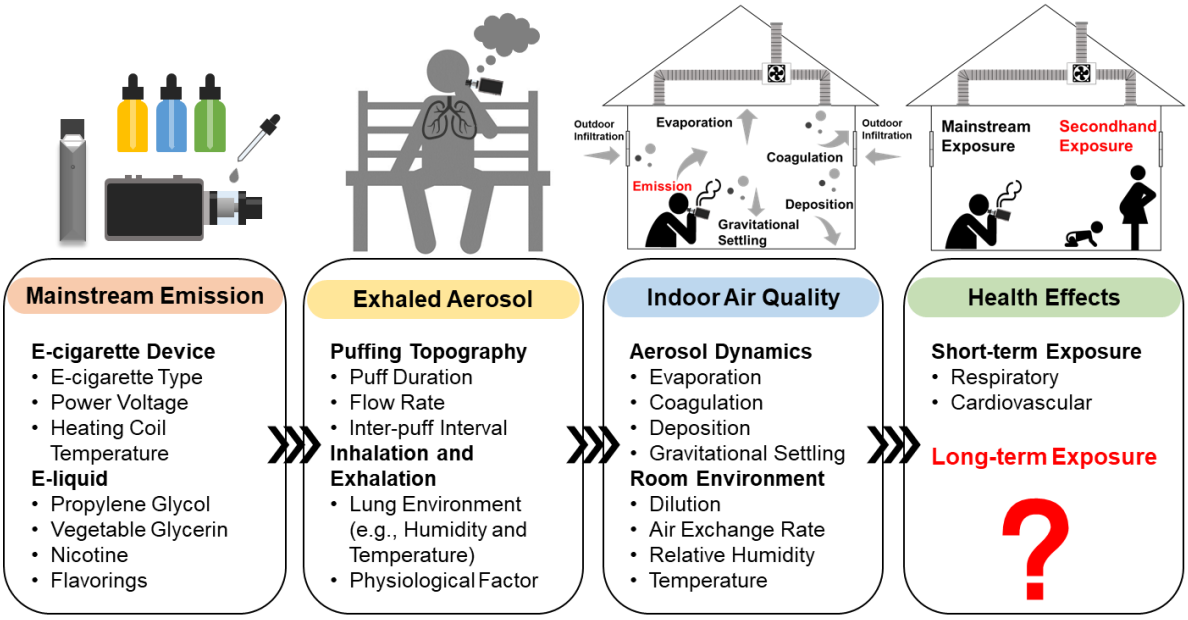


Figure 2.1. Schematic process from electronic cigarette emissions, to secondhand exposures, and to potential health effects.

2.3. The literature search

We reviewed articles published in English and listed on PubMed and the Web of Science before April 2019 that investigated either particulate matter (PM) or chemical compositions in e-cig aerosols, as well as associated health effects. Inclusion criteria include (*a*) e-cig aerosol studies report fine particulate matter ($PM_{2.5}$, particles with aerodynamic diameters ≤ 2.5 μm) or ultrafine

particles (UFPs; particles with a diameter ≤ 100 nm), which are approximately measured by the particle number concentration (PNC), (*b*) both mainstream and secondhand exposure studies investigated chemical compositions in e-cig aerosols, and (*c*) active and passive human exposure studies on e-cig health effects. Key search terms included: "electronic cigarette" OR "e-cigarette" OR "e-cig" OR "vaping" in combination with "aerosol" OR "particle" OR "particulate matter (PM)," "chemical composition" OR "chemical emission" OR "exposure," "mainstream" OR "secondhand" OR "indoor air quality," and "health." We extracted data on particle and chemical concentrations from the text, tables, or supporting information in the identified articles. To compare the results across different studies, here we report chemical compositions in mass per puff for mainstream and mass per cubic meter for secondhand studies, respectively.

2.4. Impacts of e-cig on indoor air quality

Studies evaluating the effects of e-cig on particulate matter (PM) were typically conducted either in a room (>30 m^3) or in a chamber (<1 m^3). Studies conducted in rooms represent real-world exposures, but were often affected by various environmental factors, such as relative humidity, air exchange rate, and temperature, which are difficult to be fully controlled. On the other hand, chamber studies usually have good control over environmental factors, thus can systematically isolate and investigate the effects of e-cig devices and e-liquid compositions. However, the concentrations of pollutants reported in chamber studies are often orders of magnitude higher than in real-world indoor environments. In the following sections, we focus on studies conducted in real-world indoor environments.

2.4.1. Indoor Particle Concentrations

Exposure to outdoor $PM_{2.5}$ is a well-established risk factor for respiratory and cardiovascular diseases (Burnett et al. 2014). Several indoor studies have reported high concentrations of $PM_{2.5}$

resulting from e-cig (**Figure 2.2a**), which could reach up to 1,121 μg/m^3, or ~45 times as high as the World Health Organization's recommended limit for 24-hour outdoor concentrations of 25 μg/m^3 (World Health Organization 2006.). In most cases, the reported indoor $PM_{2.5}$ levels during e-cig use are above 150 μg/m^3, which are similar to those produced by t-cigs. The impacts of e-cigs on indoor air quality are also similar to, if not greater than, other combustion-free nicotine delivery systems, such as waterpipe and "heat-not-burn" products (Forster et al. 2018; Ruprecht et al. 2017; Fromme et al. 2009). The $PM_{2.5}$ concentrations of 600 to 800 μg/m^3, as reported in the vape shops and vaping conventions (Soule et al. 2017; Nguyen et al. 2019), are about twice as high as those in hookah bars (Zhou et al. 2017). In comparison, the $PM_{2.5}$ concentrations observed across a wide range of common indoor environments without e-cigs, such as homes, offices, schools, and day care, are from 8 to 52 μg/m^3 (Morawska et al. 2017).

In addition to $PM_{2.5}$, UFPs are also of great health concern (Fuoco et al. 2014) because they have a greater surface area per unit mass than larger particles so that they can bind more toxic chemicals (Terzano et al. 2010). The indoor PNC can increase up to 20 times over the background during e-cig use (7.2×10^3 to 6.2×10^4 particles/cm^3; **Figure 2.2b**) (Guo et al. 2010), but still lower than those from t-cigs (7×10^4 to 2.1×10^5 particles/cm^3) (Forster et al. 2018; Ruprecht et al. 2017; Scheitel et al. 2016; Konstantopoulou et al. 2014) and other combustion-free nicotine delivery systems (7.7×10^3 to 3.2×10^5 particles/cm^3) (Fromme et al. 2009; Ruprecht et al. 2017; Forster et al. 2018). Similar to $PM_{2.5}$, indoor PNCs from e-cigs are also higher than other common indoor environments mentioned above (Morawska et al. 2017).

As shown in **Figure 2.2**, studies on t-cig secondhand smoke have been conducted worldwide, but studies on e-cigs are mainly from North America and Europe. The current prevalence of e-cig in other countries and regions is relatively low, but the e-cig market in many

populous countries (e.g., China) is expanding rapidly (Prescient & Strategic Intelligence 2018). Thus, secondhand exposures to e-cig aerosols will likely become a potential public health problem in those countries in the near future. Detailed information on $PM_{2.5}$ and PNC levels, background concentrations, emission protocol, room size, and air exchange rate for both e-cig and t-cig room studies are summarized in **Table A-1 of the Appendix**.

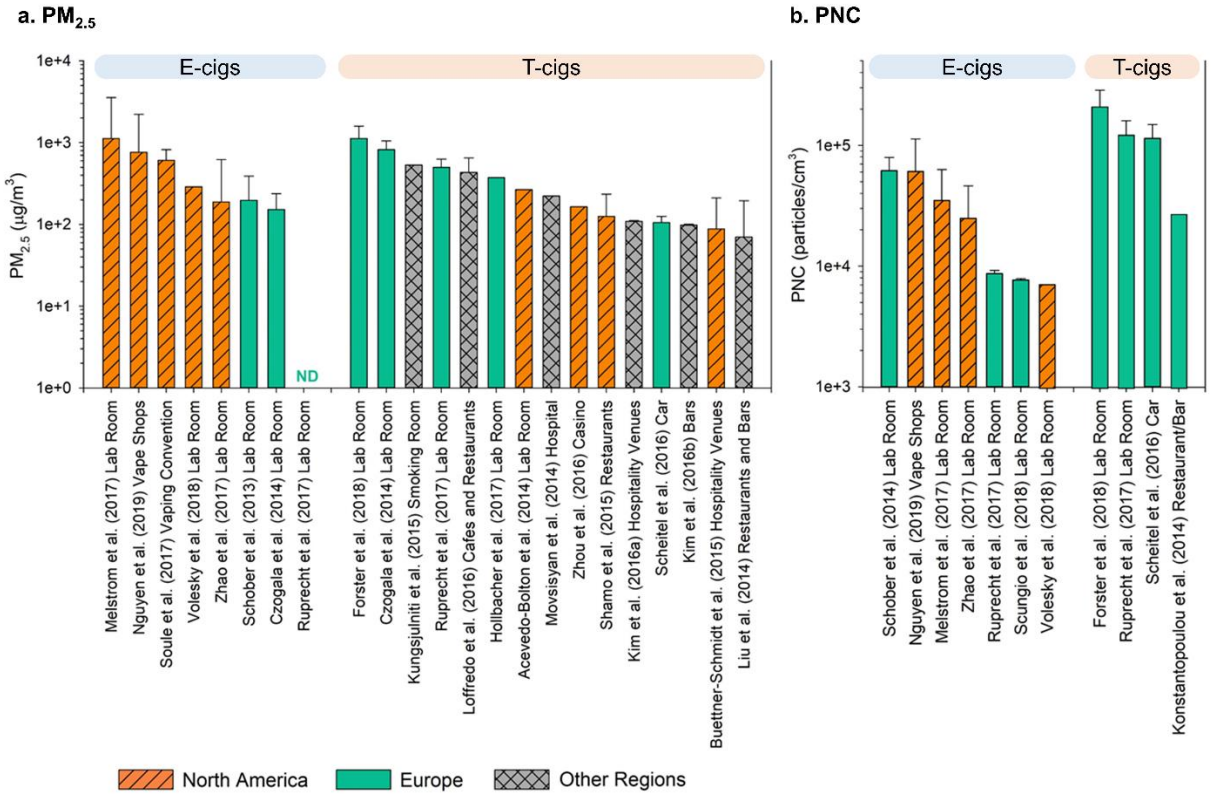


Figure 2.2. Average concentrations of (a) $PM_{2.5}$ mass concentration and (b) particle number concentration (PNC) from 11 studies on e-cigs and 16 studies on t-cigs in various indoor environments (i.e., laboratory settings and real-world public indoor spaces) by region. Abbreviation: ND = not detectable.

2.4.2. Factors Affecting Indoor Particle Concentrations

In addition to particle concentrations, particle size distribution is also important to respiratory health because smaller particles (especially UFPs) generally penetrate deeper into the lung

(Hinds 1999). E-cig particles are primarily in the submicron size range (Fuoco et al. 2014; Ingebrethsen et al. 2012) exhibiting a bimodal size distribution, with one mode located around 15-30 nm and the other around 85-100 nm (Schripp et al. 2013; Zhao et al. 2017; Scungio et al. 2018). Both particle concentration and particle size distribution are affected by emissions from the e-cig device, exhalation by the e-cig user, and indoor environmental factors, as illustrated in **Figure 2.1** and discussed below.

E-cig emissions are affected by various intrinsic factors including the e-cig device type, heating coil temperature, power voltage, and e-liquid compositions (Floyd et al. 2018; Gillman et al. 2016; Son et al. 2018; Khlystov and Samburova 2016; Sleiman et al. 2016; Zhao et al. 2016c; Fuoco et al. 2014; Baassiri et al. 2017; Pankow et al. 2017). As shown in **Figure 1.1**, e-cigs have evolved quickly over time from the "cigalike" disposable type, to the more advanced tank-style with customizable voltage and e-liquids, to the recent pod-based vaping systems (Huang et al. 2019; Glantz and Bareham 2018; McKelvey et al. 2018). The power voltage that determines the heating coil temperature has been associated with particle emissions (Floyd et al. 2018; Gillman et al. 2016). The tank-style which allows a higher voltage can produce more particles than the "cigalike" type (Melstrom et al. 2017). In addition, particle emissions from e-cigs are also influenced by the e-liquid compositions. The presence of nicotine (Fuoco et al. 2014) and higher PG/VG ratios tend to produce more particles (Baassiri et al. 2017). The recently introduced pod-based JUUL has not been studied and raises even more health concerns due to its high nicotine content and its popularity among adolescents (McKelvey et al. 2018; Goniewicz et al. 2018).

Variables related to the e-cig user, such as the puffing topography (i.e., flow rate, puff duration, and inter-puff interval) and the process of inhalation and exhalation, also affect particle concentrations. In general, the particle concentration increases with higher puffing flow rates,

longer puff durations, and greater inter-puff intervals (Gillman et al. 2016; Chen et al. 2018; Nguyen et al. 2019; Zhao et al. 2016c). E-cig particles tend to grow in human lungs under high humidity due to the hygroscopic effect (Pichelstorfer et al. 2016; Sosnowski and Kramek-Romanowska 2016). Other physiological factors in the respiratory system, such as lung capacity, air flow, and breath pattern, might also affect e-cig aerosol dynamics. Unfortunately, none of these factors have been studied and the differences between the inhaled mainstream and the exhaled secondhand e-cig aerosols remain unknown.

Once released into the room air, e-cig particles are subject to aerosol dynamics under certain environmental conditions. In contrast to t-cig smoke, e-cig particles mainly consist of droplets that are more volatile because the e-liquid main ingredient, PG, has a relatively high saturation vapor pressure. E-cig particles have been observed to evaporate within seconds (Zhao et al. 2017). At high particle number concentrations, coagulation is also an important particle-removal mechanism that reduces the number of particles, but increases particle size (Mikheev et al. 2016; Floyd et al. 2018). In addition, e-cig particles can be removed from the room air by gravitational settling and surface deposition, leading to potential third-hand exposures which also deserves future studies (Goniewicz and Lee 2015). Increasing dilution or air exchange rate may enhance particle evaporation and reduce particle concentrations and particle sizes (Meng et al. 2017; Zhao et al. 2016a; Nguyen et al. 2019; Ingebrethsen et al. 2012; Floyd et al. 2018). Similarly, increasing temperature or decreasing relative humidity may also enhance evaporation and reduce particle size (Wright et al. 2016; Schripp et al. 2013). Because e-cig particles are markedly dynamic, their concentrations decay rapidly over distances (>1.5 m) from the source (i.e., e-cig users), especially for $PM_{2.5}$ mass concentration (Zhao et al. 2017; Nguyen et al. 2019).

Understanding the dynamics of e-cig particles in an indoor environment is important as it can guide exposure assessment and mitigation strategies.

2.5. Chemical compositions of e-cig aerosols

The effects of e-cig aerosols on health are largely determined by their chemical compositions. The most commonly reported chemicals in both mainstream and secondhand e-cig aerosols are PG, VG, nicotine, carbonyls, aromatic volatile organic compounds (VOCs), trace metals, and tobacco-specific nitrosamines (TSNAs) (**Figure 2.3)**. Many chemicals are present in both gas- and particulate-phases (Schripp et al. 2013). The partition between gas- and particulate-phases affects the concentration and fate of e-cig emitted chemicals and deserves future studies.

As shown in **Figure 2.3**, the chemical profiles of the mainstream and secondhand e-cig aerosols are similar, but as expected, the concentrations of most chemicals in the secondhand are much lower than in the mainstream. Overall, the most abundant chemicals detected in the e-cig mainstream are PG and VG, followed by nicotine, carbonyls, aromatic VOCs, and trace metals. Most of the chemicals in the mainstream come from the major components of e-liquids: PG, VG, and nicotine. Although the FDA states that ingesting PG and VG in consumer and household products is safe, inhaling vaporized PG and VG at high concentrations could potentially irritate the lungs (Kienhuis et al. 2015), which is a unique health risk for e-cig aerosols (Margham et al. 2016; Liu et al. 2017). The significant amount of nicotine reported in the e-cig aerosols also poses several health risks. Existing evidence indicates that e-cig use can motivate youth to start smoking t-cig due to the highly addictive nature of nicotine (Glantz and Bareham 2018). In addition, nicotine contributes to adverse health effects on the cardiocirculatory, respiratory, and gastrointestinal systems (England et al. 2017; Benowitz and Burbank 2016; Mishra et al. 2015).

Other observed chemicals such as formaldehyde, acetaldehyde, propanol, acrolein, acetone, and benzene are likely produced by either dehydration of PG/VG or by the reactions between PG and VG at high heating coil temperatures (Sleiman et al. 2016; Ogunwale et al. 2017; Qu et al. 2019; Pankow et al. 2017). E-cig-related aldehydes might also come from flavoring additives in the e-liquid (Khlystov and Samburova 2016). Aldehydes are cytotoxic and can have adverse respiratory effects (Huang et al. 2018). In addition, formaldehyde and acetaldehyde are classified by the International Agency for Research on Cancer (IARC) as carcinogenic to humans (Group 1) and possibly carcinogenic to humans (Group 2B), respectively (Huang et al. 2018). Among the aromatic VOCs, the IARC lists benzene as a human carcinogen and toluene may be neurotoxic (Huang et al. 2018).

The likely sources of trace metals, especially those with relatively higher concentrations (i.e., chromium, aluminum, and copper), are the metal-coated wires of the heating coils (Saffari et al. 2014; Williams et al. 2013). Inhaling trace metals might irritate the respiratory system and impair respiration (Williams et al. 2013). Cadmium, lead, chromium, arsenic, and nickel are also classified as human carcinogens (IARC 2019). Although two studies found nicotine-derived nitrosamines, such as N'-Nitrosonornicotine (NNN) and 4-(methylnitrosamino)-1-(3-pyridyl)-1-butanone (NNK) (Goniewicz et al. 2014; Margham et al. 2016), which are strong carcinogens that may cause lung and oral cancers (Hecht et al. 2016), whether these compounds are products of chemical reactions of nicotine or impurities of the e-liquid is not clear (Farsalinos et al. 2015).

The concentrations of most chemicals in the e-cig mainstream aerosols are lower than those of t-cigs (**Figure 2.3**). The only exceptions are PG and VG, which are major components of e-liquid but are not used in t-cigs. Concentrations of trace metals in mainstream aerosols are similar in e-cigs and t-cigs. However, chromium, a carcinogenic and respiratory toxicant, is at

higher concentrations in e-cigs, suggesting potential risks from chromium-coated wire in heating coils (Williams et al. 2013). The concentration of nicotine in e-cig mainstream aerosol is similar to or slightly lower than that in t-cig smoke. Of note, the nicotine content in a single JUUL pod is higher than that in 20 t-cigs, and might lead to potential cytotoxicity and more significant addiction effects (Omaiye et al. 2019). The concentrations of carbonyls and aromatic VOCs are 10 to 1000 times higher in the mainstream emissions of t-cigs than in e-cigs. Because these compounds are highly toxic, the observed lower concentrations indicate that e-cig aerosols are likely less toxic than t-cig smoke (Oh and Kacker 2014; Cervellati et al. 2014).

In addition to the chemicals described above, e-cig aerosols contain a wide variety of VOCs at a much lower level, such as acetonitrile, isoprene, ethanol, diacetyl, and acetoin, which likely originate from the flavoring additives (Lee et al. 2017; Liu et al. 2017; Allen et al. 2016; Klager et al. 2017). Even weaker evidence exists in the literature on the presence of polycyclic aromatic hydrocarbons, crotonaldehyde, acetol, glyoxal, glycidol, and benzaldehyde in e-cig aerosols.

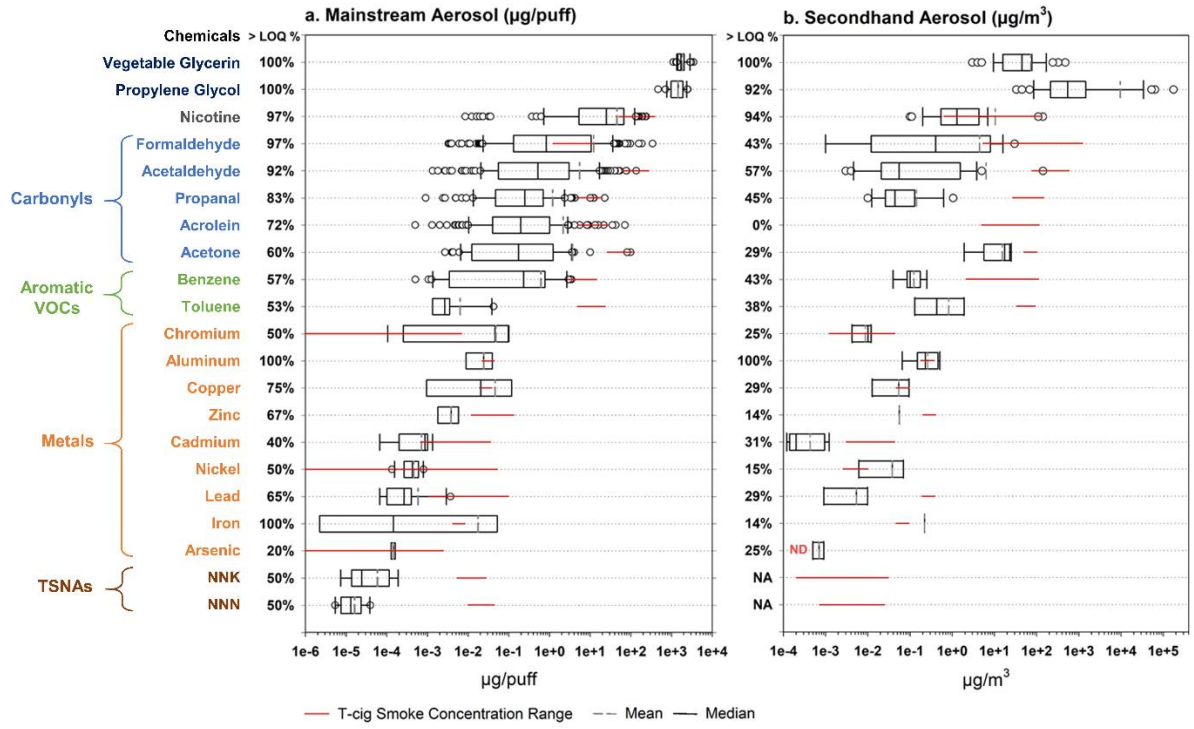


Figure 2.3. Chemical compositions of e-cig aerosols including (a) mainstream aerosols (µg/puff) from 37 studies and (b) secondhand aerosols (µg/m^3) from 11 studies. Concentrations of t-cig-emitted chemicals are presented in ranges (red line) as a reference group. All the data included are background-subtracted values, when applicable. "> LOQ%" indicates the percentage of available data points above the limit of quantification (LOQ). Abbreviations: VOCs=volatile organic compounds; TSNAs=tobacco-specific nitrosamines; NNK=4-(methylnitrosamino)-1-(3-pyridyl)-1-butanone; NNN=N'-Nitrosonornicotine.

2.6. Health effects of e-cig aerosols

The chemical profiles of mainstream and secondhand e-cig aerosols are similar (**Figure 2.3**), suggesting the results of the studies on active e-cig use and secondhand exposures likely reflect the health effects of similar chemical mixtures at different doses. As previously reviewed, many studies have shown that e-cig aerosols are safer than t-cig smoke (Oh and Kacker 2014). However, substantial evidence indicates that e-cig aerosols are not safe to cells *in vitro* or

animals *in vivo*. Results from *in vitro* studies have identified the biologic effects on various cell types including airway epithelium and vascular endothelium (Taylor et al. 2017; Dinakar and O'Connor 2016). Similarly, e-cig aerosols also impair lung functions in animals, with inflammation and immune abnormalities as the likely underlying mechanisms (Dinakar and O'Connor 2016), and perturb the cardiovascular system (Olfert et al. 2018; Qasim et al. 2018). In addition to the observed respiratory and cardiovascular effects (Crotty Alexander et al. 2018; Nguyen et al. 2018), e-cig aerosols also present marked carcinogenicity (Lee et al. 2018a) and neurological toxicity (Nguyen et al. 2018) in animals. However, it remains controversial whether the dosages used in animal studies are relevant to human exposures, and whether the results are consistent across different species.

The respiratory and cardiovascular effects of e-cig aerosols were also examined in human studies, most of which focused on the effects of active e-cig use with only a few studies on secondhand exposures. As indicated by circulating concentrations of cotinine, doses in e-cig active exposure studies are usually higher than those in secondhand studies (**Table 2.1**). The results of these studies suggest likely short-term effects (≤ 2 hours exposure) of e-cig aerosols on pre-clinical endpoints (**Figure 2.1**).

2.6.1. Respiratory Effects

Most human studies on the respiratory system examine the effects of short-term (≤ 1 hour) exposure among a small number of healthy subjects (**Table 2.1**). Lung function is one of the most commonly studied endpoints, but the results of different studies are inconsistent. Active e-cig use by healthy t-cig smokers over five minutes slightly but significantly reduced lung function measures (i.e. forced expiratory volume in 1 s (FEV1) and forced expiratory flow (FEF) 25 %) in a randomized crossover trial (Ferrari et al. 2015). However, similar effects were not

observed in two crossover trials (one randomized and one nonrandomized), in which active e-cig use over five or 30 minutes didn't change any lung function measure among healthy t-cig smokers (Flouris et al. 2013; Vardavas et al. 2012). In another two crossover trials on secondhand e-cig aerosols (one randomized and one nonrandomized), neither 30-minutes nor one-hour exposures altered the lung function measures among healthy non-smokers (Tzortzi et al. 2018; Flouris et al. 2013). In contrast, more consistent results are reported for airway resistance, which was significantly increased after active e-cig use or passive exposure in two clinical trials, as determined by impulse oscillometry (Vardavas et al. 2012; Tzortzi et al. 2018). In addition, a case-control study found substantially altered respiratory proteomic profiles among e-cig users indicative of impending airway obstruction (Dang et al. 2018). Nevertheless, the clinical importance of these early changes is not clear. It is still unclear whether increased airway resistance induced by e-cig exposures will become worse over time and eventually contribute to decreased lung function.

Also studied are the short-term effects (≤ 2 hours) of e-cig aerosols on exhaled nitric oxide, a biomarker of airway inflammation associated with increased risk of asthma and bronchitis (Taylor et al. 2006). Three studies report no effect (Flouris et al. 2013; Antoniewicz et al. 2016; Ferrari et al. 2015), and four studies show either increased (Marini et al. 2014; Schober et al. 2014b) or decreased exhaled nitric oxide concentrations after the exposures (Tzortzi et al. 2018; Vardavas et al. 2012). In two cross-sectional studies of adolescents, e-cig use was significantly associated with a greater odds of asthma attacks [odds ratio (OR), 1.12; 95% CI, 1.01 to 1.26] (Kim et al. 2017) and chronic bronchitis symptoms (OR, 1.70; 95% CI, 1.11 to 2.59) (McConnell et al. 2017). Likewise, passive exposures to e-cig aerosols were associated with asthma attacks in cross-sectional studies of adolescents with a history of asthma (OR, 1.27;

95% CI, 1.11 to 1.47) (Bayly et al. 2018), suggesting potential adverse respiratory effects of secondhand exposures, at least among susceptible populations.

2.6.2. Cardiovascular Effects

Evidence of secondhand exposures to e-cig aerosols on cardiovascular effects in humans is limited. Nevertheless, the effects of active e-cig use on cardiovascular biomarkers have been frequently documented (**Table 2.1**). Both habitual and short-term e-cig use can cause a cardiac-autonomic imbalance, as indicated by heart rate variability. Nicotine has been suggested as a likely cause (Moheimani et al. 2017b; Moheimani et al. 2017a). The existing evidence also suggests that active e-cig use induces systemic oxidative stress and inflammation and impairs endothelial function (Antoniewicz et al. 2016; Carnevale et al. 2016; Chatterjee et al. 2019; Moheimani et al. 2017b). Although oxidative stress and inflammation are important in the pathogenesis of cardiovascular diseases, to what extent the observed cardiovascular effects of e-cigs are clinically relevant is unclear. The cross-sectional National Health Interview Surveys of 2014 (n=37,000) and 2016 (n=33,000) found that daily e-cig use was associated with myocardial infarction (OR, 1.79; 95% CI, 1.20 to 2.66) (Alzahrani et al. 2018), but more evidence is needed, especially from long-term large cohort studies, before e-cigs can be linked to cardiovascular diseases.

Table 2.1. Summary of studies on the health effects in humans of active electronic cigarette use and passive exposure to secondhand electronic cigarette aerosols. Studies with the same design are shown in chronological order based on publication date.

Study	Design	Study subjects (sample size)	Exposure concentrations	Exposure duration	Health effect assessment	Findings
Respiratory Effects: Active E-cig Use						
Flouris et al. (2013)	Randomized crossover trial	Healthy t-cig smokers (n=15)	10.4 puffs, serum cotinine: 60.6 ng/mL	30 min	Lung function, eCO, and eNO	No differences before and after e-cig use
Ferrari et al. (2015)	Randomized crossover trial	Healthy t-cig smokers (n=10) and non-smokers (n=10)	–	5 min	Lung function, eCO, and eNO	Reduction in lung function after e-cig use only among smokers
Antoniewicz et al. (2016)	Randomized crossover trial	Healthy seldom smokers (n=16)	10 puffs, plasma cotinine: 4.1 ng/mL	10 min	eNO	No differences before and after e-cig use
Vardavas et al. (2012)	Nonrandomized crossover trial	Healthy t-cig smokers (n=30)	–	5 min	Lung function, eNO, and airway resistance	Increased airway resistance and decreased eNO after e-cig use
Marini et al. (2014)	Nonrandomized crossover trial	Healthy t-cig smokers (n=25)	–	5 min	eNO	Increased eNO after e-cig use
Schober et al. (2014a)	Controlled exposure study	Healthy t-cig smokers (n=9)	132 puffs	2 h	eCO and eNO	Increased eNO after the use of e-cig with nicotine
Dicpinigaitis et al. (2016)	Controlled exposure study	Healthy non-smokers (n=30)	30 puffs	15 min	Cough reflex sensitivity	Inhibited cough reflex sensitivity after the use of e-cig with nicotine
Dang et al. (2018)	Case-control study	Healthy non-smokers (n=18)	1.8 puffs/hour, serum cotinine: 97.2 ng/mL	–	Airway proteome	Markedly changed protein profiles in lungs among e-cig

		and e-cig users (n=10)				users that may have clinical implications for the development of chronic lung diseases
Kim et al. (2017)	Cross-sectional study	Adolescents (age: 12-18 years) (n=216,056)	Self-reported e-cig use in past 30 days: 8% of the total population	−	Asthma attack in the past 12 months	Higher odds of asthma attack (OR, 1.12; 95% CI, 1.01-1.26) associated with the e-cig use
McConnell et al. (2017)	Cross-sectional study	Adolescents (age: ~ 17 years) (n=2,086)	Self-reported past (24.0%) and current (9.6%) e-cig users	−	Self-reported chronic bronchitis symptoms and wheeze	Higher odds of chronic bronchitis symptoms (OR, 1.70; 95% CI, 1.11–2.59) associated with past e-cig use
			Respiratory Effects: Passive Exposure			
Flouris et al. (2013)	Randomized crossover trial	Healthy non-smokers (n=15)	Serum cotinine: 2.4 ng/mL	1 h	Lung function, eCO, and eNO	No differences before and after the exposures
Tzortzi et al. (2018)	Nonrandomized crossover trial	Healthy non-smokers (n=40)	120 puffs/hour in a 35 m^3 room	30 min	Lung function, eCO, eNO, and airway resistance	Increased air resistance and decreased eNO after the exposures
Bayly et al. (2018)	Cross-sectional study	Adolescents (age: 11-17 years) with self-reported asthma (n=11,830)	Self-reported exposure in past 30 days: 33% of the total population	−	Asthma attack in the past 12 months	Higher odds of asthma attack (OR, 1.27; 95% CI, 1.11-1.47) associated with the exposures
			Cardiovascular Effects: Active E-cig Use			

Flouris et al. (2012)	Randomized crossover trial	Healthy t-cig smokers (n=15)	10.4 puffs, serum cotinine: 60.6 ng/mL	30 min	Complete blood count	No differences before and after e-cig use
Antoniewicz et al. (2016)	Randomized crossover trial	Healthy seldom smokers (n=16)	10 puffs, plasma cotinine: 4.1 ng/mL	10 min	Endothelial function biomarkers	Increased endothelial progenitor cell counts after e-cig use
Poulianiti et al. (2016)	Randomized crossover trial	Healthy t-cig smokers (n=15)	10.4 puffs, serum cotinine: 60.6 ng/mL	30 min	Oxidative stress biomarkers	No differences before and after e-cig use
Moheimani et al. (2017a)	Randomized crossover trial	Healthy non-smokers (n=33)	60 puffs, plasma nicotine: 4.1 ng/mL	30 min	Heart rate variability, blood pressure, and biomarkers of oxidative stress and inflammation	A shift in cardiac autonomic balance after the use of e-cig with nicotine
Carnevale et al. (2016)	Nonrandomized Crossover trial	Healthy t-cig smokers (n=20) and non-smokers (n=20)	9 puffs	–	Biomarkers of endothelial function and oxidative stress	Changes of biomarkers indicative of increased oxidative stress and decreased endothelia function after e-cig use
Chatterjee et al. (2019)	Controlled exposure study	Healthy non-smokers (n=10)	16 - 17 puffs	3 min	Biomarkers of oxidative stress and inflammation	Changes of biomarkers indicative of increased oxidative stress and inflammation after e-cig use
Moheimani et al. (2017b)	Case-control study	Healthy non-smokers (n=23)	Plasma cotinine: 3.8-139 ng/mL	1.6 years	Heart rate variability, blood	A shift in cardiac autonomic balance

		and e-cig users (n=19)			pressure, and biomarkers of oxidative stress and inflammation	and an increase in oxidative stress among e-cig users
Alzahrani et al. (2018)	Cross-sectional study	Adults (age>18 years) (n= 69,725)	Self-reported daily e-cig users: 1.1% of the total population	–	Self-reported history of myocardial infarction	Higher odds of myocardial infarction (OR, 1.79; 95% CI, 1.20-2.66) associated with daily e-cig use
			Cardiovascular Effects: Passive Exposures			
Flouris et al. (2012)	Randomized crossover trial	Healthy non-smokers (n=15)	Serum cotinine: 2.4 ng/mL	1 h	Complete blood count	No differences before and after the exposures
Poulianiti et al. (2016)	Randomized crossover trial	Healthy non-smokers (n=15)	Serum cotinine: 2.4 ng/mL	1 h	Oxidative stress biomarkers	No differences before and after the exposures

Abbreviations: eCO, exhaled carbon monoxide; eNO, exhaled nitric oxide; e-cig, electronic cigarette.

2.7. Conclusions and future perspectives

The evidence in the literature confirms that e-cig emissions impair indoor air quality and that bystanders are at risk of secondhand exposures. Indoor particle concentrations due to e-cigs are similar to those due to t-cigs. Although studies of secondhand e-cig aerosols are limited, their chemical composition profiles are similar to those of mainstream e-cig aerosols but have much lower concentrations. E-cigs generate less carcinogenic and toxic compounds than t-cigs, but still produce substantial amounts of PG, VG, and nicotine, as well as some toxic compounds such as aldehydes and heavy metals. Current health effect studies in humans focus on the acute effects and early biomarkers. These studies have suggested potential respiratory and cardiovascular effects of e-cig aerosol. However, results from these studies are inconsistent, calling for large cohort and long-term exposure studies that examine the linkage between e-cigs and clinical endpoints.

Although the effects of e-cigs on human health are not yet fully understood, the high levels of indoor air pollutants due to e-cig call for precautionary measures to protect public health. As of October 2016, 32 countries have banned e-cigs from public spaces (Kennedy et al. 2017). In the United States, 15 states and 814 municipalities have already expanded smoke-free laws to e-cigs and have prohibited their use in smoke-free places (American Nonsmokers' Rights Foundation 2019). Until the long-term health effects are fully established, we recommend restricting the use of e-cigs in public indoor spaces to protect bystanders from secondhand exposures.

Given the uncertainties of the heating process and complexity of flavoring additives, the e-cig design features and e-liquid compositions should be further studied to better understand their effects on e-cig aerosol toxicity to support future regulations. Indoor air pollution due to e-

cigs could be potentially reduced by enhancing ventilation and air filtration, but limited studies have been conducted on these mitigation measures that can inform policy. Future studies also need to focus on identifying susceptible and vulnerable populations and monitor places that may contribute to high levels of secondhand exposures, such as vape shops.

3. EFFECTS OF PROPYLENE GLYCOL, VEGETABLE GLYCERIN, AND NICOTINE ON EMISSIONS AND DYNAMICS OF ELECTRONIC CIGARETTE AEROSOLS

Published in Aerosol Science and Technology [2020, Volume 54 (11), pp. 1270 – 1281]

DOI: 10.1080/02786826.2020.1771270

3.1. Abstract

An electronic cigarette (e-cig) generates aerosols by vaporizing the e-liquid, which mainly consists of propylene glycol (PG), vegetable glycerin (VG), and nicotine. Understanding the effects of e-liquid main compositions on e-cig aerosols is important for exposure assessment. This study investigated how the PG/VG ratio and nicotine content affect e-cig aerosol emissions and dynamics. A tank-based e-cig device with 10 different flavorless e-liquid mixtures (e.g., PG/VG ratios of 0/100, 10/90, 30/70, 50/50, and 100/0 with 0.0% or 2.4% nicotine by weight) was used to puff aerosols into a 0.46 m^3 stainless steel chamber for 0.5 h. Real-time measurements of particle number concentration (PNC), fine particulate matter ($PM_{2.5}$), and particle size distributions were conducted continuously throughout the puffing and the following 2-h decay period. During the decay period, particle loss rates were determined by a first-order log-linear regression and used to calculate the emission factor. The addition of nicotine in the e-liquid significantly decreased the particle number emission factor by 33%. The $PM_{2.5}$ emission factor significantly decreased with greater PG content in the e-liquid. For nicotine-free e-liquids, increasing the PG/VG ratio resulted in increased particle loss rates measured by PNC and $PM_{2.5}$. This pattern was not observed with nicotine in the e-liquids. The particle loss rates, however, were significantly different with and without nicotine especially when the PG/VG ratios were greater than 30/70. Compared with nonvolatile di-ethyl-hexyl subacute (DEHS) aerosols, e-cig particle concentration decayed faster

inside the chamber, presumably due to evaporation. These results have potential implications for assessing human exposure to e-cig aerosols.

3.2. Introduction

A cluster of respiratory syndromes has been recently identified among patients after using electronic cigarettes (e-cigs) (Layden et al. 2019a). With the rapid growth of e-cig users worldwide (Cullen et al. 2018; Breland et al. 2017; Yoong et al. 2018), exposure to e-cig aerosols has become an important public health concern. The global e-cig market is anticipated to reach $48.9 billion by 2025, with the largest revenue in the United States (Adroit Market Research 2018). E-cigs have become a popular alternative to tobacco cigarettes, but the efficacy of e-cigs as smoking cessation aids remains inconclusive (Malas et al. 2016; Hartmann-Boyce et al. 2018). Recent studies (Polosa and Caponnetto 2016; Chun et al. 2017) have reported the potential toxicity of e-cig aerosols even though they typically contain lower levels of toxic chemicals than tobacco smoke (Li et al. 2020c).

Similar to tobacco smoke, high levels of particle number concentration (PNC) and fine particulate matter ($PM_{2.5}$) have been observed in e-cig emissions (Ingebrethsen et al. 2012; Fuoco et al. 2014; Zhao et al. 2016b; Nguyen et al. 2019; Zhao et al. 2017; Williams et al. 2013). Unlike tobacco cigarettes, which produce smoke by combustion of tobacco leaves, e-cigs generate aerosols via vaporization of the e-liquid, which is made of propylene glycol (PG), vegetable glycerin (VG), nicotine, water, and flavoring compounds (Geiss et al. 2015; Etter et al. 2013; Kim and Shin 2013). Previous studies have investigated the relationship between the e-liquid composition (i.e., PG/VG ratio and nicotine) and e-cig particle emissions. A few studies have found that the total mass of PM in e-cig aerosols is elevated with the increasing volume ratios of PG/VG with nicotine in the e-liquid (Baassiri et al. 2017; El-Hellani et al. 2018; Talih et al. 2017). In addition to PG/VG ratio, several studies have found that adding nicotine to e-liquids produces

more particles (Fuoco et al. 2014; Manigrasso et al. 2015; Scungio et al. 2018). Conversely, Schober et al. (2014a) reported that higher PNC and $PM_{2.5}$ were observed for nicotine-free e-liquids. Moreover, Zervas et al. (2018) did not detect a significant difference in PNC with and without nicotine in the e-liquid. These inconsistent results in the literature call for a systematic study on the effects of e-liquid main compositions on e-cig aerosols.

E-cig aerosols are highly dynamic since they contain a significant amount of volatile or semi-volatile materials (Vo and Morris 2014; Ingebrethsen et al. 2012). In indoor environments, e-cig particle concentrations decay rapidly over a short distance (>1.5 m) from the source and largely disappear within a few seconds (Zhao et al. 2017; Martuzevicius et al. 2018). This is likely attributable to both indoor air exchange rate (AER) and particle dynamics which include particle evaporation, surface deposition, coagulation, and gravitational settling (Meng et al. 2017; Nguyen et al. 2019; Ingebrethsen et al. 2012; Floyd et al. 2018; Goniewicz and Lee 2015; Mikheev et al. 2016; Zhao et al. 2016b). These particle dynamic processes not only change e-cig aerosol concentrations but also affect the particle size distribution which determines the extent and location of particle deposition in the respiratory tract (Hinds 1999), and thus need to be better understood.

E-cig particles are primarily in the submicron size range (Fuoco et al. 2014; Ingebrethsen et al. 2012), exhibiting considerable differences in terms of size distribution ranging from a single mode to a tri-modal distribution reported by different studies (see **Table A-2** in the Appendix). Previous studies have also reported that the e-cig particle size distributions varied depending on e-cig puffing parameters (i.e., puffing flow rate, particle residence time, and the amounts of puffs) and environmental factors (i.e., temperature, relative humidity, and dilution factor) (Zhang et al. 2013; Schripp et al. 2013; Fuoco et al. 2014; Manigrasso et al. 2015; Zhao et al. 2016b; Zhao et al. 2017; Mikheev et al. 2016; Mikheev et al. 2018; Zervas et al. 2018; Scungio et al. 2018; Nguyen

et al. 2019; Meng et al. 2017; Floyd et al. 2018; Feng et al. 2015; Wright et al. 2016; Sosnowski and Odziomek 2018; McAuley et al. 2012). However, limited studies have focused on the effects of e-liquid compositions on e-cig particle size distribution, which is important for assessing exposure and related health effects. To fill these knowledge gaps, this study aims to investigate how PG/VG ratio and nicotine in the e-liquid affect the emissions and dynamics of e-cig aerosols under well-controlled experimental conditions.

3.3. Materials and methods

3.3.1. Experimental setup

A 0.46 m^3 stainless steel test chamber equipped with sampling instruments was used in this study (**Figure 3.1**). A well-mixed condition was achieved with two mixing fans inside the chamber. With the total air flow rate of sampling instruments at 0.47 m^3/h, the AER was maintained at a constant level of 1.0 h^{-1}. This AER was verified with measurements of CO_2 concentration decay inside the chamber. The interior of the chamber was made of stainless steel to achieve a minimal loss of the emitted aerosols due to surface adsorption. This chamber has been well characterized through our previous studies (Fung et al. 2014; Liu et al. 2014; Shi et al. 2016). The test chamber was supplied with aerosols generated by the e-cig device. The chamber exhaust connected with a high efficiency particulate air (HEPA) filter was led into the laboratory exhaust system. During the experimental period, temperature and relative humidity inside the chamber were maintained at 24.0 ± 0.5 °C and 35% ± 15%, respectively.

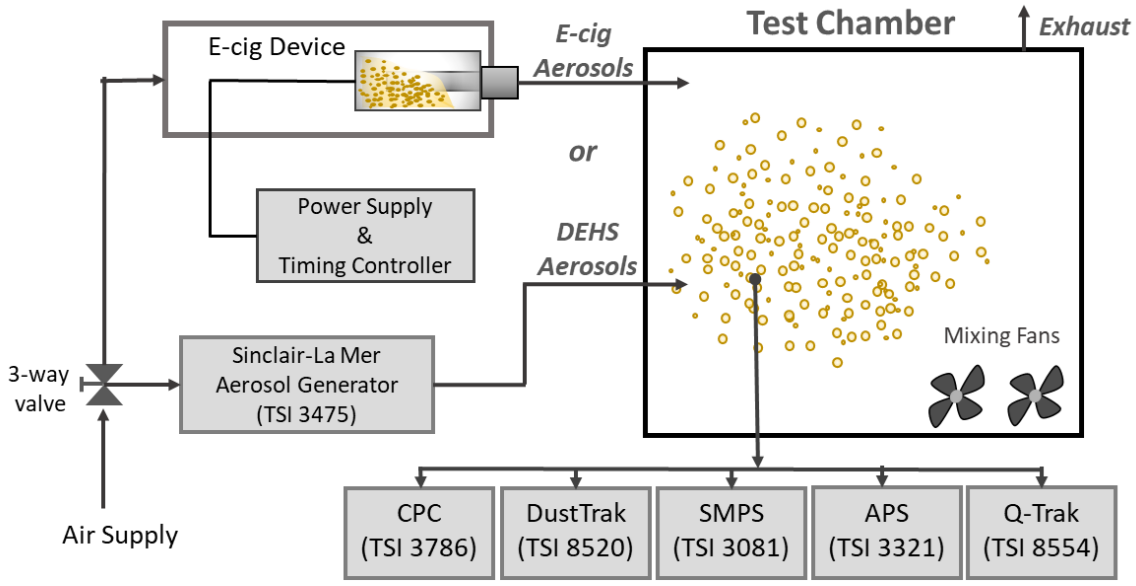


Figure 3.1. A schematic diagram of the aerosol generation and sampling system.

3.3.2. Aerosol generation

E-cig aerosols were generated by using an e-cig device, Vapor-fi model Volt Hybrid Tank, which was equipped with a refillable tank, high capacity batteries, and adjustable power settings. This type of e-cig device was selected because it is popular among experienced e-cig users (Yingst et al. 2015; Baweja et al. 2016). The e-cig device with a heating coil of 0.5 Ω thermal resistance was powered at 18.75 W, which is within the manufacturer's recommended range. However, in the real world, depending on e-liquid flavors and e-cig devices, the wattages used by e-cig users vary greatly and their effects on e-cig aerosols warrant future study. To better control the e-liquid composition, homemade e-liquids were used to avoid unknown compounds in the commercial e-liquids (Flora et al. 2016). The e-liquids were prepared from individual chemical compounds of PG ($C_3H_8O_2$, ≥ 99.5%), VG ($C_3H_8O_3$, ≥ 99.5%), and nicotine ($C_{10}H_{14}N_2$, ≥ 99%) (see Appendix **Table A-3** for chemical properties). In total, 10 e-liquids were tested at five different PG/VG

volume ratios (i.e., 0/100, 10/90, 30/70, 50/50, and 100/0) with either 0.0% or 2.4% nicotine by weight.

A homemade puffing machine composed of a compressed air source and an Arduino Uno R3 microcontroller board (Arduino, Italy), which served as a programmable timer, was used to power the e-cig device. The inlet air was filtered by a HEPA filter and was continuously pushed through the e-cig tank at an airflow rate of 1 L/min. For each e-liquid mixture, the e-cig device was puffed for 0.5 h to achieve a steady-state condition followed by a 2-h decay. During the puffing session, the e-cig device was controlled to repeat a continuous puffing cycle (i.e., 4 s/puff, every 30 s) to mimic a typical puff topography of e-cig users (Farsalinos et al. 2013; Behar et al. 2015; Hua et al. 2013; Robinson et al. 2015). For a given puff duration and puff flow rate, the corresponding dilution ratio was derived by dividing the chamber volume by the puff volume (i.e., puff duration × puff flow rate). The dilution ratio for the chamber was 6900:1.

Di-ethyl-hexyl sebacate (DEHS) with an extremely low saturation vapor pressure (1.2×10^{-6} Pa) was used as the nonvolatile baseline to compare with the e-cig aerosols. DEHS aerosols were produced by the Sinclair–La Mer aerosol generator (model 3475, TSI, Inc., Shoreview, MN). The generator was adjusted to produce DEHS aerosol resembling e-cig aerosols in terms of particle concentration and size distribution. The DEHS aerosol was also monitored for the 2-h decay period inside the same chamber (**Figure 3.2**).

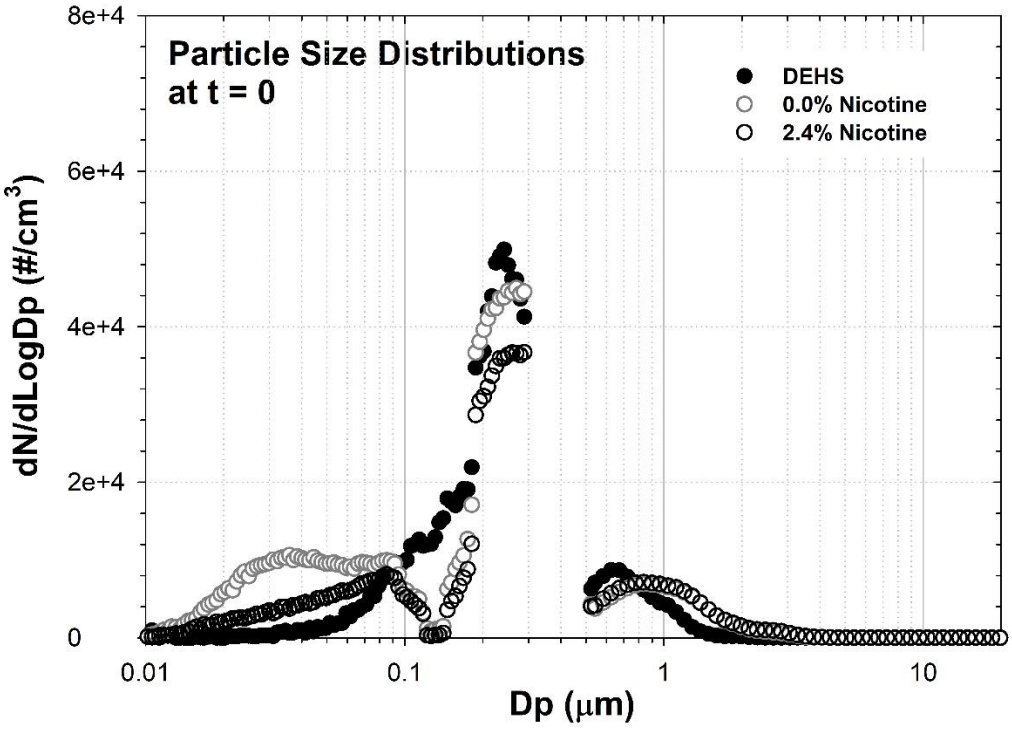


Figure 3.2. Overall particle size distributions (dN/dLogDp) of DEHS and e-cig aerosols at the start of the decay cycle (t = 0). The plotted data are the means of all measurements conducted with each type of e-liquid mixture evaluated in this study. The plotted data also compare the initial particle size distribution of e-cig aerosols with and without nicotine.

3.3.3. Measurements

For each experimental session, during the 0.5-h puffing and the 2-h decay, PNC and $PM_{2.5}$ were continuously measured inside the chamber using a set of real-time instruments. A condensation particle counter (CPC 3786, TSI Inc.) was used to monitor PNC. $PM_{2.5}$ mass concentrations were measured with DustTrak Aerosol Monitors (DustTrak 8520, TSI Inc.). An indoor air quality monitor (Q-Trak 8554 TSI Inc.) was also used to collect temperature and relative humidity data inside the chamber. All instruments were calibrated prior to the study, and the DustTrak was zero

calibrated before each experiment. The data logging interval was set to 2 min for the CPC, DustTrak, and Q-Trak. These real-time instruments provided high time-resolution measurements for PNC and $PM_{2.5}$. A scanning mobility particle sizer (SMPS 3080, TSI Inc.; 100 s up scan, 20 s down scan) and an Aerodynamic Particle Sizer (APS 3321, TSI Inc.) were used to measure particle size distribution. The particle size range measured by SMPS and APS were 7-289 nm and 0.5-19.8 μm, respectively. The real-time measurements were repeated six times for the DEHS aerosol as well as e-cig aerosols generated from each of the ten e-liquid mixtures.

To ensure data quality, before each experiment, PNC and $PM_{2.5}$ in the chamber were maintained at a background level of less than 1000 particles/cm^3 and 2 μg/m^3, respectively. A notable upward $PM_{2.5}$ bias of DustTrak when sampling ambient air has been observed in previous studies (Zhang and Zhu 2010; Jenkins et al. 2004). From our previous e-cig study, a calibration factor of 0.27 was obtained through gravimetric calibration of DustTrak $PM_{2.5}$ measurements in chamber-puffed e-cig aerosols. This calibration factor was applied to correct all $PM_{2.5}$ data in this study (Zhao et al. 2017; Nguyen et al. 2019).

3.3.4. Data analysis

Assuming a well-mixed chamber, Equation (1) can be used to calculate particle concentrations by considering factors such as particle levels inside and outside of the chamber, AER, and particle loss rate (Dockery and Spengler 1981; He et al. 2004):

$$\frac{dC_{in}}{dt} = P\alpha C_{out} + \frac{S}{V} - (\alpha + k)C_{in} \quad (1)$$

where C_{in} and C_{out} are the particle concentrations inside and outside the chamber, respectively, P is the penetration efficiency, α is the AER, k is the particle loss rate due to evaporation, surface

deposition, coagulation, and gravitational settling, S is the particle emission rate in number or mass per hour, t is the time, and V is the volume of the chamber.

After 60 puffs were generated over 0.5 h, the particle concentration approached an equilibrium value under a steady-state condition with $dC_{in}/dt = 0$. This equilibrium value was defined as the initial concentration $C_{t=0}$ representing the beginning of the decay. Since the room air outside of the chamber was filtered by HEPA filters, $C_{out} = 0$. Thus, the e-cig emission rate (S) in this study is a function of the initial concentration before decay started ($C_{t=0}$), chamber volume (V), and total removal rate $(\alpha + k)$, and was calculated using Equation (2):

$$S = C_{t=0} \times V(\alpha + k) \tag{2}$$

A total of 60 puffs were generated during the 0.5 h emission period, and the puff number normalized emission factor (S_p) in number or mass per puff was calculated using Equation (3):

$$S_p = [C_{t=0} \times V(\alpha + k) \times 0.5]/60 \tag{3}$$

Previous studies have used a regression of the first-order decay to determine the particle loss rates (Schripp et al. 2008; Gong et al. 2009). The first-order log-linear regression is described as follows:

$$\ln\left(C_t / C_{t=0}\right) = -(\alpha + k) \times t \tag{4}$$

where t is the elapsed time, C_t and $C_{t=0}$ are particle concentrations in the chamber measured at times t and t=0, respectively, during the decay. The particle loss rate (k), was calculated by fitting a line to the plot of the log of $C_t/C_{t=0}$ versus times and subtracting the AER (α) from the total removal rate $(\alpha + k)$. This method was employed in this study. For both e-cig and DEHS aerosols,

we estimated the particle loss rate [h^{-1}] based on PNC and $PM_{2.5}$ collected during the decay periods mentioned above.

As an example, **Figure 3.3a** presents normalized concentration ($C_t/C_{t=0}$) decay data collected with an e-liquid mixture made of 30% PG, 70% VG, and 0.0% nicotine. The total removal rates ($\alpha + k$) were determined by fitting a log-linear regression to normalized concentration data shown in **Figure 3.3b**. For each e-liquid mixture, the total removal rate ($\alpha + k$) was determined from six repeated measurements. For each e-liquid mixture evaluated in this study, the six repeated measurements had high coefficients of determination (R^2) greater than 0.93 for PNC and greater than 0.90 for $PM_{2.5}$, respectively. Similarly, DEHS data also had high R^2 values of 0.98 and 0.99 for PNC and $PM_{2.5}$, respectively. **Table A-4** in the Appendix summarizes the details of the log-linear regression results.

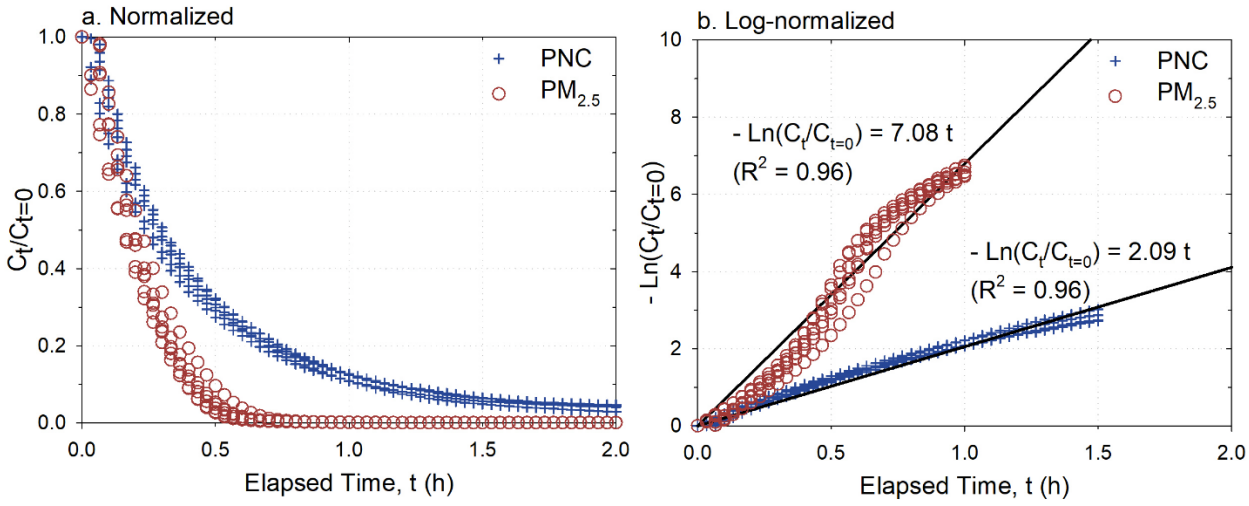


Figure 3.3. Decay curves for PNC and $PM_{2.5}$ shown in (a) $C_t/C_{t=0}$, and (b) ln ($C_t/C_{t=0}$). The plotted data were collected with the e-liquid mixture having a PG/VG ratio of 30/70 without nicotine.

Both simple and multiple linear regression analyses were used to study the effect of PG/VG ratio and nicotine level on the e-cig emission factor, t_{50}, and particle loss rate in terms of PNC and $PM_{2.5}$. The comparison between the e-liquids with and without nicotine for each PG/VG ratio was performed by using Student's t-test. All statistical analyses were conducted using SAS version 9.4. All figures were generated with Sigmaplot 12.5 (Systat Software Inc., San Jose, CA). While there is a size range gap between SMPS and APS output (289 nm- 540 nm), the plotting software automatically fits the data gap by linear interpolation. The level of statistical significance was set as $p < 0.05$.

3.4. Results and discussion

3.4.1. Particle emission

For all tested e-liquid mixtures, the e-cig was a strong source of particles with the mean (standard deviation) number and mass emission factors of 2.5×10^7 (7×10^6) particles/puff and 113 (42) µg/puff, respectively (**Table 3.1**). The multiple linear regression results indicated that the addition of 2.4% nicotine in the e-liquid significantly decreased the particle emission factor from $3.0\times10^7(6.6\times10^6)$ particles/puff to $2.0\times10^7(2.0\times10^6)$ particles/puff ($p < 0.001$). The decreases in particle emission from nicotine-containing e-liquid were also reported by Zervas et al. (2018) and Schober et al. (2014a). However, no significant difference in $PM_{2.5}$ emission was detected with and without nicotine in the e-liquid mixture.

Interestingly, we found that the PG/VG ratio was negatively associated with the $PM_{2.5}$ emission factor ($p < 0.001$). However, two previous studies reported the opposite results in that the total mass of e-cig-emitted particles increased with greater PG/VG ratios using filter-based methods (El-Hellani et al. 2018; Baassiri et al. 2017). This discrepancy may be attributable to the different dilution conditions between the current study with a dilution factor of 6900 and the

previous two studies with a minimal dilution factor of 1.75 (El-Hellani et al. 2018; Baassiri et al. 2017). PG aerosols with higher saturation vapor pressure (i.e., 20 pa) are more volatile than VG (i.e., 0.01 pa). Thus, the higher dilution in the current study is likely resulting in more evaporation with high levels of PG in the e-liquid compared to the low-dilution conditions.

Table 3.1. The mean (standard deviation) of emission factor (S_p), initial concentrations ($C_{t=0}$), and the time (t_{50}) taken to achieve 50% of $C_{t=0}$ for each e-liquid mixture and DEHS aerosols evaluated in the study.

Aerosol Type	PG/VG	PNC			$PM_{2.5}$		
		S_p (#/puff)	$C_{t=0}$ (#/cm^3)	t_{50} (min)	S_p (µg/puff)	$C_{t=0}$ (µg/m^3)	t_{50} (min)
E-cig with 0.0% Nicotine	0/100	4.04×10^7 (5.96×10^6)	56346 (6503)	23.9	186 (9)	3570 (410)	11.6
	10/90	2.70×10^7 (1.04×10^7)	32159 (8775)	18.6	102 (22)	1920 (420)	10
	30/70	2.62×10^7 (4.30×10^6)	32693 (4666)	16.6	116 (7)	2180 (440)	11.1
	50/50	2.39×10^7 (2.69×10^6)	29527 (3277)	16.5	95 (10)	1900 (270)	11.2
	100/0	3.25×10^7 (5.65×10^6)	39314 (8253)	14.8	85 (58)	1630 (1460)	6.2
E-cig with 2.4% Nicotine	0/100	1.92×10^7 (4.99×10^6)	26343 (5356)	21.9	83 (15)	1670 (320)	11
	10/90	2.19×10^7 (3.17×10^6)	31692 (1504)	21.1	147 (4)	2740 (220)	9.2
	30/70	1.81×10^7 (2.10×10^6)	27626 (2493)	19.4	172 (7)	3250 (190)	10
	50/50	2.22×10^7 (8.72×10^6)	30378 (9858)	20.8	88 (23)	1950 (580)	11.6
	100/0	1.80×10^7 (1.69×10^6)	28615 (2995)	21.6	57 (9)	1380 (240)	11.7
DEHS	NA	NA	21864 (6717)	23.7	NA	1630 (610)	20.3

3.4.2. Decay of PNC and $PM_{2.5}$

Using the initial concentration ($C_{t=0}$) shown in Table 1, we normalized PNC and $PM_{2.5}$ ($C_t/C_{t=0}$), averaged over the six repeated measurements, and plotted the data as a function of time for each e-liquid mixture during the 2-h decay (**Figure 3.4**). For both PNC and $PM_{2.5}$, the decay was faster for e-cig aerosols than for the DEHS aerosols inside the chamber. More noticeable differences between DEHS and e-cig aerosols were observed for $PM_{2.5}$ compared with PNC. For nicotine-free

e-liquid, a faster decay of e-cig particle concentration was observed at an increasing PG/VG ratio (**Figures 3.4a and c**). For both PNC and $PM_{2.5}$, the fastest decay was observed when the PG/VG ratio was 100/0. Interestingly, once nicotine was added to the e-liquids, the decay curves became closer to each other without a clear difference (**Figures 3.4b and d**).

During the 2-h decay, the $t_{50,}$ which is the time needed to achieve 50% of the initial PNC and $PM_{2.5}$ for each e-liquid mixture, is also presented in Table 1. For e-cig aerosols, the t_{50} was within a range of 15-24 min for PNC and 6-12 min for $PM_{2.5}$. In comparison, for DEHS aerosols, the t_{50} was 24 and 20 min for PNC and $PM_{2.5}$, respectively. There is a significant difference in t_{50} between e-liquids with and without nicotine for PNC ($p < 0.001$), where the difference increased noticeably when PG/VG ratios increased. For $PM_{2.5}$, however, we observed a significant difference only when the PG/VG ratio reached 100/0 ($p < 0.01$). For the nicotine-free e-liquid, t_{50} was found to decrease with increasing PG/VG ratios ($p = 0.005$ for PNC; $p = 0.002$ for $PM_{2.5}$). In contrast, the t_{50} for e-liquid with nicotine showed a slightly rising pattern with increasing PG ($p = 0.003$ for PNC; $p < 0.05$ for $PM_{2.5}$).

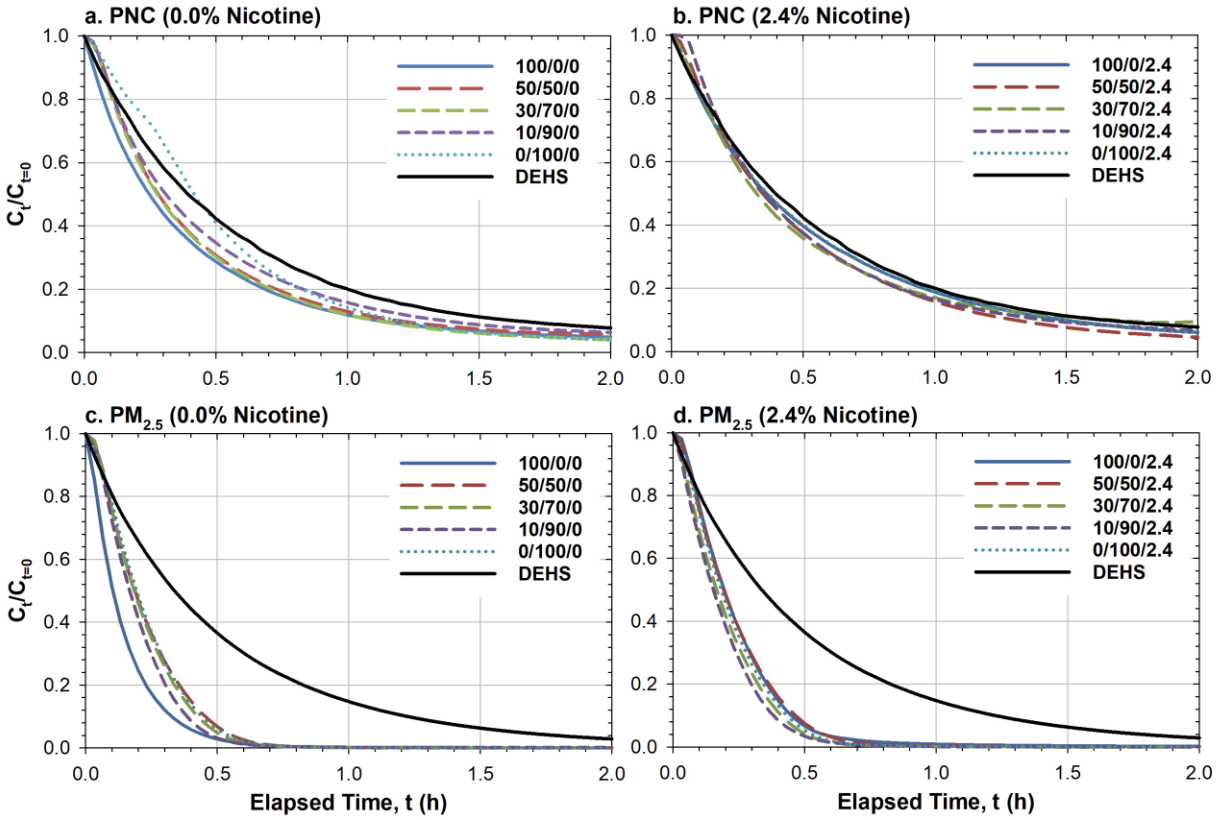


Figure 3.4. Averaged normalized concentration ($C_t/C_{t=0}$) decay curves for PNC (a and b) and $PM_{2.5}$ (c and d). The plotted data provide the means of six repeated measurements without nicotine (0.0%; a and c) and with nicotine (2.4%; b and d) in comparison to DEHS aerosols.

3.4.3. Particle loss rate

To further illustrate the effect of nicotine and PG/VG ratios on the dynamic of e-cig aerosols, we determined the particle loss rate under each experimental condition and compared those to the DEHS aerosol (**Figure 3.5**). Since the evaporation of DEHS aerosols is negligible relative to that of e-cig aerosols, we used the particle loss rate of DEHS aerosols as a nonvolatile baseline. The error bars are one standard deviation, σ, of the six repeated measurements, which show larger variability in the estimated particle loss rates for $PM_{2.5}$ (i.e., σ = 0.26-1.76) compared to PNC (i.e., σ = 0.04-0.24).

Overall, the particle loss rates measured by $PM_{2.5}$ (i.e., 4.4-7.0 h^{-1}) were substantially greater than those measured by PNC (i.e., 0.6-1.2 h^{-1}). This is likely because particle mass decreased rapidly by evaporation, but the change of particle number was less prominent. The multiple linear regression results showed a significant interaction effect of the nicotine level and PG/VG ratio on the particle loss rate ($p < 0.001$ for both PNC and $PM_{2.5}$). For nicotine-free e-liquid, the particle loss rates significantly increased with increasing PG/VG ratios ($p = 0.001$ for PNC; $p < 0.05$ for $PM_{2.5}$; **Figures 3.5a and b**). Once nicotine was added to the e-liquid, significant decreases in the particle loss rate were observed as the PG/VG ratio increased ($p = 0.004$ for PNC; $p < 0.001$ for $PM_{2.5}$).

According to Raoult's law, the evaporation rate of each component in the e-liquid is subject to the product of its saturation vapor pressure and its mole fraction. The PG/VG ratio that determines the saturation vapor pressure of the e-liquid mixtures likely governs the volatility of e-cig aerosols. For example, the PG-based mixture makes e-cig aerosols more volatile (i.e., P_{sat} = ~ 20 Pa), whereas the VG-based mixture makes them much less volatile (i.e., P_{sat} = 0.01 Pa). However, this principle can be only applied to nicotine-free e-liquids. The addition of nicotine, whose vapor pressure falls between that of PG and VG, will also affect the overall e-liquid saturation vapor pressure. The fundamental principle determining the saturation vapor pressure of the e-liquid mixture, however, is complicated and is beyond the scope of the current work. Future research is warranted to systematically evaluate to what extent the interactions between PG, VG, and nicotine could affect the change of e-cig particle production and loss.

The change from positive to negative association between PG/VG ratio and particle loss rate is mainly driven by the significant differences in the particle loss rates between e-liquids with and without nicotine when the percentage of PG is greater than 30% for PNC and 50% for $PM_{2.5}$,

respectively (**Figure 3.5**). The significant effect of nicotine on the particle loss rates suggests that the presence of nicotine might contribute to reducing the volatility of e-cig aerosols when the PG/VG ratio is high enough. The change of volatility in mainstream e-cig aerosols could potentially affect the particle concentration and deposition pattern after particles are inhaled. In an indoor environment, the concentration and transport of secondhand e-cig aerosols might also be affected by nicotine in the e-liquid.

PG and VG could undergo thermal degradation when in contact with the heating coil of the e-cig atomizer to form a significant amount of volatile carbonyl compounds, such as formaldehyde, acetaldehyde, acrolein and acetone (Ogunwale et al. 2017; Sleiman et al. 2016; Kosmider et al. 2018; Geiss et al. 2016). PG is more susceptible to thermal decomposition than VG, leading to more volatile carbonyls generated from PG-based e-liquids (Kosmider et al. 2014). With greater nicotine content in the e-liquid, however, lower levels of these carbonyls are generated potentially reducing the volatility of e-cig aerosols (Kosmider et al. 2018). On the other hand, under certain temperature and oxidative conditions and in the presence of metals, these carbonyls might further degrade to acidic products that can protonate the nitrogen on the pyrrolidine ring in nicotine when the e-liquid is aerosolized (Liang and Pankow 1996; Rossiter et al. 1985). Compared to VG-based e-liquids, PG-based e-liquids with lower pH could facilitate the formation of the protonated nicotine with lower volatility than the free-base nicotine in the e-cig aerosol (El-Hellani et al. 2015; Son et al. 2018). Consequently, depending on the chemistry and rate at which these possible acidic degradation compounds can form in the aerosol, nicotine may interact more strongly with these acidic products causing the particle volatility to decrease (Jensen et al. 2017).

During the vaporization process, ß-nicotyrine can be formed as a result of catalytic dehydrogenation of nicotine at 300-500 ºC. Thus, another plausible reason that nicotine contributes to reducing particle loss rate is the increased interactions between the aromatic electrons in ß-nicotyrine and polar PG and VG (Abramovitz et al. 2015). The nicotyrine to nicotine ratio (NNR) in e-cig aerosols was higher for PG-based e-liquids than e-liquids containing both PG and VG, suggesting that as the PG/VG ratio increases, the NNR may also increase (Abramovitz et al. 2015). Furthermore, nicotyrine is one order of magnitude less volatile than nicotine, rendering it more likely than nicotine to remain in the particle phase (Abramovitz et al. 2015). Therefore, with nicotine in the e-liquid, nicotyrine's increased affinity for the particle phase in PG-based aerosols may cause the particles to be less volatile compared to VG-based aerosols.

With the same amount of nicotine in the e-liquid, more nicotine was found in the e-cig aerosol with increasing PG/VG ratios (Baassiri et al. 2017; El-Hellani et al. 2018; Talih et al. 2017), suggesting even larger impacts of nicotine on the dynamics of e-cig aerosols with elevated PG content. In addition, the newly introduced pod-based e-cigs with extremely high nicotine concentrations of 5.0% or greater might deliver more particles and warrants future studies (Huang et al. 2019; Goniewicz et al. 2018).

This study used the regression of first-order decay rate of particle concentration to determine particle loss rate. Since coagulation may play a role in decreasing particle number concentrations, we used SMPS data to estimate the t_{50} (time required to achieve 50% $C_{t=0}$) solely due to coagulation. We found the t_{50} due to coagulation was approximately 5-6 hours, which was 14-17 times longer than the overall t_{50} (i.e., ~ 20 min) for all the e-liquid mixtures summarized in **Table 3.1**. Therefore, coagulation during the decay period was negligible compared to other particle loss mechanisms in this study (see details in Appendix B). One limitation of this study

was that the mass of e-liquid consumed per puff was not measured and should be addressed in future studies to account for other potential mass loss.

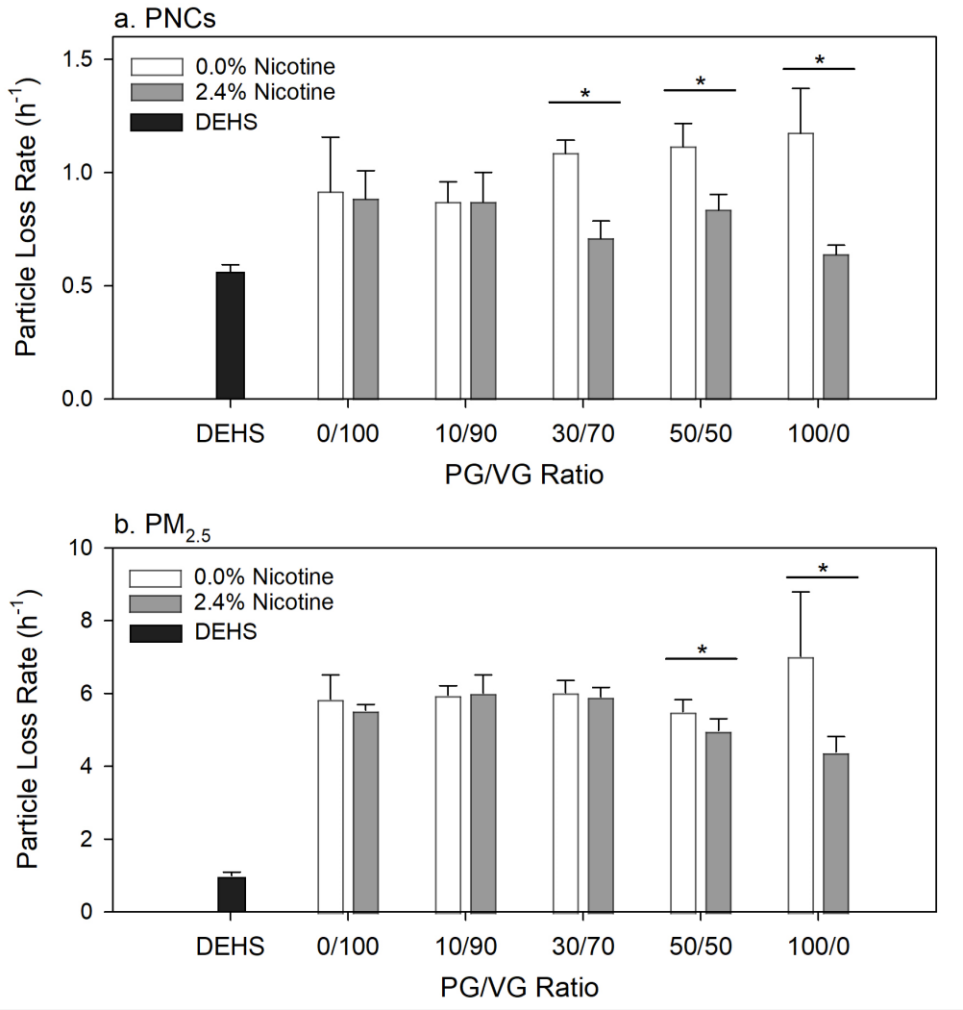


Figure 3.5. Particle loss rates as measured by (a) PNC and (b) $PM_{2.5}$ at different PG/VG ratios with 0.0% and 2.4% nicotine compared with DEHS. Statistically significant differences are noted with * ($p < 0.001$, Student's t-test).

3.4.4. Particle size distribution

Time-resolved particle size distributions measured for the three e-liquid mixtures (i.e., PG/VG= 0/100, 50/50, and 100/0) with and without nicotine are shown as contour plots in **Figure 3.6**. These three PG/VG ratios were chosen because PG-based and VG-based e-liquids represent the two extreme conditions, and significant differences in particle loss rate between with and without nicotine were observed for both PNC and $PM_{2.5}$ at the PG/VG of 50/50 (see **Figure 3.5**).

In **Figure 3.6**, the x-axis presents the elapsed time at which data were collected, the y-axis is the particle size in log scale, and the color intensity indicates normalized PNC (dN/dLogDp) for a given size at a given time. The same normalized concentration scale was used for all plots. Overall, most e-cig particles were within the submicron size range, which was in good agreement with previous studies (Ingebrethsen et al. 2012; Fuoco et al. 2014). Before decay started, we observed similar tri-modal particle size distributions across all e-liquid mixtures with a primary mode at 250 nm and two secondary modes at approximately 30-80 nm and 1 μm. During the 2-h decay, the mode diameter at approximately 1 μm decreased, while the mode of nanoparticles (< 100 nm) increased. This finding is consistent with Mikheev et al.'s results (2016) which have shown that under a high dilution condition, evaporation reduces the diameter of larger e-cig particles and increases the number of nanoparticles. As a result, the e-cig aerosol shifted from a tri-modal size distribution to a bi-modal distribution and even a single-mode after aging.

For nicotine-free e-liquid, a clear pattern was observed showing that the e-cig particle concentration decayed faster with an increasing PG/VG ratio (**Figures 3.6a, b, and c**). In contrast, the decay of e-cig particle concentration with nicotine showed an opposite trend (**Figures 3.6d, e, and f).** Under the extreme condition of PG-based mixtures (PG/VG ratio=100/0; **Figures 3.6c and f**), the addition of nicotine in the e-liquid slowed down the decay. Based on these observations, the

interference of nicotine in e-liquid plays an important role in the physical properties of e-cig aerosols and warrants further study.

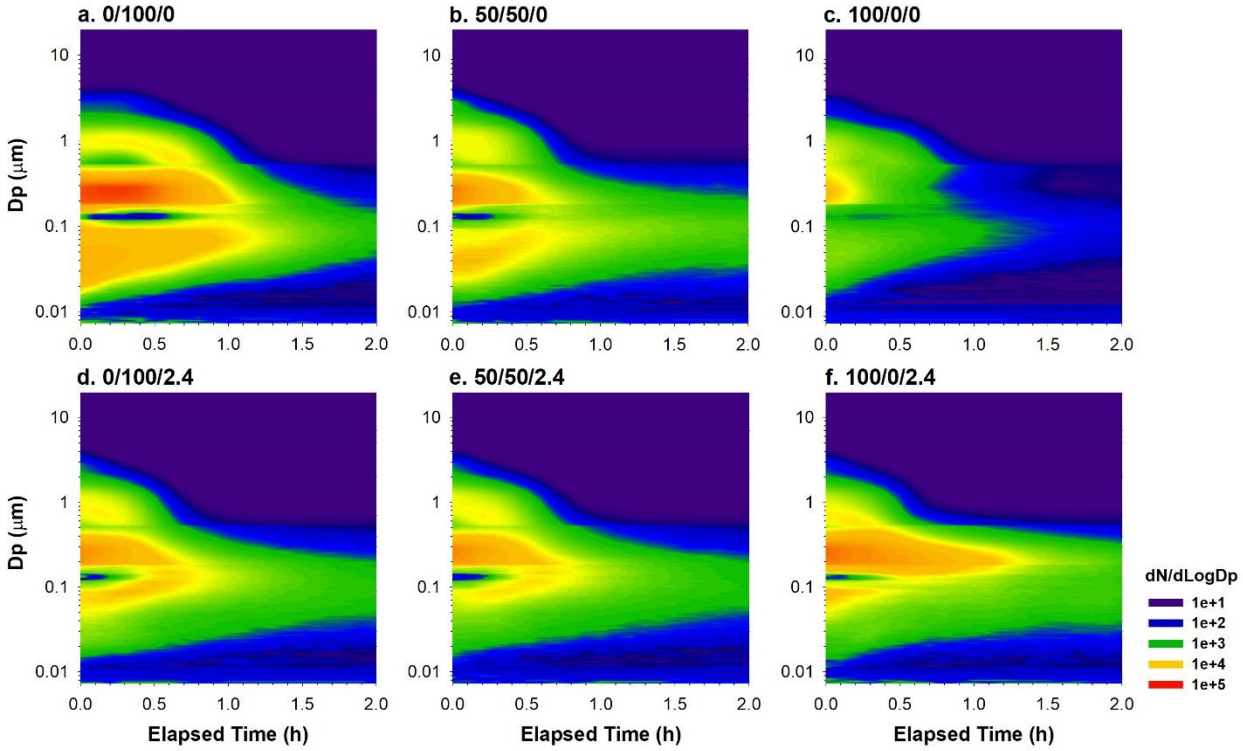


Figure 3.6. Averaged particle size distributions (dN/dLogDp) for e-liquid mixtures (i.e., PG/VG =0/100, 50/50, and 100/0) without nicotine (0.0%; a, b, and c) and with nicotine (2.4%; d, e, and f). The vertical axes represent particle size on a logarithmic scale, the horizontal axes represent elapsed time in hours from the start of sampling, and the color scale represents particle number concentration at a certain time and diameter. Linear interpolation is used to fill the data gap between the SMPS and APS output (289 nm- 540 nm).

3.5. Conclusions

This study characterized e-cig mainstream aerosols generated using e-liquids of different PG/VG ratios with and without nicotine in terms of particle emission, particle loss rate, and particle size distribution. For the 10 tested e-liquid mixtures, the mean emission factors of PNC and $PM_{2.5}$ were

2.5×10^7 (7×10^6) particles/puff and 113 (42) µg/puff, respectively. The addition of nicotine in the e-liquid significantly decreased the particle number emission factor by 33%. The $PM_{2.5}$ emission factor was negatively associated with PG content in the e-liquid. The multiple linear regression analysis showed a significant interaction effect of the nicotine level and PG/VG ratio on the particle loss rate. For nicotine-free e-liquid, a greater PG content increased the particle loss rate. On the other hand, with nicotine in the e-liquid, the greater PG content decreased the particle loss rates. For both PNC and $PM_{2.5}$, significant differences in particle loss rates were observed between e-liquids with and without nicotine when the PG/VG ratios were greater than 30/70. Overall, the particle loss rate measured by $PM_{2.5}$ was about 5-6 times greater than that measured by PNC. In addition, we observed a tri-modal particle size distribution with the primary mode around 250 nm and two secondary modes at 30-80 nm and ~1 µm across all tested e-liquid mixtures. As they aged in the test chamber, e-cig aerosols shifted to a bimodal and then a single-mode distribution. Understanding the dynamics of e-cig aerosols is important for modeling respiratory deposition and for estimating exposures in an indoor environment.

4. IMPACTS OF ELECTRONIC CIGARETTES USAGE ON AIR QUALITY OF VAPE SHOPS AND THEIR NEARBY AREAS

Published in Science of The Total Environment (2021, Volume 760, pp. 143423)

DOI: 10.1016/j.scitotenv.2020.143423

4.1. Abstract

With the rapid growth of the electronic cigarette (e-cig) market, there is an increasing number of vape shops that exclusively sell e-cigs. The use of e-cigs in the vape shop is a primary source of indoor particles, which might transport to its nearby indoor spaces in the multiunit setting. In this study, six pairs of vape shops and neighboring businesses in Southern California were recruited for real-time measurements of particulate pollutants between February 2017 and October 2019. The mean (SD) particle number concentration (PNC) and $PM_{2.5}$ concentration in the studied vape shops were 2.8×10^4 (2.3×10^4) particles/cm^3 and 276 (546) μg/m^3, which were substantially higher than those in neighboring businesses and outdoor areas. In addition, 24-h time-weighted average (TWA) nicotine sampling was conducted in the six pairs and three additional pairs. Nicotine was detected in the air of all the studied vape shops and neighboring businesses, in which the mean (SD) concentration was 2.59 (1.02) and 0.17 (0.13) μg/m^3, respectively. Inside vape shops, the dilution-corrected vaping density (puffs/h/100 m^3) is a strong predictor of the particle concentration, and nicotine concentration highly depends on the air exchange rate (AER). Out of the six studied pairs, PNCs in five vape shops and $PM_{2.5}$ in two vape shops were significantly correlated with those in their neighboring businesses. This correlation was stronger when the door of the vape shop was closed. When the door was open, environmental electronic vaping (EEV) aerosols, especially smaller particles, could transport from the vape shop to the outdoor environment. Overall, e-cig usage in the vape shop impacts both its own and nearby air

quality, raising concerns regarding the risk of exposure to EEV aerosols in the surrounding environments.

4.2. Introduction

An electronic cigarette (e-cig), belonging to the group of electronic alternatives to tobacco cigarettes (EATCs) (Protano et al. 2020), is a battery-powered nicotine delivery system that generates aerosols by vaporizing e-liquids. Widely serving as an alternative to smoking tobacco cigarettes, the use of e-cigs (also known as vaping) has grown exponentially worldwide (Yoong et al. 2018; Hammond et al. 2020). In addition, there has been a high demand for flavored e-cig products among never-smoking adolescents and young adults since e-cigs were introduced (Vallone et al. 2020; Glantz and Bareham 2018; McMillen et al. 2019). With the rapid growth of the e-cig markets, various e-cig devices, ranging from the disposable cigalike to a more advanced tank style and the emerging pod-based JUUL with thousands of appealing flavors, have been introduced to the public (Glantz and Bareham 2018; Huang et al. 2019; McKelvey et al. 2018; Galstyan et al. 2019). As a result, a new type of retailer, the vape shop, where customers can exclusively purchase e-cig products and sample e-liquids with a combination of flavors and varying levels of nicotine, has emerged (Lee et al. 2018b; Galstyan et al. 2019). In the United States, the growing vape shop industry accounts for 20% of the e-cig retail markets in 2019 and has proliferated globally over the past few years (Truth Initiative 2019; Sussman et al. 2016; Galstyan et al. 2019). While many states have established smoking bans in workplaces and public spaces, the use of e-cigs is unrestricted in vape shops. Exposure to the visible massive “clouds” produced in vape shops brings an environmental and public health concern (Nguyen et al. 2019).

At the end of 2019, many cases and deaths of e-cigarette or vaping product use-associated lung injury (EVALI) have been reported in the United States (Layden et al. 2019a; Carlos et al. 2019), suggesting the potential serious health risks of vaping. Using e-cigs may not only pose health harms to active users but also bystanders who are involuntarily exposed to environmental electronic vaping (EEV) aerosols (Protano et al. 2018). Although the information on the health effects of exposure to EEV aerosols is limited, a review article summarizing more than 20 studies on secondhand exposure has shown that vaping degrades indoor air quality by generating high levels of particles that are comparable to other tobacco products (Li et al. 2020b). Many studies have reported that the average fine particulate matter ($PM_{2.5}$) during active vaping in the indoor environments are mostly greater than 150 $\mu g/m^3$ and can even reach 1.5×10^3 $\mu g/m^3$ (Nguyen et al. 2019; Melstrom et al. 2017; Soule et al. 2017; Volesky et al. 2018; Zhao et al. 2017; Schober et al. 2014a; Czogala et al. 2014; Son et al. 2020; Protano et al. 2020; Protano et al. 2018). The average indoor particle number concentrations (PNCs), an approximate measure for ultrafine particles (UFPs), ranged from 7.2×10^3 to 6.2×10^4 particles/cm^3 (Schober et al. 2014a; Nguyen et al. 2019; Melstrom et al. 2017; Zhao et al. 2017; Volesky et al. 2018; Scungio et al. 2018). Additionally, substantial amounts of propylene glycol, vegetable glycerin, and nicotine, as well as relatively low levels of toxic compounds such as carbonyls, aromatic volatile organic compounds (VOCs), and heavy metals, have been observed in EEV aerosols in indoor environments (Li et al. 2020b). In addition to the secondhand exposure, the deposited residuals from vaping might be reemitted into the gas phase and serve as a potential source of thirdhand exposure (Khachatoorian et al. 2019; Goniewicz and Lee 2015). The health effects of thirdhand exposure are understudied which warrant future research.

Different from typical laboratory studies in which volunteers vape an e-cig following a standard puffing protocol for a short period, continuous vaping by multiple e-cig users occurs in vape shops during business hours. Nguyen et al. (2019) found that the PNC and $PM_{2.5}$ in vape shops fluctuated dramatically and can even reach up to 4.8×10^5 particles/cm^3 and 37,500 µg/m^3, respectively. The exhaled particles can persist and mix in the indoor environment, leading to elevated concentrations at distances greater than 3.6 m away from the vaping sources (Nguyen et al. 2019). Because vape shops are typically located in multiunit buildings with at least one neighboring business, such as an office, restaurant, retail store, or clinic, the EEV particles may also travel to their neighboring businesses (Nguyen et al. 2019). Additionally, vape shops were found disproportionately located in proximity to vulnerable communities such as the low-income, minority, and youth (Berg 2018). Vulnerable individuals who are bystanders in a vape shop or neighboring the vape shops can be at increased risks of exposure to EEV aerosols.

It has been well established that secondhand smoke (SHS) can transfer from smoking units to smoke-free adjacent units through shared ventilation, open windows, holes in walls, hallways, and electric outlets (Hood et al. 2014; Russo et al. 2015; Bohac et al. 2011; King et al. 2010). Analogous to SHS, these transfer mechanisms might also be applicable to EEV aerosols. Khachatoorian et al. (2019) detected tobacco-specific residues, including nicotine, minor alkaloids, and TSNAs, on surfaces in an indoor space adjacent to a vape shop, suggesting potential thirdhand exposures to e-cig emissions. In a laboratory setting, Zhang et al. (2020) found that the EEV aerosols transferred from a vaping room to its adjacent non-vaping room, which could be effectively reduced by blocking the door between the two rooms. However, no study has assessed the transport of EEV aerosol from vape shops to neighboring units in multiunit commercial buildings. Therefore, the aim of this study was to (1) assess the impacts of

e-cig usage in vape shops on the indoor air quality of neighboring businesses, (2) identify major factors that influence the behaviors of EEV aerosols, and (3) evaluate the transport of EEV particles from the vape shop to its outdoor environment.

4.3. Materials and methods

4.3.1. Study sites

Both vape shops and their neighboring businesses in Southern California were recruited via phone calls, site visits, and brochure postings. Vape shops for this study were identified from a Yelp.com search using the keywords “vape shops”. For each selected vape shop, a neighboring business was identified through the Google Maps search and site visits. The selection criteria for each pair (i.e., vape shop and its neighboring business) include: (a) The pair was adjacent to each other on the same floor in a multiunit commercial building; (b) no other tobacco products other than e-cigs were used in the vape shops; and (c) neighboring businesses were smoke-free indoor spaces. Because high levels of particles have been reported in restaurants serving barbecued, boiling, and pan-fried food (Lee et al. 2001), these restaurants were excluded in this study. A total of nine pairs of vape shops and neighboring businesses (pair IDs A - I) agreed to participate in this study.

The characteristics of the study sites such as building location, shop volume, ventilation type, air exchange rate (AER), and vaping density for each pair are summarized in **Table 4.1** (see Appendix **Table A-5** for ventilation and sampling details). All of the studied pairs A-I were located in multiunit commercial buildings, which were either in a plaza or storefront along a street. No e-cigs or other tobacco products were consumed in the studied neighboring businesses due to the smoking ban in all enclosed workplaces in California (AB-13, enacted as California Labor Code LC 6404.5). However, the smoking ban did not apply to vape shops.

Table 4.1. Characteristics and nicotine concentrations of the nine studied vape shops and their neighboring businesses.

		Vape Shop					Neighboring Business				
[a]Pairs ID	Location	Volume (m^3)	Ventilation Type	AER (h^{-1})	[b]Vaping Density (TVF/h/100 m^3)	24-h TWA nicotine ($\mu g/m^3$)	Volume (m^3)	Ventilation Type	AER (h^{-1})	24-h TWA nicotine ($\mu g/m^3$)	[c]Nicotine transfer (%)
A	Plaza	168	Natural Ventilation	0.29	13 (14)	3.43 (1.21)	> 400	Rooftop A/C and natural ventilation	0.21	0.09 (0.04)	2.7
B	Plaza	242	Natural Ventilation	0.21	13 (12)	3.08 (0.69)	> 400	Rooftop A/C	0.17	0.37 (0.32)	12
C	Plaza	217	Window A/C	0.39	11 (8)	1.72 (0.51)	278	Rooftop A/C with an exhaust fan	0.60	0.42 (0.14)	24.7
D	Plaza	323	Rooftop A/C with a mixing fan	0.20	8 (4)	3.99 (1.07)	357	Rooftop A/C with mixing fans	0.20	0.13 (0.05)	3.4
E	Storefront	418	Rooftop A/C	0.22	5 (8)	3.15 (2.67)	181	Rooftop A/C	0.21	0.11 (0.04)	3.6
F	Storefront	361	Rooftop A/C	0.81	5 (6)	1.89 (1.27)	358	Rooftop A/C	0.78	0.14 (0.05)	7.5
G	Storefront	212	Rooftop A/C	1.06	[d]NA	0.65 (0.35)	160	Natural Ventilation	NA	0.09 (0.04)	13.2
H	Plaza	402	Rooftop A/C	0.31	NA	2.72 (0.26)	376	Rooftop A/C	0.58	0.07 (0.05)	2.6
I	Plaza	260	Rooftop A/C or natural ventilation	0.24	20 (6)	2.71 (1.50)	116	Rooftop A/C	0.30	0.06 (0.03)	2.4

Abbreviations: AER, air exchange rate; TVF: total vaping frequency; A/C, air conditioning; TWA, time-weighted average; NA, not applicable

[a]Real-time particle samplings were conducted in pairs A-F while nicotine samplings were conducted in all nine pairs

[b]Vaping density (TVF/h/100 m^3): total number of puffs per hour normalized by the shop volume for each vape shop.

[c]Nicotine transfer: the percentage of nicotine transferred from vape shop to neighboring business = (neighboring business nicotine concentration/ vape shop nicotine concentration) × 100%.

[d]NA due to lack of access

4.3.2. Sampling protocol

Air samplings in each pair of vape shops and neighboring businesses were conducted for 3-4 days between February 2017 and October 2019. **Figure 4.1** illustrates the sampling types and sampling locations in the study site: (a) Sampling location 1: inside the vape shop within 1.2 m away from the vaping bar which was the main vaping activity area, (b) sampling location 2: inside the neighboring business, (c) sampling location 3: outside of the vape shop about 1-3 m away from the front door of vape shop, and (d) an additional sampling location 4 for vape shop I only: outdoor about 6-8 m away from the front door of vape shop. Real-time PNC and $PM_{2.5}$ mass concentrations were monitored concurrently in pairs A-F at sampling locations 1-3. No particle sample was collected concurrently in pairs G-I because we were not able to install the particle sampling instruments in the neighboring businesses. The transport of EEV particles from the vape shop to its outdoor area was investigated in vape shop I at sampling locations 1, 3, and 4 when the door of vape shop I was open. Particle size distributions were measured inside pair B (sampling locations 1 and 2) and vape shop C (sampling location 1 only). The 24-h time-weighted average (TWA) airborne nicotine samplings were conducted in all pairs A-I at sampling locations 1 and 2.

On each sampling day, particle monitoring was conducted for about 5-8 hours during overlapping business hours between a vape shop and its neighboring business. Observation notes were recorded by research staff who stayed in the vape shop during the 5-8 sampling hours including (1) characteristic information such as shop volume (m^3), ventilation type, and location; (2) total number of puffs generated by e-cig users including customers and employees in the vape shops every minute, which allowed us to calculate the total vaping frequency (TVF); (3)

any changes of ventilation settings such as opening or closing the shop doors and A/C switching on or off; and (4) activities with any potential particle emissions.

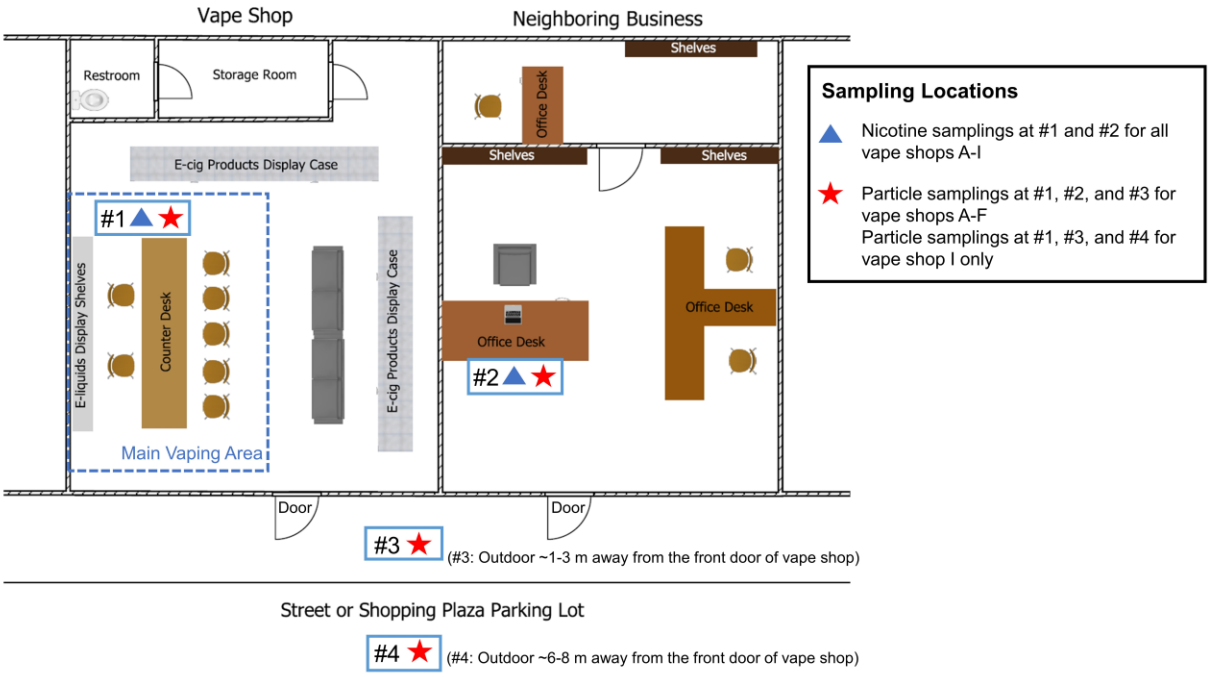


Figure 4.1. The schematic diagram of sampling types and sampling locations in a representative pair of vape shop and its neighboring business.

4.3.3. Measurement of particle number, $PM_{2.5}$, and particle size distribution

Three sets of instruments were installed at sampling locations 1-3 to measure real-time PNC and $PM_{2.5}$ mass concentration simultaneously. At each sampling location, a portable Condensation Particle Counter (CPC 3007, TSI Inc., Shoreview, MN) or a DiSCmini (Diffusion Size Classifier Miniature, Testo SE & Co. KGaA, Germany) and a DustTrak II Aerosol Monitor (DustTrak II 8532, TSI Inc.) were used to measure PNC and $PM_{2.5}$, respectively, at 2-min logging intervals. Real-time carbon dioxide (CO_2) concentrations, temperature, and relative humidity were measured at 1-minute intervals by two indoor air quality monitors (Q-Trak 7575, TSI Inc.) in vape shops and neighboring businesses. Using the CO_2 concentration data, we calculated the room AER by the CO_2 tracer gas decay method (Batterman 2017; Nguyen et al.

2019). In addition, particle size distributions in the size range of 7-289 nm and 0.5-19.8 μm were measured in pair B and vape shop C with a Scanning Mobility Particle Sizer (SMPS 3080, TSI Inc.) (100 s up scan, 20 s down scan) and Aerodynamic Particle Sizer (APS 3321, TSI Inc.), respectively.

4.3.4. Measurement of airborne nicotine concentrations

Airborne nicotine was collected using a modified sampling method (Lopez et al. 2013; Chen et al. 2017) that was first developed by Hammond and Leaderer (Hammond and Leaderer 1987). The sampler with a 37 mm filter pretreated with sodium bisulfate was connected to a pump at a sampling rate of 3 L/min. The sampling flow rate were verified by a mass flow meter (Model 4140, TSI Inc.) at the start and end of each sampling session. The average flow rate of the two values was used to calculate the total air volume. The active nicotine samplers were installed at sampling locations 1 and 2 in each pair for a period of 24 hours. A total of 3-5 nicotine samples were collected in each pair. To ensure nicotine data quality, an outdoor sample for each pair of shops was also collected. All the nicotine filters were extracted using dichloromethane with an internal standard (i.e., 2 μg/ml quinoline) and analyzed by gas chromatography-mass spectrometry (GC-MS). The limit of quantification (LOQ) of GC-MS was 0.2 μg per filter, equivalent to 0.05 $\mu g/m^3$ 24-h TWA nicotine. The TWA airborne nicotine concentration was calculated by dividing the total mass of nicotine collected in the filter by the product of flow rate (i.e., 3 L/min) and sampling time in minutes.

4.3.5. Quality control/quality assurance for data collection and analysis

Before each sampling session, particle sampling instruments were zero checked and collocated for at least 30 min for quality assurance. Regression results from the collocation tests have been applied to correct all the PNC and $PM_{2.5}$ data throughout this study.

DustTrak is sensitive to the composition and size distribution of airborne particles leading to notable upward $PM_{2.5}$ bias during air sampling (Moosmuller et al. 2001; Zhao et al. 2017). Therefore, we have conducted gravimetric calibration of DustTrak II $PM_{2.5}$ measurements in this study. The detailed process has been described previously (Zhao et al. 2017; Nguyen et al. 2019). Briefly, $PM_{2.5}$ gravimetric samples were collected using personal cascade impactors side by side with the DustTrak II inside selected vape shops and outdoor sampling locations. A calibration factor of 0.25 ± 0.009 (R^2 = 0.95; 95% CI, 0.22 to 0.28) and 0.48 ± 0.026 (R^2 = 0.98; 95% CI, 0.41 to 0.55) was determined for $PM_{2.5}$ data in vape shop and ambient sampling locations (i.e., outdoor and neighboring business), respectively, from gravimetric analysis.

4.3.6. Data analysis

The arithmetic mean and standard deviation (SD), as well as median and interquartile range (IQR), of PNC, $PM_{2.5}$, and nicotine concentrations were calculated for each pair of vape shops and neighboring businesses during overlapping business hours. Kruskal-Wallis ANOVA on Ranks was used to compare e-cig-related air pollutant levels in vape shop with neighboring business and outdoor sampling locations. In an effort to examine the temporal dynamics of particle transfer, linear regression analyses were used to determine the correlation between particle concentrations in vape shops and vaping-free areas (i.e., neighboring businesses or outdoor sampling locations) using 10-min averaged data. Based on field observation notes,

vaping density (puffs/h/100 m^3), defined as the total number of puffs per hour normalized by the shop volume, for each vape shop was estimated. The effects of parameters such as AER and vaping density on the e-cig-related air pollutant levels in vape shops were also assessed by linear regression. Hourly averaged data were used to investigate the effects of vaping density on particle concentrations.

R 3.4.0 and Microsoft Excel 2016 (Microsoft, Seattle, WA, USA) were used to summarize data and perform statistical analyses. All figures were generated with Sigmaplot 14.0 (Systat Software Inc., San Jose, CA). The level of statistical significance was set at $p < 0.05$.

4.4. Results and discussion

4.4.1. E-cig related air pollutants in the vape shops and neighboring businesses

Particle concentrations. The PNC and $PM_{2.5}$ concentrations for pairs A-F during overlapping business hours are presented with respect to mean vaping density in **Figure 4.2** (see Appendix **Table A-6** and **Table A-7** for the mean and median particle concentrations, respectively). The median (IQR) PNCs in the six vape shops during the sampling sessions ranged from 1.4×10^4 (1.1×10^4, 1.7×10^4) to 3.5×10^4 (2.0×10^4, 5.0×10^4) particles/cm^3. For $PM_{2.5}$, the median (IQR) concentration was within the range of 15 (6, 145) – 134 (33, 541) µg/m^3. Although there are no guidelines for PNC indoors, the $PM_{2.5}$ levels inside most vape shops were largely above the 24-h average standard of 35 µg/m^3(U.S. Environmental Protection Agency 2016). Both PNC and $PM_{2.5}$ observed in vape shops were at the comparable level to a previous vape shop study (Nguyen et al. 2019). When customers were at high volumes, the peak PNCs and $PM_{2.5}$ concentrations in the vape shop can even reach 2.9×10^5 particles/cm^3 and 4,988 µg/m^3, respectively. As the vaping density decreased from 13 to 5 puffs/h/100 m^3, the mean $PM_{2.5}$ in the vape shops A-F significantly decreased ($r = 0.97$, $p = 0.002$). A similar but less prominent trend

was observed for PNCs ($r = 0.81$, $p < 0.05$). As to the median concentrations, however, there is no significant correlation detected. It should be noted that vape shops A and B enhanced their natural ventilation by opening their shop doors only for 18% and 20% of sampling time, respectively, but did not use any ventilation for most of the time (Appendix **Table A-5**).

The PNC and $PM_{2.5}$ in vape shops A-F were significantly higher than their neighboring businesses (Kruskal-Wallis, $p < 0.001$), except for $PM_{2.5}$ in vape shop E. The mean (SD) PNCs in the neighboring businesses reached up to 1.8×10^4 (7.3×10^3) particles/cm^3 which was higher than most of the common indoor environments such as homes, offices, and schools (Morawska et al. 2017). The mean $PM_{2.5}$ concentrations in neighboring businesses A, C, and E exceeded the U.S. Environmental Protection Agency's annual standard of 12 μg/m^3, which is the maximum allowable concentration for outdoor air quality (U.S. Environmental Protection Agency 2016). Although there is currently no standard for $PM_{2.5}$ in the indoor environments, the indoor $PM_{2.5}$ levels are expected to be the same as, or lower than, outdoor levels when there is no other indoor emission source (U.S. Environmental Protection Agency 2020).

On the other hand, PNC and $PM_{2.5}$ in vape shops A-F were all significantly greater than those measured at outdoor sampling locations (Kruskal-Wallis, $p < 0.001$; see Appendix **Table A-6**), suggesting that the high concentration measured in vape shops were not due to outdoor impacts such as vehicular emissions.

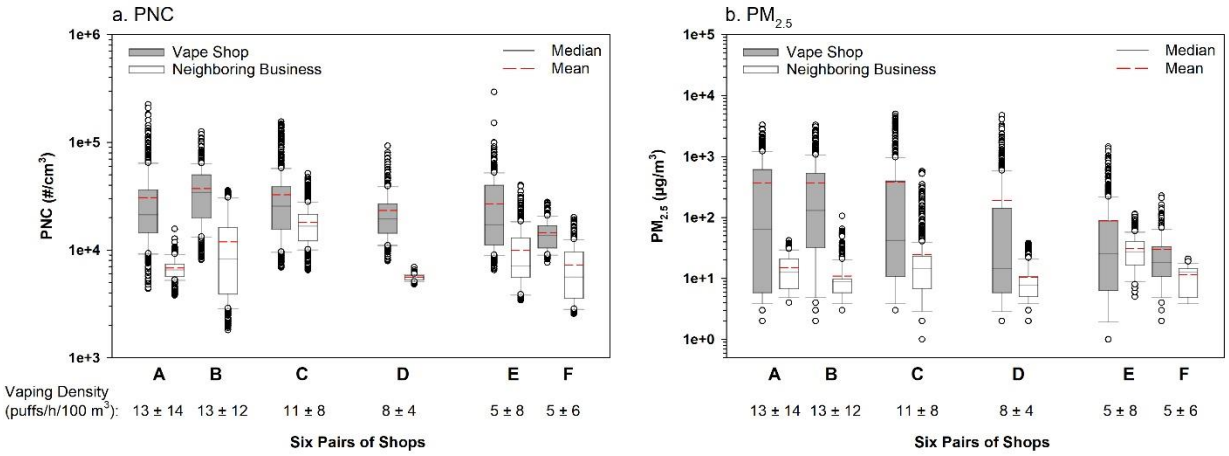


Figure 4.2. Box plots summarizing (a) PNC and (b) $PM_{2.5}$ mass concentrations measured during all sampling sessions for the six pairs of vape shops and neighboring businesses A-F by vaping density. The solid line in each box represents the median value, and the dash line in each box represents the mean value.

Airborne nicotine concentration. Gas-phase nicotine, as a tracer for EEV aerosols, was detected in all nine pairs, suggesting EEV aerosol transfer from vape shops to neighboring businesses (**Table 4.1**). The median (IQR) concentration of the 24-h TWA nicotine measured in vape shops and neighboring businesses were 2.72 (1.80, 3.29) µg/m^3 and 0.11 (0.08, 0.26) µg/m^3, respectively. Although the measured 24-h TWA nicotine concentrations were lower than the ACGIH/OSHA 8-h standard of 500 ug/m^3, the long-term health hazards are largely unknown and warrant future studies. The nicotine levels estimated in the vape shops were comparable to previous studies that recruited volunteers to use e-cigs in a room (0.20 - 6.23 µg/m^3) (Schober et al. 2014a; Geiss et al. 2015; Melstrom et al. 2017; Czogala et al. 2014; Johnson et al. 2018; Liu et al. 2017). The nicotine levels in vape shops were found to be similar to those in smoking hospitality venues in Ghana where nicotine samples were passively collected for 7 days

(Agbenyikey et al. 2011). However, the nicotine levels in vape shops were about 5 – 10 times lower than those measured in smoking allowed restaurants and bars where nicotine samples were collected during 4 busy hours (Bolte et al. 2008). The nicotine levels in all the studied vape shops and four of the neighboring businesses were significantly higher than those at e-cig users' homes (0.11 μg/m^3) (Ballbè et al. 2014). On the other hand, Chen et al. (2017) reported an exceptionally high nicotine concentration ~ 125 μg/m^3 at a vaping convention with more than 1,000 participants in a 13,475 m^3 venue (i.e., 13 m^3 per person or 7 occupants per 100 m^3). In the current study, there were usually 2 – 7 people inside vape shops (i.e., ~ 41 - 145 m^3 per person or ~1-2 occupants per 100 m^3) during our sampling time. Therefore, the difference in nicotine concentration may be explained by two factors: (1) the space occupied by each person in the vaping convention is lower than that in vape shops, suggesting less dilution for EEV aerosols; (2) our sampling inside vape shops included overnight periods when there was no vaping; in contrast, sampling in the vaping convention was conducted only during active vaping periods. Nevertheless, Johnson et al. (2018) reported a low median concentration of nicotine ~ 1.1 μg/m^3 in four e-cig vaping events where the occupancy densities were ~17-200 m^3 per person (1-6 occupants per 100 m^3), which were closer to what observed in the vape shops.

Similar to previous e-cig indoor studies (Ballbè et al. 2014; Chen et al. 2017; Johnson et al. 2018), our method only measured gas-phase not particulate phase nicotine. To understand the total exposure to nicotine from EEV aerosols, the gas/particle partitioning of nicotine should be considered in future studies. Assuming the nicotine measured in the neighboring business was all from its adjacent vape shop, the percentage of nicotine transfer ranged from 2.4 to 24.7%. Although the airborne nicotine levels varied depending on the level of nicotine in the e-liquids selected by e-cig users as well as the customer traffic, the identification of nicotine in all studied

vape shops and neighboring businesses confirmed that involuntary exposures to EEV aerosols occurred in these indoor environments.

4.4.2. Predictors of air pollutants concentrations inside vape shops

A previous study (Nguyen et al. 2019) used TVF every 30 min as a predictor which had strong correlation with both PNC (r = 0.74, $p < 0.001$) and $PM_{2.5}$ concentrations (r = 0.75, $p < 0.001$) in vape shops when the shop door was closed. After considering the different vape shop volumes, we found that the dilution-corrected vaping density (puffs/h/100 m^3) had an even stronger positive correlation with PNC (r =0.82, $p < 0.001$) and $PM_{2.5}$ (r =0.88, $p < 0.001$), respectively (**Figure 4.3**). This result is in agreement with recent findings that EEV aerosols can be substantially affected by the dilution condition (Floyd et al. 2018; Ingebrethsen et al. 2012; Meng et al. 2017; Zhao et al. 2016a). Additionally, the $PM_{2.5}$ mass concentration showed a better correlation with vaping density compared to PNC, suggesting that fine particles are more sensitive to dilution compared to smaller particles.

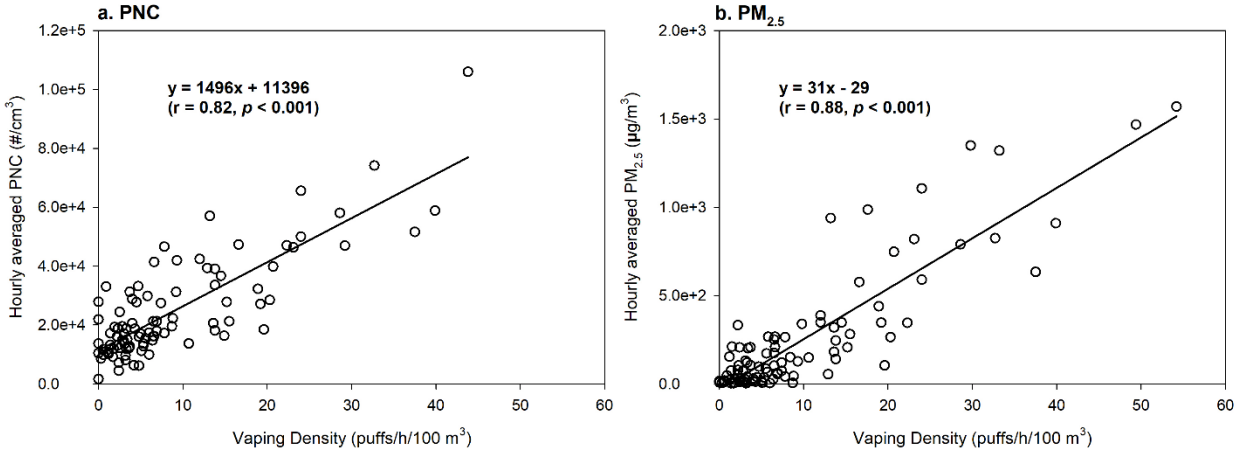


Figure 4.3. Relationships between hourly averaged PNC and $PM_{2.5}$ and vaping density (puffs/h/100 m^3) when the shop door was closed for vape shops A-F and I with particle samplings.

In addition to vaping density, we previously found that lower AERs in vape shops could increase the particle levels measured from opening to closing of business on busy days (Nguyen et al. 2019). In this study, all of the studied vape shops and neighboring businesses did not use any central ventilation during sampling sessions. Only either A/C (without outdoor air supply) or natural ventilation was observed in the shops. Accordingly, the AERs for all of the pairs ranged from 0.20 to 1.06 h^{-1}. We found a negative, significant association between the AER and 24-h TWA airborne nicotine concentration in vape shops (**Figure 4.4**; r = -0.86, p = 0.003). This finding confirms that the mitigation of nicotine pollution in vape shops can be achieved by enhancing ventilation despite the varying levels of nicotine in different e-cig products. Due to a small number of studied vape shops with relatively low AERs in this study, future research is warranted to systematically evaluate the effects of ventilation on indoor airborne nicotine levels.

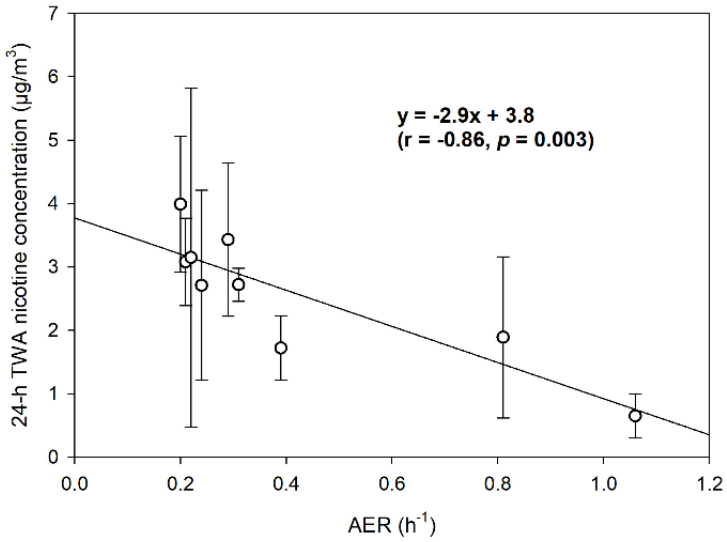


Figure 4.4. Relationships between the 24-h time-weighted average (TWA) nicotine concentration and air exchange rate (AER) in all the studied vape shops.

4.4.3. Impacts of EEV emissions from vape shops on nearby areas

Indoor air quality of neighboring businesses. The relationship between the 10-min averaged concentrations (i.e., both PNC and $PM_{2.5}$) inside vape shops and those in neighboring businesses A-F were summarized in **Table 4.2** (see Appendix **Figure A-1 and Figure A-2** for the regression analysis). For PNCs, significant correlations ($r > 0.33$, $p < 0.001$) were detected in 5 out of 6 pairs (i.e., A, B, C, E, and F). A moderate or strong correlation ($r > 0.40$) was observed in pairs A, B, and C, which had higher vaping density compared to other pairs. The weakest correlation shown in pair E among the five pairs with significant correlations was likely because their ventilation systems were separated by a wall while the ventilation system of other pairs were connected. The slopes of the linear regression relating the PNCs in neighboring businesses to those in vape shops ranged from 0.035 to 0.368. In other words, PNCs in the neighboring businesses were expected to increase by 35 to 368 particles/cm^3 when the PNC in vape shops increased by 1000 particles/cm^3. Notably, the regression slopes for pairs B and F were 3 – 10 times higher than other pairs possibly because multiple pathways such as the ductwork in their shared ventilation systems, doors, shared walls, and building cracks contributed to the particle transfer between the two indoor spaces. Future studies are needed to identify these potential pathways in multiunit buildings for mitigation purposes. No significant correlation was observed for pair D likely because the sampling instruments were installed behind several large massage chairs in the corner of the neighboring business, creating an enclosed area in which the EEV particles could hardly reach.

Regarding $PM_{2.5}$, while the correlations were weak for most pairs, significant results ($r > 0.33$, $p < 0.001$) were observed in 2 out of 6 pairs (i.e., A and C). The regression slopes were 0.010 and 0.041 for pairs A and C, respectively. Interestingly, the correlation coefficient for

$PM_{2.5}$ in pair C reached as high as 0.83, which was likely driven by the extremely high $PM_{2.5}$ levels (1,000 - 4,500 μg/m^3) in vape shop C. The reason why the transfer of UFPs in pair C is less prominent compared to $PM_{2.5}$ can be explained by the change of particle size in vape shop C (**Figure 4.5**). When vaping density increased from 10 to 44 puffs/h/100 m^3, the particle mass distribution shifted from a typical single mode at 1 μm, which has been observed in previous studies (Baassiri et al. 2017; Floyd et al. 2018), to a trimodal pattern of 0.3, 0.8, and 3 μm. The increase of the micron-sized particles can be explained by the fact that the emitted UFPs coagulated with the 1 μm particles resulting in a growth of particle mass to the 3 μm mode. Mikheev et al. (2016) and Floyd et al. (2018) have demonstrated that coagulation effectively increases the e-cig particle mass while depleting smaller particles. As a result, the increase of PNC (from 2.3 $\times 10^4$ to 2.8 $\times 10^4$ particles/cm^3) was less prominent than $PM_{2.5}$ which surged by 6 times to 127 μg/m^3 in the neighboring business when emission increased in vape shop C. These results show that both UFPs and $PM_{2.5}$ from the vape shops can impact the indoor air quality in their neighboring businesses.

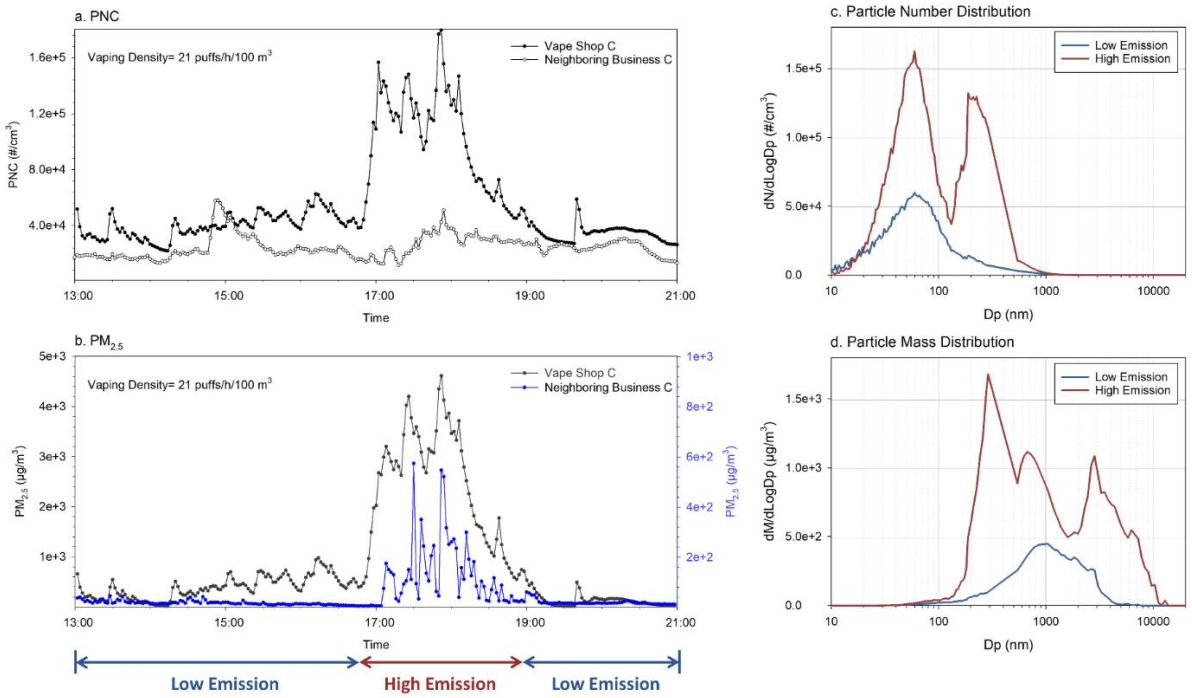


Figure 4.5. Temporal profile of PNC and $PM_{2.5}$ in vape shop C and neighboring business C (a and b) as well as the particle size distributions in vape shop C for both low emission and high emission periods (c and d).

The higher particle transfer rates were observed in pairs B, C, and F, which also had higher nicotine transfer rates compared to other pairs (see **Table 4.1**). The highest nicotine transfer rate (i.e., 24.7%) was observed in pair C likely because the neighboring business C experienced significant impacts of both particle number and mass on their indoor air quality. Notably, despite no significant correlation observed for particles in pair D, 3.4 % of gas-phase nicotine still transferred from vape shop D to its neighboring business suggesting indoor air pollution due to vaping.

Outdoor air quality. As the EEV aerosols in the vape shop can transfer to its neighboring business in the multiunit building, we were also interested in whether the EEV particles can travel to the outdoor environment. The relationship between the 10-min averaged concentrations

(i.e., both PNC and $PM_{2.5}$) inside and outside vape shops A-F is also summarized in **Table 4.2** (see Appendix **Figure A-3** and **Figure A-4** for the regression analysis). For PNCs, significant correlations ($r > 0.33$, $p < 0.001$) were detected only in vape shops A and B with natural ventilation. Both vape shops A and B also had the highest vaping density among the six studied vape shops, which contributed to increasing the particle concentration gradient between indoors and outdoors. According to the Fick's first law of diffusion, particles might transport from vape shops to outdoor areas through the open doors and holes on the wall. The regression slope for vape shop B was 7 times higher than vape shop A possibly because of the higher vaping frequency (i.e., 46.2 puffs/h) in vape shop B when the door was open compared to vape shop A (i.e., 25.4 puffs/h). For $PM_{2.5}$, a significant correlation was only observed in vape shop A.

Table 4.2. Linear regression analysis relating the 10-min averaged PNC and $PM_{2.5}$ in neighboring businesses and outdoors (sampling location 3) to those in vape shops for pairs A-F.

Vape shops	PNC			$PM_{2.5}$		
	Slope (95% CI)	p-value	r	Slope (95% CI)	p-value	r
Neighboring Businesses						
A	0.035 (0.027, 0.043)	<0.001	0.59	0.010 (0.008, 0.013)	< 0.001	0.56
B	0.316 (0.238, 0.394)	<0.001	0.62	-0.002 (-0.006, 0.002)	0.329	-0.09
C	0.136 (0.105, 0.168)	<0.001	0.55	0.041 (0.0369, 0.045)	<0.001	0.83
D	-0.008 (-0.017, 0.001)	0.075	-0.22	-0.003 (-0.006, 0.001)	0.148	-0.12
E	0.111 (0.054, 0.167)	<0.001	0.37	0.020 (-0.003, 0.042)	0.084	0.15
F	0.368 (0.119, 0.616)	0.005	0.39	0.016 (-0.044, 0.077)	0.595	0.07
Outdoors						
A	0.076 (0.043, 0.109)	<0.001	0.37	0.006 (0.005, 0.008)	<0.001	0.64
B	0.584 (0.451, 0.716)	<0.001	0.66	0.013 (-0.009, 0.034)	0.251	0.12
C	0.054 (-0.010, 0.117)	0.099	0.13	-0.000 (-0.002, 0.002)	0.937	-0.01
D	0.222 (-0.050, 0.495)	0.107	0.27	-0.001 (-0.003, 0.001)	0.428	-0.07
E	-0.056 (-0.106, -0.006)	0.030	-0.30	-0.005 (-0.011, 0.001)	0.120	-0.17
F	0.088 (-0.033, 0.210)	0.149	0.28	0.089 (0.037, 0.141)	0.001	0.43

4.4.4. Effects of vape shop door open and close on particle transport

Neighboring businesses. The effects of door open and close on UFP transfer from a vape shop to its neighboring business for pair B are further illustrated in **Figure 4.6**. During the sampling period, the vape shop door was closed before 14:30 except for customers walking in and out, and then kept open after 14:30. Following the PNC spikes in the vape shop, the PNC levels were also elevated in the neighboring business (**Figure 4.6a**). Shortly following the vape shop door open, the PNC started to diminish in the neighboring business (**Figure 4.6a**). Consequently, the mean PNC decreased by 19% to 4.3×10^4 (2.0×10^4) particles/cm^3 in the vape shop (Kruskal-Wallis, $p < 0.05$) and decreased by 33% to 1.8×10^4 (4.8×10^3) particles/cm^3 in neighboring business (Kruskal-Wallis, $p < 0.001$).

Figure 4.6b and c present the contour plots of the number-based particle size distribution for pair B. The color intensity indicates the normalized particle number concentration (dN/dLogDp) for a given particle size at a given time. As demonstrated by Nguyen et al. (2019), the particles emitted in the vape shop was characterized by a bimodal particle number distribution of 60 nm and 250 nm when the shop door was closed. Meanwhile, UFPs largely penetrated into the neighboring business showing a single mode at 60 nm. Since UFPs may deposit deep into the human lung and induce greater adverse respiratory effects (Sturm 2016; Peters et al. 1997), the exposure to EEV related UFPs might bring more health concerns for employees and patrons in the neighboring business. Under the effect of door open, the particle size distribution in the vape shop shifted to a single mode while the UFPs started to decrease shortly after door open.

Opening and closing the vape shop doors changed the condition of ventilation in vape shops A and B. When the door of the vape shop was closed, an even stronger correlation in

terms of PNC was observed for pairs A (r= 0.62, $p < 0.0\ 01$) and B (r = 0.66, $p < 0.001$). This was most likely a result of the enhanced particle concentration gradient between the vape shop and neighboring business because particles persisted and remained at high concentrations in the vape shop during door closed periods (Nguyen et al. 2019). However, no significant correlations were observed for both pairs A (r = 0.36, p > 0.05) and B (r = 0.25, p > 0.05) when their shop doors were open due to the enhanced dilution from outdoor air. For $PM_{2.5}$, a similar but less prominent effect was observed in pair A, but no significant correlation was presented in pair B at all. Future research is warranted to systematically evaluate more mitigation strategies that would effectively reduce exposure to EEV aerosols in public multiunit buildings.

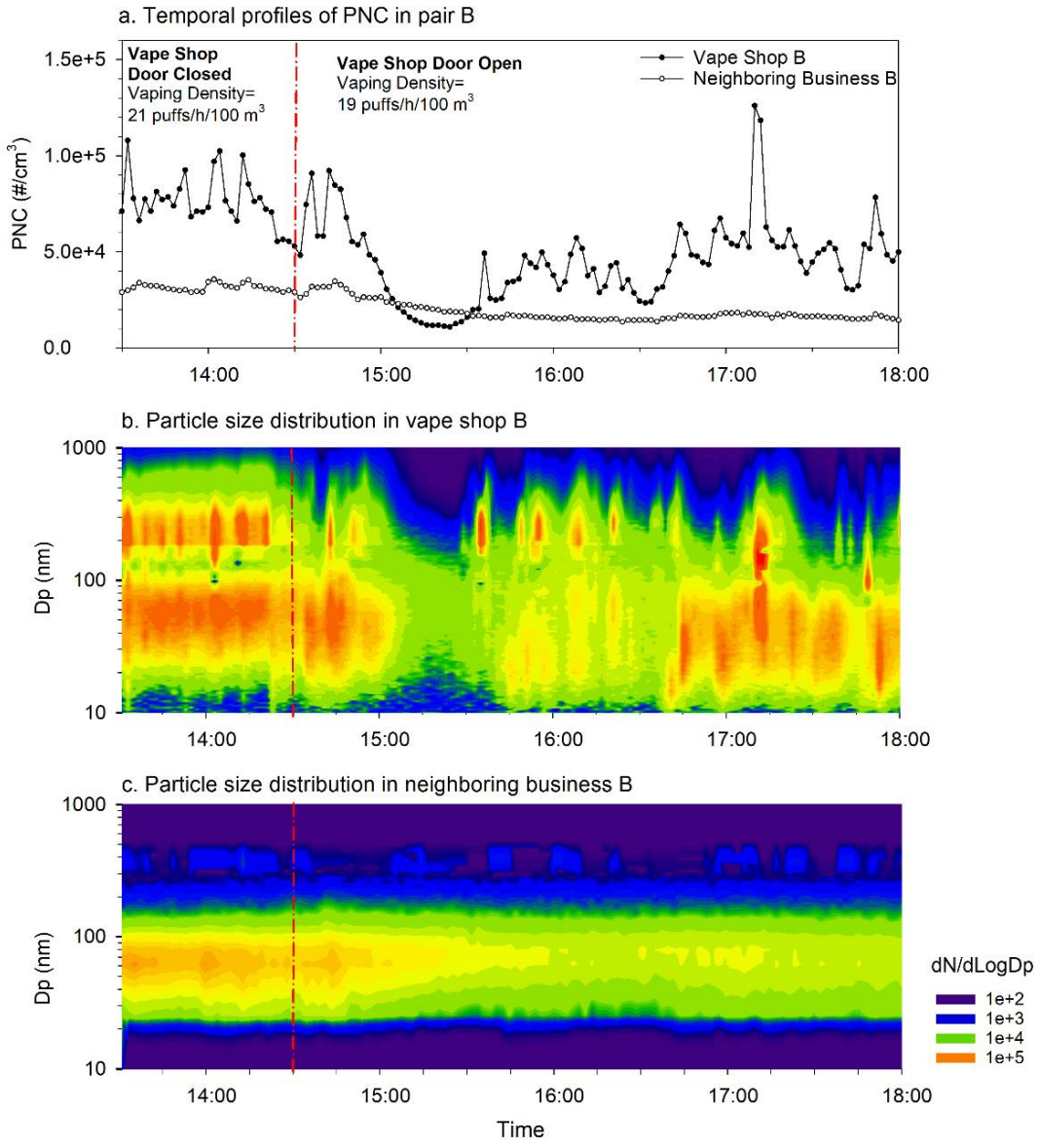


Figure 4.6. Temporal profile of (a) PNC in vape shop B and its neighboring business B as well as particle size distributions in (b) vape shop B and (c) neighboring business B during overlapping business hours on a day with ventilation changes. Note: The door of vape shop was closed during 13:30-14:30 and the door was open during 14:30-18:00.

Outdoor environment. While opening doors significantly reduced particle levels inside vape shops and neighboring businesses, it might increase the transport of EEV particles from vape

shops to outdoor areas. Indeed, as shown in **Figure 4.7**, linear regression demonstrated that the correlation between particle concentrations (i.e., PNC and $PM_{2.5}$) inside and outside vape shop B was stronger when the shop door was open compared to that was closed. In addition, the regression slope was greater during the door open periods, suggesting particles due to vaping largely transported from vape shop to its outdoor environment, compared to the door closed. Similar results were also observed for vape shop A (**Figure 4.8**). As shown in **Figure 4.9**, the exceptionally high ratio between the indoor and outdoor particle concentration (or I/O) demonstrated that vaping was a major indoor emission source in vape shops A and B regardless of door opening or closing. Compared to door closed periods, door opening significantly reduced the I/O ratios for both PNC and $PM_{2.5}$. Like indoor spaces with smoking cigarettes that showed $PM_{2.5}$ I/O ratio reached ~11 with the minimal AER (Li and Chen 2003), the median I/O ratio in vape shops was up to 34 during door closed periods where the ventilation was dominated by infiltration (Chen and Zhao 2011). After the shop door was open, the AER between indoor and outdoor likely increased, resulting in significantly lower I/O ratios around 2 – 4. This is because that the outdoor air with a lower particle concentration penetrated into vape shops more quickly and diluted the indoor EEV aerosols. At the same time, EEV aerosols traveled to the outdoor environment.

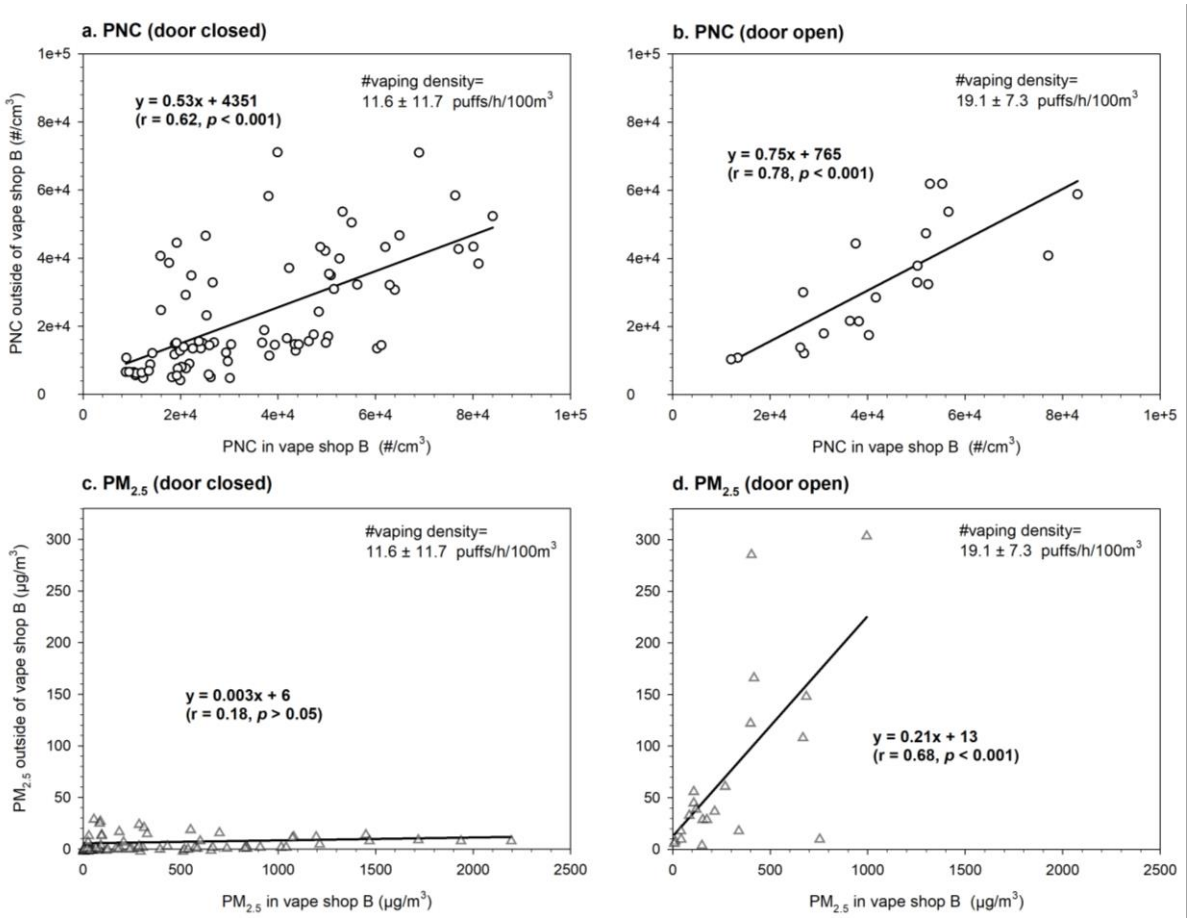


Figure 4.7. Effects of door open and close on the particle transport from vape shop B to the outdoor environment (i.e., sampling location 3: ~1-3 m away from the front door of vape shop B).

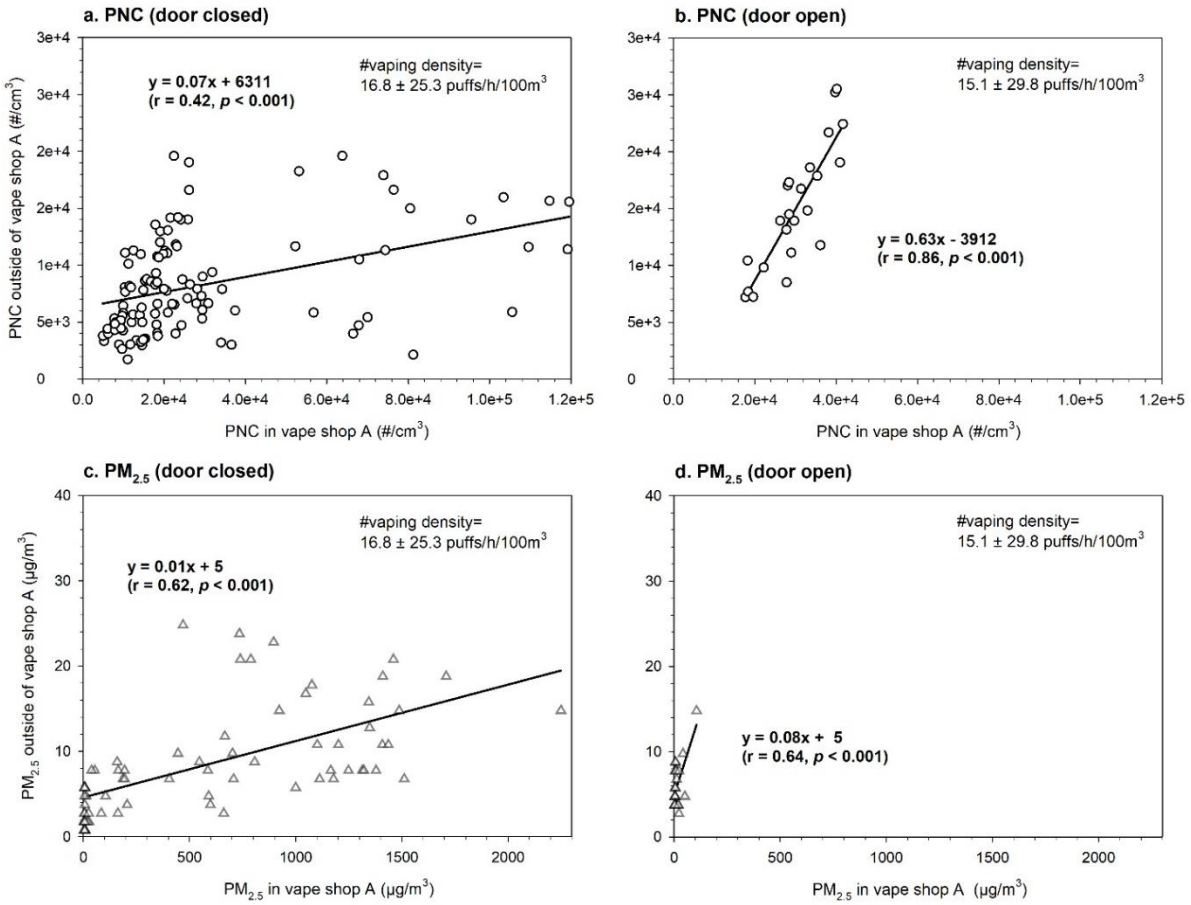


Figure 4.8. Effects of door opening and closing on the particle transport from vape shop A to the outdoor environment (i.e., sampling location 3: ~1-3 m away from the front door of vape shop A).

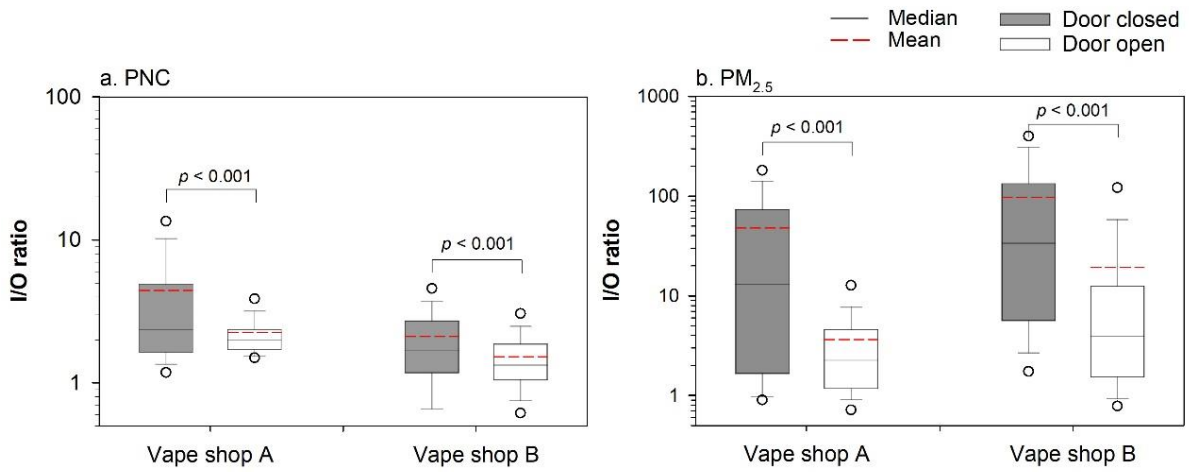


Figure 4.9. I/O ratios for (a) PNC and (b) $PM_{2.5}$ in vape shops A and B with the effects of door opening and closing. The Mann-Whitney U test was used to compare the I/O ratios during door closed vs. door open.

To further study the effect of proximity to vape shop on outdoor particle concentrations, additional particle measurements were conducted simultaneously at indoor sampling location 1 and outdoor sampling locations 3 and 4 for vape shop I (**Figure 4.10**). As seen in **Figure 4.10a**, the mean PNCs were 3.1×10^4, 1.3×10^4, and 8.9×10^3 particles/cm^3 at sampling locations 1, 3, and 4, respectively. When the sampling location moved from indoor location 1 to outdoor locations 3 and 4, the PNC dropped to 41% and 29% of what was measured in the vape shop, respectively. The significant correlations of location 1 with location 3 ($r = 0.51$, $p < 0.001$) and 4 ($r = 0.37$, $p = 0.004$) indicate that small particles measured by PNC transported from the vape shop to the outdoor area and could even reach ~6-8 m away from the shop.

In **Figure 4.10b**, the mean $PM_{2.5}$ was 472, 27, and 5 µg/m^3 at sites 1, 3, and 4, respectively. When the sampling location moved to 3 and 4, $PM_{2.5}$ dropped to 6% and 1%, of what was measured in the vape shop. Compared to UFPs, the stronger correlation between locations 1 and 3 ($r = 0.75$, $p < 0.001$) observed for $PM_{2.5}$ indicates that fine particles traveled to

outdoor location 3 from the vape shop despite at a low level. However, the insignificant correlation between locations 1 and 4 ($r = 0.01$, $p > 0.05$) for $PM_{2.5}$ showed that large particles hardly traveled for a long distance because EEV particle mass decreased more rapidly due to evaporation compared to particle number (Li et al. 2020a).

Previously, Zhao et al. (2017) found that only 7% of PNC and 1% of $PM_{2.5}$ remained beyond 2.5 m away from an e-cig user in an indoor environment. With more vaping events in the vape shop than a laboratory setting, our results indicate that EEV particles not only persisted in the indoor environment but also traveled to outdoor areas from the vape shop, especially for small particles. Both UFPs and $PM_{2.5}$ transported from the vape shop to outdoor areas, leading to exposure risk for passersby and patrons in the shopping strip or plaza. On the other hand, EEV particles with the capability to travel farther away may enter the neighboring business through infiltration. A trade-off should be considered between using natural ventilation as the mitigation strategy to reduce exposure to EEV aerosols. However, the natural ventilation was the only method used by the studied vape shops. Other ventilation types such as mechanical ventilation with either an exhaust or supply air system should be considered in future studies.

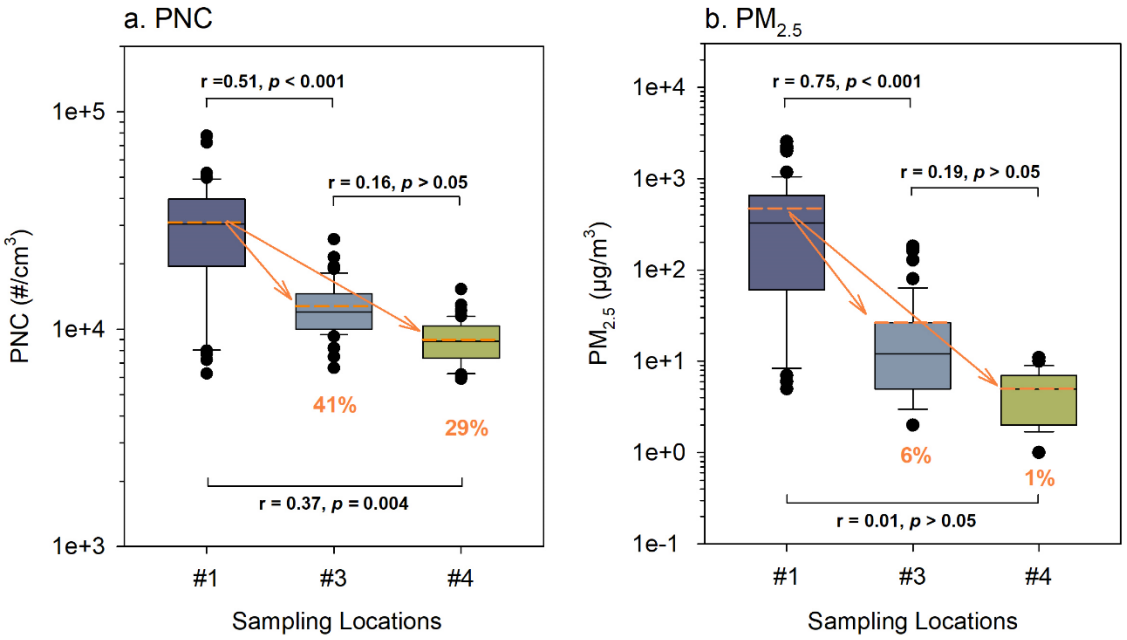


Figure 4.10. (a) PNC and (b) $PM_{2.5}$ at indoor sampling locations 1 (inside vape shop) as well as outdoor sampling locations 3 (outside ~1-3 m away from the vape shop door) and 4 (outside ~ 6-8 m away from the vape shop door) for vape shop I. The solid line in each box represents the median value, and the dash line in each box represents the mean value.

4.5. Conclusions

This is the first study that focuses on the transport of EEV aerosols from vape shops to neighboring indoor spaces in multiunit buildings and the outdoor environment. The PNC and $PM_{2.5}$ concentration in the studied vape shops were substantially higher than those in neighboring businesses and outdoor areas. Gas-phase nicotine was detected in all the studied vape shops and neighboring businesses. The results of this study indicate that EEV aerosols can transfer from the vape shops to neighboring businesses. Compared to $PM_{2.5}$, UFPs are more likely to travel to nearby indoor spaces. Under the extremely high level of $PM_{2.5}$ in the vape shop, the particle mass transfer from the vape shop to a neighboring business could also occur. Opening the door of the vape shop substantially reduced the aerosol transport from the vape shop to its neighboring

business. During door open periods, EEV aerosols, especially small particles, could transport from vape shop to outdoor areas. These data provide strong policy implications in terms of protecting employees, patrons, and bystanders from exposures to EEV aerosols in indoor and outdoor spaces adjacent to vape shops. Further research on mitigation measures is needed to better inform policy. The high levels of indoor air pollutants produced by using e-cigs call for precautionary measures to protect public health.

5. DEVELOPMENT OF A VENTILATED ARTIFICIAL LUNG SYSTEM FOR CHARACTERIZING THE PHYSICOCHEMICAL PROPERTIES OF INHALED E-CIGARETTE AEROSOLS

5.1. Abstract

Given the increasing popularity of e-cigarettes (e-cig), such as JUUL, and their potential health risks, it is important to understand how e-cig aerosols behave when inhaled into the human lungs. A ventilated artificial lung system was developed that allows physicochemical characterization of e-cig aerosols while independently controlling puffing, breathing, retention, temperature, and relative humidity (RH). We used this system to evaluate the impacts of the presence of ventilation, varying respiratory rates [10 or 15 breaths per min (BPM)], breath volumes (480 or 720 ml), and environmental conditions on particle number concentration (PNC), particle decay rates, and particle size distributions during a 4-puff vaping cycle and 10-min decay period. Three environmental conditions inside the artificial lung were created including a dry environment (3% RH, 25°C), an ambient room environment (38% RH, 25°C), and a simulated lung environment (88 % RH, 37°C). Compared to the static condition (i.e., no breath), the presence of breathing (10 BPM, 480 ml/breath) decreased the peak PNC by 35% and increased the particle decay rates from 8 to 32 h^{-1}. Increasing the respiratory rate (from 10 to 15 BPM) and breath volume (from 480 to 720 ml) resulted in enhanced particle decay rates from 32 to 80 h^{-1} in the ambient room environment. The decay rates under all breathing patterns increased by ~ 11 – 20% when changing the temperature and RH from ambient room to simulated lung conditions. As to the particle size distributions, simulated lung conditions resulted in hygroscopic particle growth that significantly enhanced the presence of supermicron (> 1 μm) e-cig particles compared to dry and ambient room conditions. This work provides novel insight into the

physiochemical transformation of inhaled e-cig particles with the effects of breathing, temperature, and RH in the respiratory system.

5.2. Introduction

Electronic cigarettes (e-cigs), such as JUUL, are increasingly popular among adolescents and young adults even though emerging data raise concerns about their health effects (Overbeek et al. 2020; Huang et al. 2019; Layden et al. 2019b). The e-cig aerosols generated by vaporizing e-liquids are fundamentally different from those generated during the combustion of conventional tobacco cigarettes (t-cigs). Although existing studies generally agree that e-cig aerosols contain lower level of toxic chemicals than t-cigs (Li et al. 2020b; Oh and Kacker 2014; Margham et al. 2016), there is still limited knowledge regarding the health effects of short- and long-term exposure to e-cig aerosols.

The physiochemical characteristics of e-cig aerosols are different from those of t-cigs (Ingebrethsen et al. 2012). Previously, e-cig particles were found highly volatile which make their size distribution sensitive to dilution and humidity (Li et al. 2020a; Luo et al. 2021; Zhao et al. 2016a; McAuley et al. 2012; Zhang et al. 2013). Nevertheless, it is not yet clear how e-cig particles behave when inhaled into human lungs. Many studies have used a conventional static exposure chamber under typical indoor room temperature and humidity to evaluate the e-cig emissions (Zhao et al. 2016b; Schripp et al. 2013; Lee et al. 2017; Li et al. 2020a; Allen et al. 2016; Zhao et al. 2016a). However, air entering the lung is rapidly humidified and warmed to body temperature as it is admixed within the lung volume and then expelled from the lung during breathing. As such, the conditions that occur within a ventilating lung are fundamentally different from those occurring within large conventional static exposure chambers. The dynamic nature of e-cig aerosols has been documented with respect to temperature, humidity, dilution,

and holding time when studied in a mixing chamber (Schripp et al. 2013; Sundahl et al. 2017; Feng et al. 2015). As particle sizes directly affect the location and mechanisms of deposition in the respiratory tract (Hinds 1999), the shifts in e-cig particle size due to breathing, temperature, and humidity need to be better understood. Although studies have extensively modeled the aerosol dynamics of e-cig aerosols in the human respiratory tract to predict the aerosol behaviors with the effects of evaporation and condensation (Pichelstorfer et al. 2016; Sosnowski and Kramek-Romanowska 2016; Feng et al. 2015; Pichelstorfer et al. 2020; Asgharian et al. 2018; Sundahl et al. 2017), there is still a lack of experimental data to support the predictions.

Understanding to what extent e-cig aerosol transformations, such as evaporation, coagulation, and hygroscopic growth in the respiratory system affect the particle size distribution may also provide insights into secondhand exposure to e-cig aerosols. Although many studies have investigated the effects of direct-emitted e-cig aerosols (Jiang et al. 2020; Baassiri et al. 2017; Luo et al. 2021; Ingebrethsen et al. 2012; Fuoco et al. 2014) as well as the exhaled aerosols by e-cig users on indoor air quality (Li et al. 2020d; Zhao et al. 2017; Scungio et al. 2018; Schripp et al. 2013; Zhang et al. 2020), how the human lung environment alters and transforms the inhaled e-cig aerosols into exhaled aerosols is largely unknown. One major difficulty lies in the lack of access to the inhaled e-cig aerosols in the human lung and the tremendous person-to-person variations that occur with respect to vaping topography, lung size, and breathing pattern.

In order to address these knowledge gaps, we developed and evaluated a ventilated artificial lung system that recapitulated major aspects of the lung environment which allowed us to assess e-cig aerosol characteristics while independently controlling puffing, breathing, retention, temperature, and humidification simulating the human respiratory conditions. The

effects of breathing, temperature, and relative humidity (RH) on the e-cig aerosols were investigated by measuring the particle number concentration (PNC), particle decay rate, as well as particle size distributions. The comparisons of different experimental conditions enabled a detailed assessment of differences between the static chamber and the ventilated lung system.

5.3. Materials and methods

5.3.1. Development of the ventilated artificial lung system

As demonstrated in **Figure 5.1a**, the ventilated artificial lung system consists of three major components: (1) a temperature-controlled and pressure-regulated artificial lung exposure chamber; (2) ventilator-controlled inspiratory and expiratory limbs with humidification; and (3) an e-cig puffing machine for aerosol generation. Chemically resistant polycarbonate sheet material was custom-fabricated into a gas-tight model that reproduced the size, shape, and volume of the average male human lung (i.e., 6 L). Two calibrated test lung balloons (Venti.Plus^{TM} Test Lung for Ventilator) were attached to the lung model, allowing expansion and contraction of the simulated lung with each breath. They were used to regulate pressure changes that occur during breathing, control the flow pattern of inhaled air, and simultaneously generate exhalation forces. Aerosol sampling ports were integrated into the system. Temperature and RH were monitored using a gas sensor (model USB-VOC100, Dracal Technologies, Quebec, Canada), and internal lung pressures were monitored using a digital manometer (model TK277PLUS, Tekoplus, Hong Kong). The lung model was assembled within a temperature-controlled chamber (– 10 °C to 100 °C, model KBF-115, Binder GmbH, Tuttlingen, Germany) equipped with an internal video recording system. A mini magnetic stirrer was introduced at the bottom of the lung chamber to create a well-mixed and suspended aerosol condition.

Active ventilation/breathing of the artificial lung (i.e., inhalation and exhalation) was managed by attaching the trachea of the chamber to a clinical-grade lung ventilator (Allied Healthcare EPV100 Portable Ventilator) fitted with an in-line humidifier (FL-9000U, Flexicare Inc.). Adjustable ventilator controls allowed for independent adjustment of inspiratory time (set for 2 s), breath volume (200 to 1200 ml), and respiratory rate (8-20 breaths per minute; BPM). Dynamic airway pressure at the ventilator source was monitored in real-time. For example, a simulated normal breath for a normal person was set at 10 BPM and 480 ml/breath, thereby creating a 6-s breath cycle (i.e., 2-s inhalation and 4-s exhalation) with a 480 ml breath. A compressed gas cylinder containing 5% CO_2/Air regulated at 50 psi powered the ventilator in order to deliver the gas composition normally occurring within the lung environment. The inspiratory limb directed each breath through the humidifier system, which could be independently controlled, through a sterile filter and then into the airway. An integrated one-way valve allowed passive exhalation to occur through an open low-resistance expiratory port. By independently controlling temperature and RH, we created three environmental conditions inside the artificial lung chamber including a dry environment (3% RH, 25°C), an ambient room environment (38% RH, 25°C), and a simulated lung environment (88% RH, 37°C).

The Virginia Tobacco-flavored JUUL pod containing 5% nicotine, which is extremely popular and accounts for nearly half of the e-cig market share in recent years (Huang et al. 2019; Williams 2020), was used in this study. An e-cig puffing machine composed of a compressed air source, JUUL pod holder (Automate Sci., Berkeley, CA, USA), and programmable timer (Arduino Uno R3 microcontroller board, Italy) to power the e-cig device was used to generate e-cig aerosols. The JUUL pod was powered at 3.7 V as recommended by the manufacturer. The flow rate of HEPA-filtered compressed air passing through the JUUL pod was set at 1 L/min

which both regulated the puff volume and delivered the generated e-cig aerosol into the inspiratory limb of the ventilator circuit. After each puff was drawn into the lung chamber, a control valve between the e-cig and inspiratory limb was closed until next puff or the end of the decay. A 4-puff vaping cycle (i.e., 2-s puff duration, 33-ml puff volume, 60-s inter-puff interval) was employed to mimic a typical puffing topography of e-cig users and the aerosol delivered into the inspiratory limb during the 2-s inhalation. The 4-puff vaping cycle (i.e., ~ 3 min) was immediately followed by a 10-min decay period, which was the washout phase with continuous breathing. As an example, **Figure 5.1b** presents the real-time particle number concentration (PNC) during the 4-puff vaping cycle and 10-min particle decay period as well as the pressure changes due to the continuous 6-s breath cycles (i.e., 2-s inhalation and 4-s exhalation) at 10 BPM and 480 ml/breath in the artificial lung chamber. In the presence of ventilation, PNC readings fluctuate, which is attributed to the pressure changes during the inhalation and exhalation process.

In order to better understand the impact of ventilation on inhaled particles, a static chamber condition was created using the same lung chamber, ventilator, and aerosol-generating conditions except for the following modifications. Only one breath was administered from the ventilator with each puff in order to deliver the e-cig aerosol into the lung. The ventilator was turned off between puffs and during the decay period after the 4-puff vaping cycle was completed.

5.3.2. Aerosol characterization and data analysis

PNC and particle size distribution were measured separately in this study (**Figure 5.1a**). The diluted PNC was monitored in real time using a Water-based Condensation Particle Counter (WCPC 3788, TSI Inc., Shoreview, MN) during a 4-puff vaping cycle (i.e., ~ 3 min) and 10-min

decay period. The data logging interval was set to 1 s. A flow rate of 0.55 L/min compressed air was used to dilute the e-cig aerosols that entered the WCPC sampling inlet. The dilution ratio is 1:7, which has been used to correct all the PNCs measured to reflect the actual values. As summarized in **Table 5.1**, the real-time PNC was measured with ventilator on and off, and under different environmental conditions and breathing patterns.

Assuming a well-mixed chamber, we used a regression of the first-order decay to determine the particle decay rates during the 10-min decay period in the absence of vaping (Schripp et al. 2008; Gong et al. 2009; Li et al. 2020a). The first-order log-linear regression is described as follows:

$$\ln\left(C_t/C_{t=0}\right) = -k \times t \qquad (1)$$

where k is the particle decay rate, t is the elapsed time, C_t and $C_{t=0}$ are PNCs in the lung chamber measured at times t and t = 0, respectively, during the decay period. The particle decay rate (k), was calculated by fitting a line to the plot of $\ln(C_t/C_{t=0})$ versus time. Due to the PNC fluctuation, the peak values were employed to calculate PNC decay rates. For each experimental condition, the particle decay rate (k) was determined from the average of triplicate measurements.

A scanning mobility particle sizer (SMPS 3080, TSI Inc.; 50 s up scan, 10 s down scan) and an Aerodynamic Particle Sizer (APS 3321, TSI Inc.) were used to measure the particle size distributions. The particle size range measured by SMPS and APS were 12 – 445 nm and 0.54 – 19.8 μm, respectively. Using a normal breathing pattern (i.e.,10 BPM, 480 ml/breath), the 1-min particle size distribution sample was collected at three time points during the decay - i.e., 0, 5, and 10 min after the last puff, respectively. To collect these samples, all ventilation was turned off at the specified time points to allow for the extended sample collection times and volumes that could not be performed in real-time. As such, each time point was measured from a separate

set of replicate lung exposures and the measures represent a "snap shot" of the particle size distribution at the indicated time. Six conditions were evaluated including the dry, ambient room, and simulated lung environments during either continuous ventilation or under static chamber conditions as already detailed. Recorded by the internal video system, the qualitative visualizations of the e-cig aerosols immediately after the 4^{th} puff (t = 0 min during the decay) for the lung model under the six experimental conditions are presented in **Figure 5.1c**. All the experimental conditions for PNC and particle size distribution measurements are demonstrated in **Table 5.1**.

All figures were generated with Sigmaplot 14.0 (Systat Software Inc., San Jose, CA). While there is a size range gap between SMPS and APS output (445 - 540 nm) and a time gap between the three discrete time points (i.e., t = 0, 5, and 10 min) during the decay, the plotting software automatically fits the data gaps by linear interpolation. All experiments were executed in triplicates.

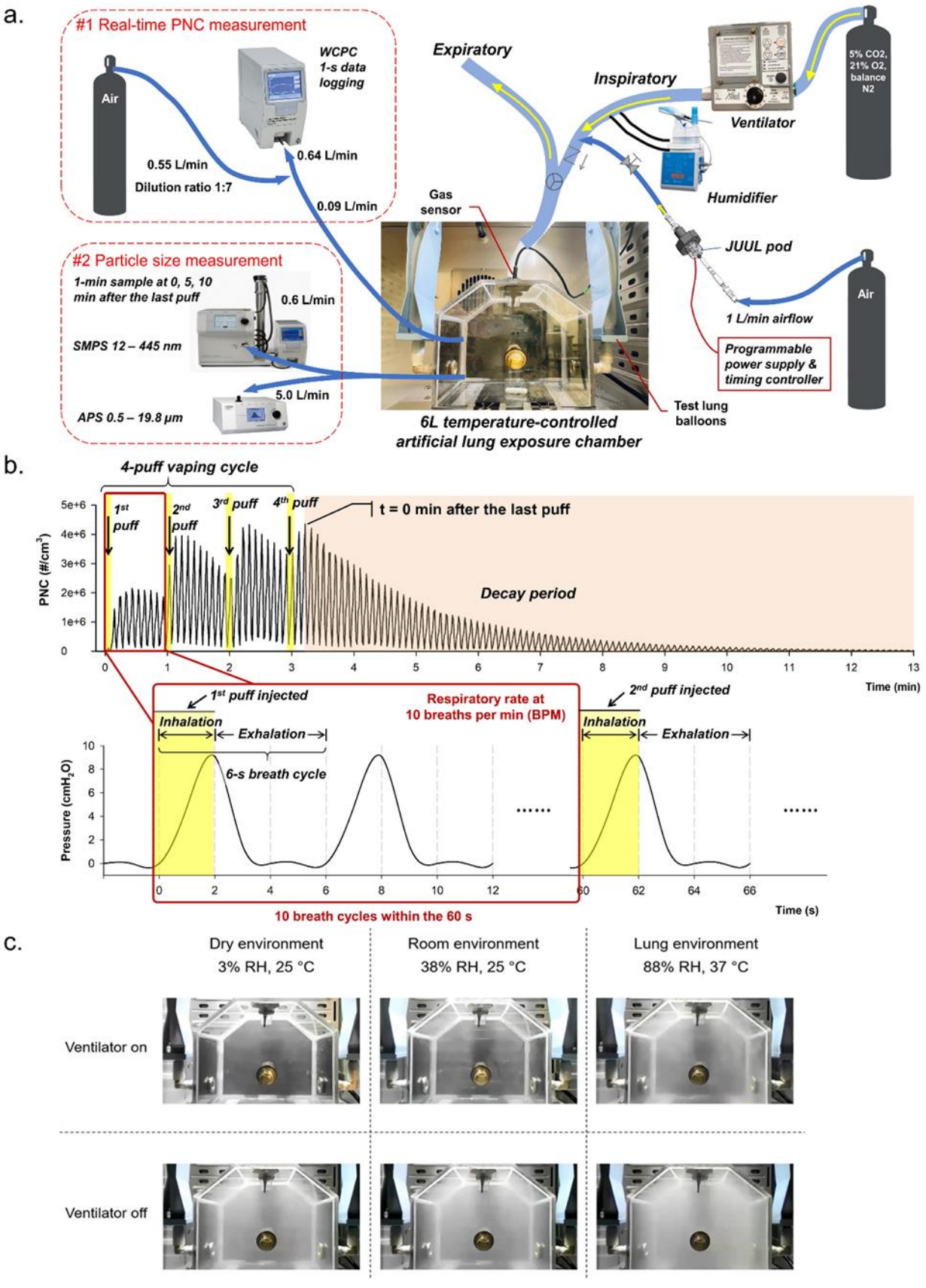

a.
#1 Real-time PNC measurement
Air
WCPC
1-s data
logging
0.55 L/min
Dilution ratio 1:7
0.64 L/min
0.09 L/min
#2 Particle size measurement
1-min sample at 0, 5, 10
min after the last puff
0.6 L/min
SMPS 12 – 445 nm
5.0 L/min
APS 0.5 – 19.8 µm
Expiratory
Inspiratory
Ventilator
5% CO2,
21% O2,
balance
N2
Humidifier
Gas
sensor
JUUL pod
Air
1 L/min airflow
Programmable
power supply &
timing controller
Test lung
balloons
6L temperature-controlled
artificial lung exposure chamber
b.
4-puff vaping cycle
1st puff
2nd puff
3rd puff
4th puff
t = 0 min after the last puff
Decay period
PNC (#/cm3)
Time (min)
1st puff injected
Inhalation
Exhalation
6-s breath cycle
Respiratory rate at
10 breaths per min (BPM)
2nd puff injected
Pressure (cmH2O)
Time (s)
10 breath cycles within the 60 s
c.
Dry environment
3% RH, 25 °C
Room environment
38% RH, 25 °C
Lung environment
88% RH, 37 °C
Ventilator on
Ventilator off

Figure 5.1. (a) Schematic diagrams of the ventilated artificial lung system with aerosol generation and lung chamber particle sampling methods; (b) The time series of PNC during a 4-puff vaping cycle and decay period as well as pressure changes due to continuous breathing at 10 BPM and 480 ml/breath; (c) Images recorded immediately after the 4^{th} puff (t = 0 min) for the lung model with the effects of ventilation and environmental conditions.

Table 5.1. Summary of experimental conditions.

Ventilator	Environmental conditions	Breathing patterns	Data collection
On	Dry (3 ± 3% RH, 25 ± 0.5°C)	10 BPM, 480 ml/breath	Particle size distribution
	Room (38 ± 3% RH, 25 ± 0.5°C)	10 BPM, 480 ml/breath	PNC, particle size distribution
		10 BPM, 720 ml/breath	PNC
		15 BPM, 480 ml/breath	PNC
		15 BPM, 720 ml/breath	PNC
	Lung (88 ± 5% RH, 37 ± 0.5°C)	10 BPM, 480 ml/breath	PNC, particle size distribution
		10 BPM, 720 ml/breath	PNC
		15 BPM, 480 ml/breath	PNC
		15 BPM, 720 ml/breath	PNC
Off	Dry (3 ± 3% RH, 25 ± 0.5°C)	N/A	Particle size distribution
	Room (38 ± 3% RH, 25 ± 0.5°C)		PNC, particle size distribution
	Lung (88 ± 5% RH, 37 ± 0.5°C)		Particle size distribution

Abbreviations: PNC = particle number concentration, BPM = breaths per min, RH = relative humidity

5.4. Results and discussion

5.4.1. Effects of ventilation and lung chamber conditions on the e-cig particle concentration and decay

Real-time temporal profiles of PNCs within the artificial lung chamber were measured during a 4-puff vaping cycle and a 10-min decay period (**Figure 5.2**). The particle decay rates were calculated under both static conditions (ventilator off) and with the ventilator on (**Figures 5.2a and d**). In addition, the effect of respiratory rate and breath volume were independently studied (**Figures**

5.2b and d), as were the environmental conditions of ambient room (38% RH, 25°C) vs. simulated lung (88% RH, 37°C) (**Figures 5.2c and d**).

A noticeable difference in PNC and particle decay rate between with and without ventilation was observed in **Figure 5.2a**. In the ambient room environment and with a normal breathing pattern (10 BPM, 480 ml/breath), the dilution-corrected peak PNC reached 4.4×10^6 #/cm^3 after 3 puffs and maintained the same level of exposure with additional puffs - i.e. reaching an equilibrium between new particles introduced by the puff and the fraction removed by ventilation. With continued breathing after the last puff, the PNC was washed out by 93% after 5 min. In comparison, the peak PNC measured under static conditions was identical to that occurring with ventilation for the first breath but subsequently accumulated to higher levels with each subsequent breath, ultimately exceeded the maximum concentration observed with ventilation by 35%. In addition, the PNC had only decreased by 54% at 5 min after the last puff. The calculated particle decay rate in the setting of a normal breathing pattern (10 BPM, 480 ml/breath) was approximately 4 times that occurred under static conditions. Overall, breathing leads to a dramatic difference in both the peak PNC and the integrated particle level over time that should be considered when modeling and setting up exposure conditions to assess e-cig toxicity.

Different breathing patterns considerably affected the particle level and washout of e-cig aerosols inhaled into the lung chamber (**Figure 5.2b**). When the respiratory rate was held constant (10 BPM) but the breath volume was increased by 1.5 fold (480 ml to 720 ml/breath) under ambient room environment, the peak PNC decreased by approximately 23% and the particle decay rate increased approximately 1.66-fold to 53 h^{-1}. Similarly, the peak PNC decreased by 48% and the decay rate increased 1.4-fold to 45 h^{-1} when the respiratory rate was increased from 10 to15 BPM but the breath volume kept constant at 480 ml. The overall impact of increasing both the respiratory

rate (10 to 15 BPM) and the breath volume (480 to 720 ml/breath) were cumulative with peak PNC decreasing by 71% and the decay rate increasing 2.5-fold to 80 h^{-1}. In addition, with the heightened ventilation rate and volume, the equilibrium between new particles introduced by the puff and the fraction removed by ventilation was achieved even earlier leading to a plateau in the peak PNC after just 2 puffs. As such, this model results in a direct but inverse correlation ($r = 0.93$) between minute ventilation (respiratory rate × breath volume) and the peak PNC exposure and a direct correlation ($r = 0.99$) between minute ventilation and PNC decay rate, replicating the established effect of ventilation on lung clearance (Ratjen et al. 2019).

Significant effects were also observed when the ventilated lung model was set up to simulate the lung environment (88 % RH, 37°C) as compared to the ambient room environment (38 % RH, 25°C; **Figure 5.2c**). With the same breathing pattern (10 breaths/min, 480 ml/breath), the higher humidity and temperature associated with the lung environment reduced the peak PNC by 18% and increased the particle decay rate from 32 to 38 h^{-1}. Furthermore, a similar increase in the particle decay rate of approximately 11 – 20% was observed under all breathing patterns when changing the temperature and RH from ambient room to simulated lung conditions (**Figure 5.2d**). The saturation environment within the lung likely facilitated rapid condensation of e-cig aerosols, resulting in enhanced droplet depositions due to the hygroscopic growth and facilitating the removal of inhaled e-cig particles in the simulated lung (Feng et al. 2015; Sosnowski and Kramek-Romanowska 2016; Pichelstorfer et al. 2016).

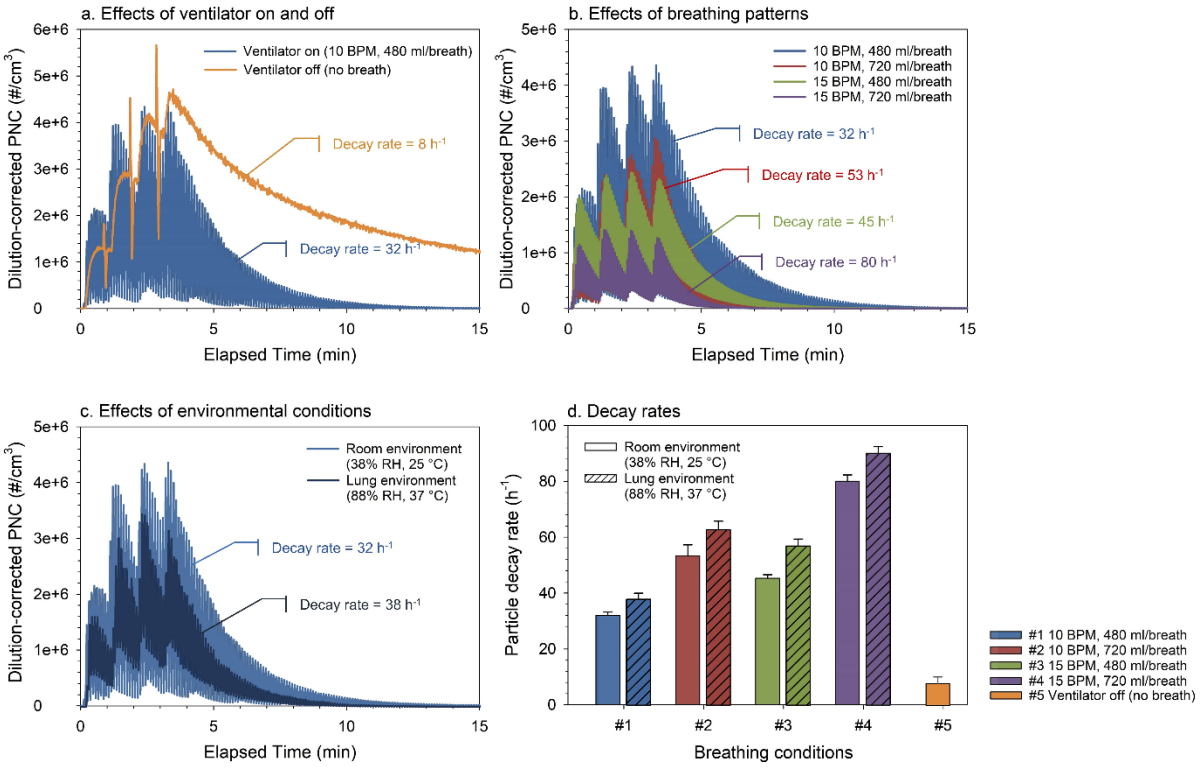


Figure 5.2. The temporal profiles of the dilution-corrected PNC during the 4-puff vaping cycle and decay period under different experimental conditions: (a) ventilator on and off (ambient room environment), (b) varying breathing patterns (ambient room environment), and (c) ambient room vs. lung environmental conditions [10 breaths per min (BPM), 480 ml/breath]. The calculated particle decay rates under all experimental conditions are presented in panel (d). Error bars show the standard deviation of the mean. Please note different scale on Y-axis.

5.4.2. Particle size distribution

The particle size distributions were measured immediately after the last puff (t = 0 min) and at 5 and 10 min thereafter during the decay period. The time-resolved particle number distributions are shown as contour plots in **Figure 5.3**. The x-axis presents the elapsed time at which data were collected, the y-axis is the particle size in log scale, and the color intensity indicates normalized

PNC (dN/dLogDp) for a given size at a given time. In the presence of ventilation, we observed a clear bimodal distribution with a primary mode at 250 nm and secondary mode at ~ 20-30 nm, and more than 90% of submicron particles were depleted within 5 min (**Figures 5.3a–c**). In contrast, the particles tended to show a single-mode distribution (~ 300 nm) and persisted for more than 10 min in the absence of breathing (**Figures 5.3d–f**). However, a less prominent secondary mode ~ 60 – 70 nm was observed in the dry environment without ventilation. The shrinking of the particle size mode is likely attributed to the faster evaporation in the dry air. The lower level of PNCs observed in the dry and lung environments compared to the ambient room environment may be explained by the following reasons: (1) the dry environment accelerated the PNC decay process by facilitating evaporation, (2) small particles were depleted by absorption of water vapor in the lung environment due to the hygroscopic effect.

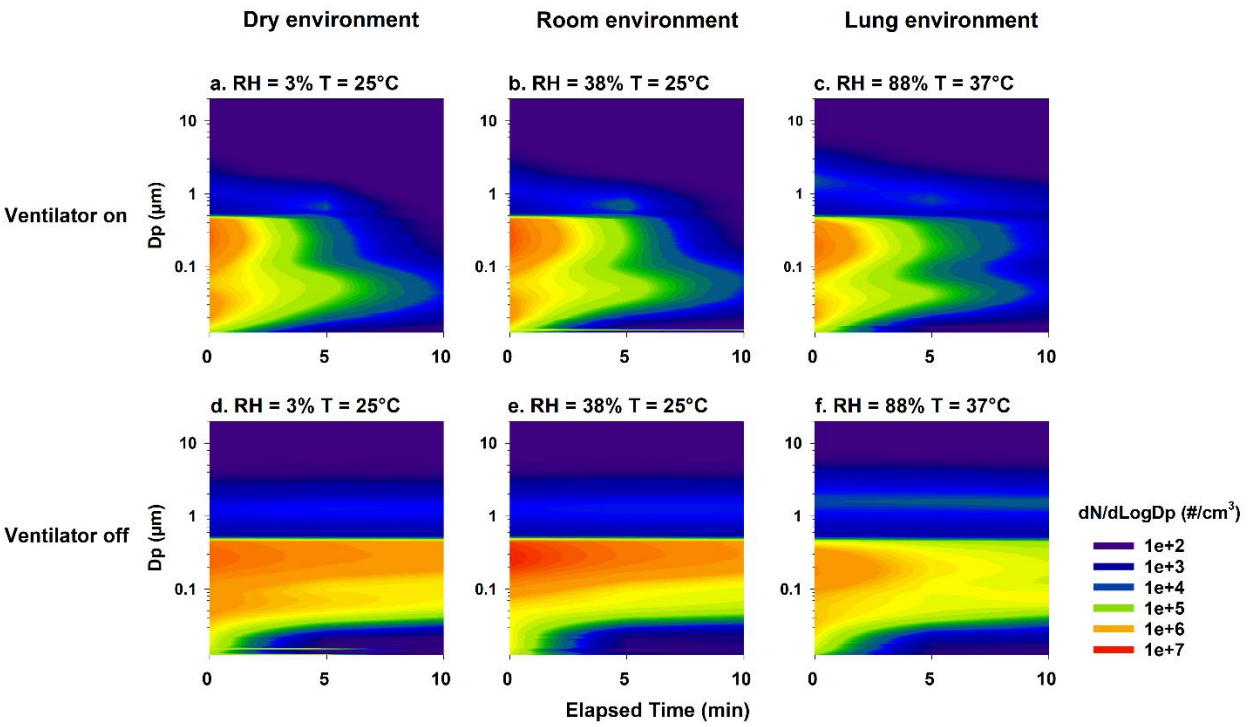


Figure 5.3. Average particle number distributions (dN/dLogDp) at t = 0, 5, and 10 min during the decay under the three environmental conditions (i.e., dry, room, and lung environments) with

ventilator on (a – c) and off (d – f). The vertical axes represent particle size on a logarithmic scale, the horizontal axes represent elapsed time in minutes during the decay, and the color scale represents particle number concentration at a certain time and diameter.

In addition to the particle number distributions, the time-resolved particle mass distributions in terms of PM mass concentration (dM/dLogDp) are shown in **Figure 5.4**. In the presence of ventilation, the PM mass concentration decayed slower when the RH increased. Compared to the dry and ambient room environments, a lower mass concentration was observed for submicron particles while the PM level of supermicron particles, especially with a diameter of 3 – 4 μm, was substantially higher in the saturated lung environment. The increase of particle sizes lasted even longer in the static chamber condition. The increase of PM mass further confirmed that the particle size grew due to the hygroscopic growth in the highly humid environment. As visualized in the images recorded at the 4th puff for the lung model (**Figure 5.1c**), the shifts to larger particle sizes from dry (or ventilated) to lung (or static) environment can be reflected by the visible "clouds" observed in the lung model. As stated in previous modeling studies (Sosnowski and Odziomek 2018; Feng et al. 2015), larger particles (> 0.5 μm) tend to grow more significantly than smaller particles resulting in mass gaining, which explained the considerable growth of supermicron particles (> 1 μm) instead of submicron particles. In the absence of breathing, the increased particle size and concentration persisted for more than 5 min and then started to slowly decay. In the highly humid lung chamber, e-cig aerosols continued to absorb water from the environment after inhaled. As the particle size increased, more enlarged particles could be removed by inertial deposition and gravitational settling.

These data provide experimental evidence showing that the dynamic changes of inhaled e-cig aerosols in the simulated lung environment. They are consistent with the results of Wright et

al. (2016), who found that glycerol particles, essential components of e-cig aerosols, gained mass from hygroscopic growth in the highly humid environment and decreased size in the dry air due to evaporation. These findings are also in good agreement with previous model predictions (Sosnowski and Odziomek 2018; Feng et al. 2015; Pichelstorfer et al. 2016), which discussed that e-cig aerosols containing volatile materials have much higher hygroscopic growth rates compared to t-cig smoke so that the increase of particle size can be more noticeable. Previously, we found that particle sizes of exhaled e-cig aerosols tend to be larger than the mainstream aerosols directly emitted from e-cig devices (Nguyen et al. 2019; Li et al. 2020d). Results from this study confirmed that the characteristics of e-cig aerosols passing through the respiratory system can be altered by the lung environment. To better understand to what extent the respiratory tract can affect e-cig aerosol exposure, future research is warranted to better estimate particle deposition and exhalation loss, considering the effects of complex branching airways.

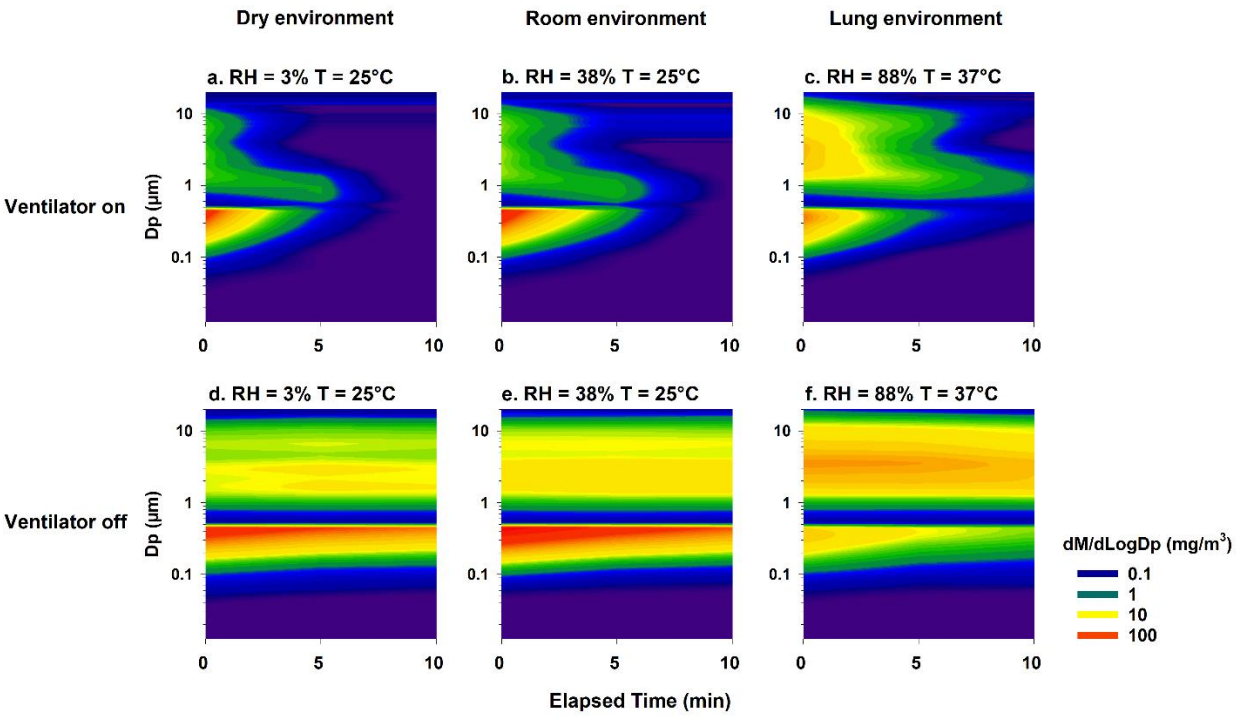


Figure 5.4. Average particle mass distributions (dM/dLogDp) at t = 0, 5, and 10 min during the decay under the three environmental conditions (i.e., dry, room, and lung environments) with ventilator on (a – c) and off (d – f). The vertical axes represent particle size on a logarithmic scale, the horizontal axes represent elapsed time in minutes during the decay, and the color scale represents PM mass concentration at a certain time and diameter.

5.5. Conclusions

We developed a dynamic ventilated artificial lung system that allowed us to replicate the inhalation of e-cig aerosols into an average-sized adult male lung and evaluate the effects of breathing pattern and physiologic lung conditions on the physicochemical characteristics of inhaled e-cig particles. Breathing and environmental conditions substantially affected both the peak particle exposure levels within the lung and the decay/clearance rates. The warm and humid

conditions that occur in the simulated lung environment (88% RH, 37°C) promoted rapid hygroscopic growth of inhaled particles and preferentially enhanced the diameters of the supermicron (> 1 μm) e-cig particles in the lung environment. This leads to higher PNC decay rates compared to what is normally measured under ambient room conditions (38% RH, 25°C). As particle number, mass, and size impact the site and rate of airway deposition, these data provide novel insights regarding the physiochemical transformation that occurs when e-cig aerosols are inhaled and the resulting lung exposure. This model also replicates the known effects of breath size, respiratory rate, and overall minute ventilation on gas exchange and clearance, providing valuable information regarding the impact of ventilation on peak particle exposure, the time to equilibrium, and the subsequent clearance of particles over time. There is a significant impact of breathing on the integrated exposure to e-cig aerosols that should be considered when modeling exposures and setting up assays to assess exposure-related toxicity. As such, this model system provides an estimation of organ-specific exposure over time that is dramatically different from and not evident when studying e-cig aerosols by conventional static chamber analysis. Data on particle size dynamics with the effects of breathing, temperature, and RH in the respiratory system can shed light on the related health effects of both inhaled and exhaled e-cig aerosols.

6. CONCLUSIONS

In this dissertation, we first summarized the evidence regarding the impacts of e-cig use on indoor air quality and human health. The results confirm that e-cigs degrade indoor air quality and pose risks of secondhand exposure to bystanders. The PM pollution levels, including both UFP and $PM_{2.5}$, due to e-cig use are comparable to t-cig smoking in the indoor environment. E-cig emissions can be affected by various factors such as device type, heating coil temperature, power voltage, e-liquid compositions, vaping topography, and the process of inhalation and exhalation. As expected, e-cig emissions contain fewer carcinogenic and toxic compounds than t-cig smoke, but substantial amounts of vaporized PG, VG, nicotine, and their degradation byproducts (e.g., aldehydes) are still identified. Although at lower levels, the chemical compositions in the secondhand/exhaled e-cig aerosols are similar to those of mainstream emissions. Current health effect studies focus on acute effects and early biomarkers, suggesting potential respiratory and cardiovascular effects from e-cig aerosols. However, these studies are limited and inconsistent, warranting large-cohort and long-term exposure studies to explore the relationship between e-cig emissions and clinical endpoints.

Understanding the dynamic characteristics of inhaled and exhaled e-cig aerosols can provide insights into deposition mechanisms of particle exposure in the respiratory system and guide exposure assessment. To explore the effects of intrinsic factors – e-liquid compositions on the dynamic and emissions of e-cig aerosols, we have characterized the e-cig aerosols generated with different PG/VG ratios with and without nicotine in terms of PNC, $PM_{2.5}$ concentration, particle loss rate, and size distribution. Our results show that particle emission factors have been associated with the e-liquid compositions. We observed a significant interaction effect of nicotine and PG/VG ratio on the particle loss rate. In the absence of nicotine in the e-liquid, the

particle loss rate increased with increasing PG levels. On the contrary, the particle loss rate has been negatively associated with PG content when nicotine is added to the e-liquid. These findings indicate that e-liquid compositions are strong determinants of e-cig emissions and dynamics, which should be accounted for in exposure assessment.

To understand the effects of e-cig use on indoor air quality in real world, we evaluated the transport of secondhand e-cig aerosols from vape shops to their neighboring businesses in multiunit buildings. The PNC and $PM_{2.5}$ concentrations in the vape shops were found positively correlated with those in the neighboring indoor spaces and outdoor environments. The tracer gas-phase nicotine was detected in all the studies pairs of vape shops and neighboring businesses. Notably, UFPs tend to reach farther distance compared to larger particles. Natural ventilation through door opening largely reduced the aerosol transfer between two neighboring spaces. The findings indicate that e-cig aerosols due to vaping can transfer between spaces in multiunit buildings and transport to outdoor areas, suggesting the secondhand exposure risk for passersby and patrons in the nearby areas. This work provides important policy implications in terms of protecting bystanders from secondhand exposure to e-cig aerosols.

Although we have investigated the mainstream e-cig emissions and secondhand exposure, little is known about the difference between physiochemical characteristics of direct-emitted e-cig aerosols and those of exhaled e-cig aerosols by e-cig users. Therefore, we have developed and evaluated a ventilated artificial lung system to better understand how e-cig particles behave after inhaled and how the lung environment changes and transforms the e-cig aerosols into exhaled aerosols. We found that breathing and environmental conditions substantially affected the particle emission and decay rate. The size of e-cig particles undergoing hygroscopic effects largely increased in the simulated lung environment (88% RH, 37°C),

resulting in higher particle decay rates attributed to the more efficient deposition and gravitational settling. These findings on particle decay and size dynamics with the effects of breathing, temperature, and RH in the respiratory system provide experimental data for modeling respiratory deposition and novel insights into the physiochemical transformation of inhaled e-cig aerosols.

In sum, the use of e-cigs generates substantial amounts of $PM_{2.5}$, UFPs, and nicotine in the air, leading to risks of secondhand exposure and related health effects. We found that e-liquid compositions, inhalation and exhalation process in the human lung, and environmental conditions with varying temperature and humidity significantly impact the emissions and dynamics of e-cig aerosols. In addition, e-cig aerosols produced by vaping have the capability to transport between neighboring spaces in multiunit buildings, where the exhaled aerosols can be affected by the air exchange rate, ventilation, dilution, vaping density (puffs/h/100m^3), and distance. Future studies need to consider the complexity of e-liquid compositions and respiratory system for assessing the vulnerable populations' exposure to secondhand e-cig aerosols.

APPENDIX

Supplementary materials for Chapter 2

Table A-1. Summary of $PM_{2.5}$ and PNC levels, background concentration, emission protocol, room size, and air exchange rate for studies in Figure 2.2.

A. $PM_{2.5}$

Study	Location	Mean, $\mu g/m^3$	Background, $\mu g/m^3$	Emission Protocol	Room Size, m^3	Air Exchange Rate, h^{-1}
E-cig Aerosols						
Melstrom et al. (2017)	Laboratory room	1121 ± 2430	18 ± 15	3 volunteers use e-cigs for 2 h	53	5.0
Nguyen et al. (2019)	6 vape shops	766 ± 1442	12 ± 6	An average of 3.9 puffs per min generated by e-cig users	168-323	0.1-4.8
Soule et al. (2017)	An e-cig vaping event in a hotel	607 ± 212	3 ± 1	A 2-day e-cig event with 59-86 active e-cig users	4023	NA
Volesky et al. (2018)	Laboratory room	290	2	1 e-cig user generated 7 puffs with 4-s puffing duration	38	NA
Zhao et al. (2017)	Laboratory room	188 ± 433	8 ± 1	1 volunteer used e-cigs with 3-s puffing duration, 3-s hold, and 24s pause for 10 min	80	4.1
Schober et al. (2013)	Laboratory room	197 ± 193	6	3 volunteers used e-cigs for 2 h	45	0.6
Czogala et al. (2014)	Laboratory room	152 ± 87	32 ± 30	5 dual volunteers used e-cigs twice for 5 min with a 30-min interval	39	2.6

Ruprecht et al. (2017)	Laboratory room	ND	0	Volunteers used e-cigs for 2 to 3 h; one puff per min for about 7 min, followed by 3 min hold	48	1.5
T-cig Aerosols						
Forster et al. (2018)	Laboratory room	1129 ± 466	6 ± 4	Volunteers smoked a puff every 30 s for 8 puffs.	38	1.2-7.7
Czogala et al. (2014)	Laboratory room	819 ± 229	32 ± 30	5 volunteers smoked twice for 5 min with a 30-min interval	39	2.6
Kungsjulniti et al. (2015)	Smoking rooms in international airports	533	14	NA	NA	NA
Ruprecht et al. (2017)	Laboratory room	500 ± 128	0	Volunteers smoked for about 7 min with 3-min intervals	48	1.5
Loffredo et al. (2016)	15 cafes and 5 restaurants allowed smoking	433 ± 217	72-81	T-cigs and waterpipes smoking observed at all sampling locations	128-235	NA
Höllbacher et al. (2017)	Laboratory room	374	0	1 volunteer smoked t-cigs for 30 min	30	0.5
Acevedo-Bolton et al. (2014)	Laboratory room	267	3-8	1 volunteer smoked 1 or 2 t-cigs for 5-10 min	121 or 460	NA
Movsisyan et al. (2014)	A hospital before smoking ban	222	NA	High frequency of smoking t-cigs observed in multiple locations in the hospital before smoking ban	NA	NA
Zhou et al. (2016)	A smoking-permitted area (i.e., employee break room) in a casino	164	23	25-43 active smokers in the smoking-permitted area in the casino	NA	NA
Shamo et al. (2015)	78 restaurants before smoking ban	126 ± 109	12 ± 23	20% smoking prevalence, 2.6 active smokers per restaurant, 1.11 burning t-cigs per 100 m^3	NA	NA

Kim et al. (2016a)	62 hospitality venues (i.e., restaurants and bars) before smoking ban	109 ± 2	46 ± 2	Smoking observed in 25 hospitality venues	90-1680	NA
Scheitel et al. (2016)	Smoking in a car	105 ± 21	2	1 volunteer smoked 1 or 2 t-cigs in a car	NA	NA
Kim et al. (2016b)	75 bars before smoking ban	98 ± 2	25 ± 2	Smoking was observed in 68-96% of the 75 sampled bars before smoking ban	NA	NA
Buettner-Schmidt et al. (2015)	135 hospitality venues (i.e., bars and restaurants)	88 ± 122	9	0.3 buring t-cigs per 100 m^3, smoking observed in 42% of the hospitality venues	494 ± 601	NA
Liu et al. (2014)	114 restaurants and bars	70 ± 124	NA	3.7 % smoking prevalence, 0.3 active smokers observed per 100 m^3	NA	4.5 (range: 0-14)

B. PNC

Study	Location	Mean, particles/cm^3	Background, particles/cm^3	Emission Protocol	Room Size, m^3	Air Exchange Rate, h^{-1}
E-cig Aerosols						
Schober et al. (2014)	Laboratory room	61682 ± 17524	4466	3 volunteers used e-cigs for 2 h	45	0.6
Nguyen et al. (2019)	6 vape shops	60667 ± 52296	14580 ± 7845	an average of 3.9 puffs per min generated by e-cig users	168-323	0.1-4.8
Melstrom et al. (2017)	Laboratory room	34961 ± 27992	3707 ± 823	3 volunteers used e-cigs for 2 h	53	5.0
Zhao et al. (2017)	Laboratory room	24800 ± 21400	6390 ± 158	1 volunteer used e-cigs with 3-s puffing duration, 3-s hold, and 24s pause for 10 min	80	4.1

Ruprecht et al. (2017)	Laboratory room	8657 ± 560	0	Volunteers used e-cigs for 2 to 3 h; one puff per min for about 7 min, followed by 3 min hold	48	1.5
Scungio et al. (2018)	Laboratory room	7690 ± 169	NA	1 volunteer used e-cigs for 10 min at 0.7-1.5 puffs/min	40	0.2
Volesky et al. (2018)	Laboratory room	7169	1389	1 e-cig user generated 7 puffs with 4-s puffing duration	38	NA
T-cig Aerosols						
Forster et al. (2018)	Laboratory room	210000 ± 75500	4297 ± 4639	Volunteers smoked a puff every 30 s for 8 puffs.	38	1.2-7.7
Ruprecht et al. (2017)	Laboratory room	122672 ± 37327	0	Volunteers smoked for about 7 min with 3-min intervals	48	1.5
Scheitel et al. (2016)	Smoking in a car	113998 ± 34382	15545	1 volunteer smoked 1 or 2 t-cigs in a car	NA	NA
Konstantopoulou et al. (2014)	A bar/restaurant before smoking ban	27172	12509	An average of 4 smokers observed	NA	NA

Supplementary materials for Chapter 3

Table A-2. Summary of studies on particle size distribution of e-cigarette (e-cig) aerosols.

Study	Type	E-cig device	E-liquid		Flow Rate (L/min)	Puff duration (s)	Puff interval	PNC (#/cm^3)	Dilution ratio or AER	Particle size distribution	Instrument
			nicotine	PG/VG							
Ingebrethsen et al. 2012	M	Cigalike	NA	NA	0.825-1.65	2-4	NA	~10^9	1:1	CMD = 296 - 458 nm	Spectral Transmission
									3400-5500:1	CMD= 14-18 nm	Electrical mobility particle sizer
McAuley et al. 2012	M	Cigalike	2.4% or 2.6 %	NA	0.75	4	30 s	~10^3	Room size 40 m^3; AER= 0.3 h^{-1}	Mode at 40 nm, 100 nm, 300 nm, 1 um, and 2 um	Wide range particle spectrometer
Zhang et al. 2013	M	NA	NA	100/0	NA	NA	30 s	~10^5	50 ml chamber	One puff: single mode at 117 nm; steady state: bimodal at 371 nm	Scanning mobility particle sizer
				0/100						One puff: single mode at 180 nm; steady state: bimodal at 414 nm	
Schripp et al. 2013	M	Tank-style	0% or 1.8%	NA	NA	3	NA	~10^5	10L glass chamber; AER = 3 h^{-1}	Bimodal at 30 and 100 nm; shifts to a single mode with increasing temperature or aging	Fast mobility particle sizer
	S					3	60 s	~10^3	8 m^3 chamber; AER = 0.3 h^{-1}	Bimodal at 30 and 100 nm	
Fuoco et al. 2014	M	Tank-style & cigalike	0%-1.8%	NA	1	2	30 s	~10^9	880:1	Bimodal at 10 and 150 nm; single modes at 120-165 nm	Fast mobility particle sizer
Manigrasso et al. 2015	M	Tank-style	0%, 1.2%, 1.4% or 1.8%	NA	1	2	30 s	~10^9	880:1	Single mode range 107-165 nm	Fast mobility particle sizer

Zhao et al. 2016	M	Cigalike	0%	NA	1	3	30s	~10^9	6400:1	Single mode range 18-29 nm	Scanning mobility particle sizer
Mikheev et al. 2016	M	Tank-style	0%-2.4%	NA	0.9	5	NA	10^7-10^8	30:1	Bimodal, CMD=11-15 and 96-175 nm	Differential Mobility Spectrometer
					0.9	5	NA	10^7-10^8	3180:1	Bimodal, CMD=16 and 75 nm	
					0.9	5	NA	10^7-10^8	10600:1	Bimodal, CMD=16 and 81 nm	
					0.9	5	NA	10^7-10^8	26500:1	Bimodal, CMD=17 and 82 nm	
Zhao et al. 2017	S	E-cig user & cigalike	0% or 2.4%	NA	NA	3	27 s	~10^4	Room size 80 m^3; AER = 4.1 h^{-1}	Bimodal at 15 and 85 nm	Scanning mobility particle sizer
Baassiri et al. 2017	M	Tank-style	1.8%	100/0, 70/30, 0/100	1	4	10 s	10^9-10^{10}	1450:1	PG/VG=100/0: bimodal, CMD 44 nm; PG/VG=70/30: bimodal, CMD= 81 nm; PG/VG= 0/100: bimodal, CMD=81 nm	Electrical mobility particle sizer
Floyd et al. 2018	M	Tank-style	2.4%	67/33	1.2	3	30 s	~10^7	4480: 1 or 14933: 1	Trimodal at 40, 200, and 1000 nm	Scanning mobility particle sizer and aerodynamic particle sizer
Mikheev et al. 2018	M	A cigalike & two tank-style	0.6%-0.9%	50/50	0.9-2.7	5	60 s	10^7-10^8	30:1	Bimodal changed to tri-modal with higher flow rate; 1) CMD 110-117 nm using SCS puff machine; 2) CMD 225-259 nm using HPP2 puff machine	Differential Mobility Spectrometer
Zervas et al. 2018	M	Tank-style	0% or 1.2%	50/50	NA	120	NA	10^6-10^7	no dilution	Bimodal at ~15 and 200-400 nm	Scanning mobility particle sizer
Scungio et al. 2018	M	Tank-style	0% or 1.2%	NA	1	2	30 s	~10^8	~880-1000:1	Single mode at 34 nm	Fast mobility particle sizer

	S	E-cig user vaped	NA	NA	NA	NA	0.7-1.5 puffs/min	~10^3	Room size 40 m^3; AER = 0.2 h^{-1}	Bimodal at 30 and 90 nm	Fast mobility particle sizer
Nguyen et al. 2019	S	Vape shop	NA	NA	NA	NA	0.53 puff/min	10^4-10^5	Room size 244 m^3; AER = 1.7 h^{-1}	Bimodal of 60 and 250 nm	Scanning mobility particle sizer

Abbreviations: M, mainstream; S, secondhand; e-cig, electronic cigarette; AER, air exchange rate; PNC, particle number concentration; PG, propylene glycol; VG, vegetable glycerin; NA, not applicable.

Table A-3. Properties of chemical compounds used in this study at 20 ºC and 1 atm.

Chemical Properties	**di-2-ethylhexyl sebacate (DEHS)**	**Vegetable Glycerin (VG)**	**Nicotine**	**Propylene Glycol (PG)**
Chemical Formula	$C_{26}H_{50}O_4$	$C_3H_8O_3$	$C_{10}H_{14}N_2$	$C_3H_8O_2$
CAS Number	122-62-3	56-81-5	54-11-5	57-55-6
Molecular Weight (g/mol)	426.67	92.09	162.23	76.09
Density (g/mL)	1.120	1.261	1.010	1.036
Dynamic Viscosity (Pa·s)	0.021	1.412	0.004	0.042
Saturation Vapor Pressure (Pa)	1.20E-06	0.01	5.3	20
Henry's Law Constant ($Pa \cdot m^3/mol$)	8.61	9.75E-06	8.20E-04	1.20E-03

Table A-4. A summary of log-linear regression analyses on log-normalized PNC and $PM_{2.5}$.

Log-linear Regression Data Summary	PNC		$PM_{2.5}$	
PG/VG/Nic	**Slope**	R^2	**Slope**	R^2
0/100/0	1.92	*0.93*	6.76	*0.96*
10/90/0	1.90	*0.95*	6.85	*0.96*
30/70/0	2.09	*0.96*	7.08	*0.96*
50/50/0	2.08	*0.97*	6.51	*0.96*
100/0/0	2.20	*0.96*	7.16	*0.90*
0/100/2.4	1.89	*0.97*	6.54	*0.97*
10/90/2.4	1.86	*0.96*	7.02	*0.97*
30/70/2.4	1.85	*0.98*	6.91	*0.97*
50/50/2.4	1.84	*0.99*	5.98	*0.96*
100/0/2.4	1.64	*0.98*	5.40	*0.96*
DEHS	1.56	*0.98*	1.95	*0.99*

Coagulation during the decay

Based on the SMPS data, the count median diameter (CMD) and geometric standard deviation (GSD) were used to estimate the average coagulation coefficient ($\bar{K}$) according to the equation (S1) (Hinds 1999; Lee and Chen 1984):

$$\overline{K} = \frac{2kT}{3\eta}\left(1+\exp(\ln^2\sigma_g)+\frac{2.49\lambda}{CMD}[\exp(0.5\ln^2\sigma_g)+\exp(2.5\ln^2\sigma_g)]\right) \quad \text{(S1)}$$

Where λ is mean free path, CMD is count median diameter, σ_g is the GSD, k is the Boltzmann's Constant, η is the gas viscosity, T is the absolute temperature. Because the experiments were conducted under the condition of 297K and 101 kPa, we obtained λ = 0.067 μm and $\eta = 1.82\times 10^{-5}$ N.s/m^2. At the initial concentrations ($C_{t=0}$) before the decay started, the e-cig aerosols from all tested e-liquid mixtures showed a similar size distribution with a similar CMD (i.e., ~ 175 nm) and GSD (i.e., ~2.35). Thus, the $\bar{K}$ was determined to be ~ 1.53×10^{-9} cm^3/s. Then, equation (S2) (Hinds 1999) was used to calculate the PNC as a function of time by coagulation, assuming the average coagulation coefficient ($\bar{K}$) to be a constant:

$$\frac{1}{C_t}-\frac{1}{C_{t=0}} = \overline{K}t \quad \text{(S2)}$$

Where $C_{t=0}$ is the initial concentration before decay started, C_t is the concentration at time t. The calculated t_{50} (i.e., time to achieve 50% $C_{t=0}$) solely due to coagulation was approximately 5-6 hours, which was 14-17 times longer than the overall t_{50} (i.e., ~ 20 min) for all the e-liquid mixtures summarized in Table 1. Therefore, coagulation during the decay was determined negligible compared to other particle loss mechanisms in this study. Additionally, the concentration changes due to coagulation were similar across all the e-liquid mixtures.

Supplementary materials for Chapter 4

Table A-5. Ventilation and sampling details of the nine studied vape shops and their neighboring businesses.

Vape Shops	Ventilation Type	Supply air from outdoor and approach	Particle sampling time with door kept open (h)	[a]Frequency of door opening during door closed periods (times/h)	Total particle sampling time (h)	Total nicotine sampling time (days)	[b]Shared ventilation system
A	Natural Ventilation	Yes, door open	5.8	12	32	3	Yes
B	Natural Ventilation	Yes, door open	5.0	NA	25	3	Yes
C	Window A/C	No	/	5	27	4	Yes
D	Rooftop A/C with a mixing fan	No	/	12	26	5	Yes
E	Rooftop A/C	No	/	9	26	3	No
F	Rooftop A/C	No	/	15	18	5	Yes
G	Rooftop A/C	No	/	/	/	5	Yes
H	Rooftop A/C	No	/	/	/	3	Yes
I	Rooftop A/C or natural ventilation	Yes, door open	7.5	16	26	4	Yes

[a]During the periods of door closed, customers occasionally walked in and out with the door opening and closing

[b]The ventilation systems were off for all studied pairs during all sampling days

Table A-6. The mean (SD) PNC and $PM_{2.5}$ concentrations in the vape shops, neighboring businesses, and outdoor area (sampling location 3) for the six pairs A-F.

Pairs of Shops	PNC (particles/cm^3)			$PM_{2.5}$ (µg/m^3)		
	Vape Shop	Neighboring business	Outdoor	Vape Shop	Neighboring business	Outdoor
A	30714 (26920)	6814 (1536)	9497 (5815)	373 (551)	15 (9)	8 (6)
B	37098 (20962)	11902 (9851)	26967 (24750)	374 (525)	11 (10)	21 (49)
C	32550 (25998)	17983 (7339)	22679 (12800)	379 (775)	25 (48)	12 (11)
D	23331 (13154)	5604 (343)	8634 (2832)	189 (457)	10 (8)	8 (4)
E	26995 (22008)	9894 (6206)	7141 (3390)	89 (171)	31 (19)	9 (4)
F	14387 (4563)	7214 (4059)	6191 (2365)	30 (34)	11 (5)	13 (3)

Table A-7. The median (IQR) PNC and $PM_{2.5}$ concentrations in the vape shops, neighboring businesses, and outdoor area (sampling location 3) for the six pairs A-F.

Pairs of Shops	PNC (particles/cm^3)			PM2.5 (µg/m^3)		
	Vape Shop	Neighboring business	Outdoor	Vape Shop	Neighboring business	Outdoor
A	21629 (14639, 36590)	6625 (5800, 7536)	7807 (5158, 12052)	66 (6, 620)	13 (7, 22)	7 (3, 10)
B	34631 (20168, 50479)	8423 (3955, 16470)	16419 (11283, 37129)	134 (33, 541)	9 (6, 10)	4 (2, 14)
C	25878 (15845, 39093)	16904 (12306, 21793)	18487 (13165, 28752)	44 (11, 404)	15 (7, 24)	9 (6, 14)
D	19614 (14518, 27212)	5629 (5372, 5878)	7463 (6730, 9905)	15 (6, 145)	8 (5, 11)	8 (5, 9)
E	17433 (11269, 40493)	7248 (5661, 13082)	7093 (4195, 9204)	26 (7, 90)	28 (17, 42)	9 (7, 11)
F	13859 (10603, 17087)	5711 (3633, 9796)	5481 (4515, 7443)	19 (11, 34)	13 (5, 15)	13 (10, 16)

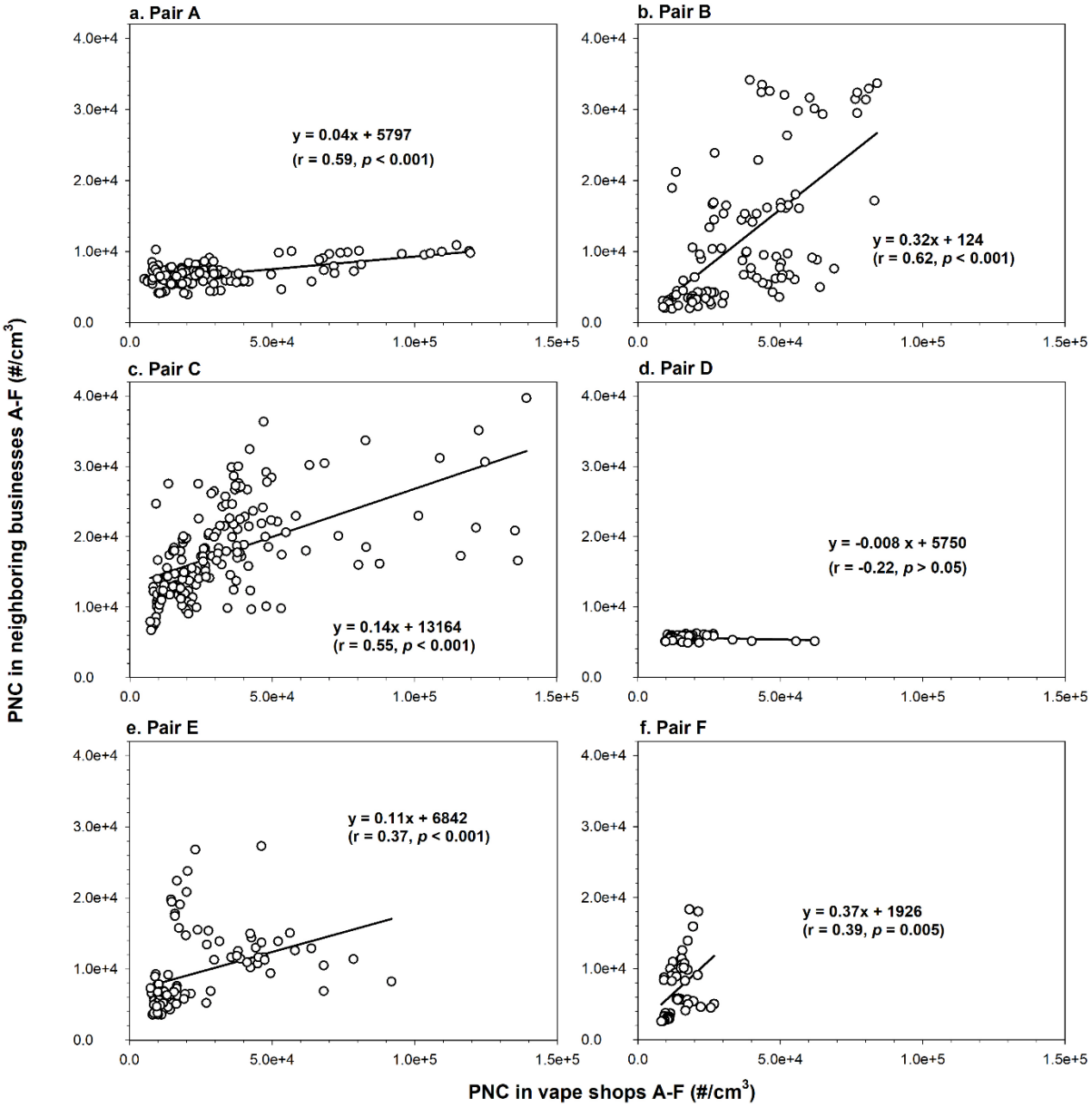


Figure A-1. Correlations between 10-min averaged PNCs in vape shops and neighboring businesses A-F. Linear regression equations and lines are provided.

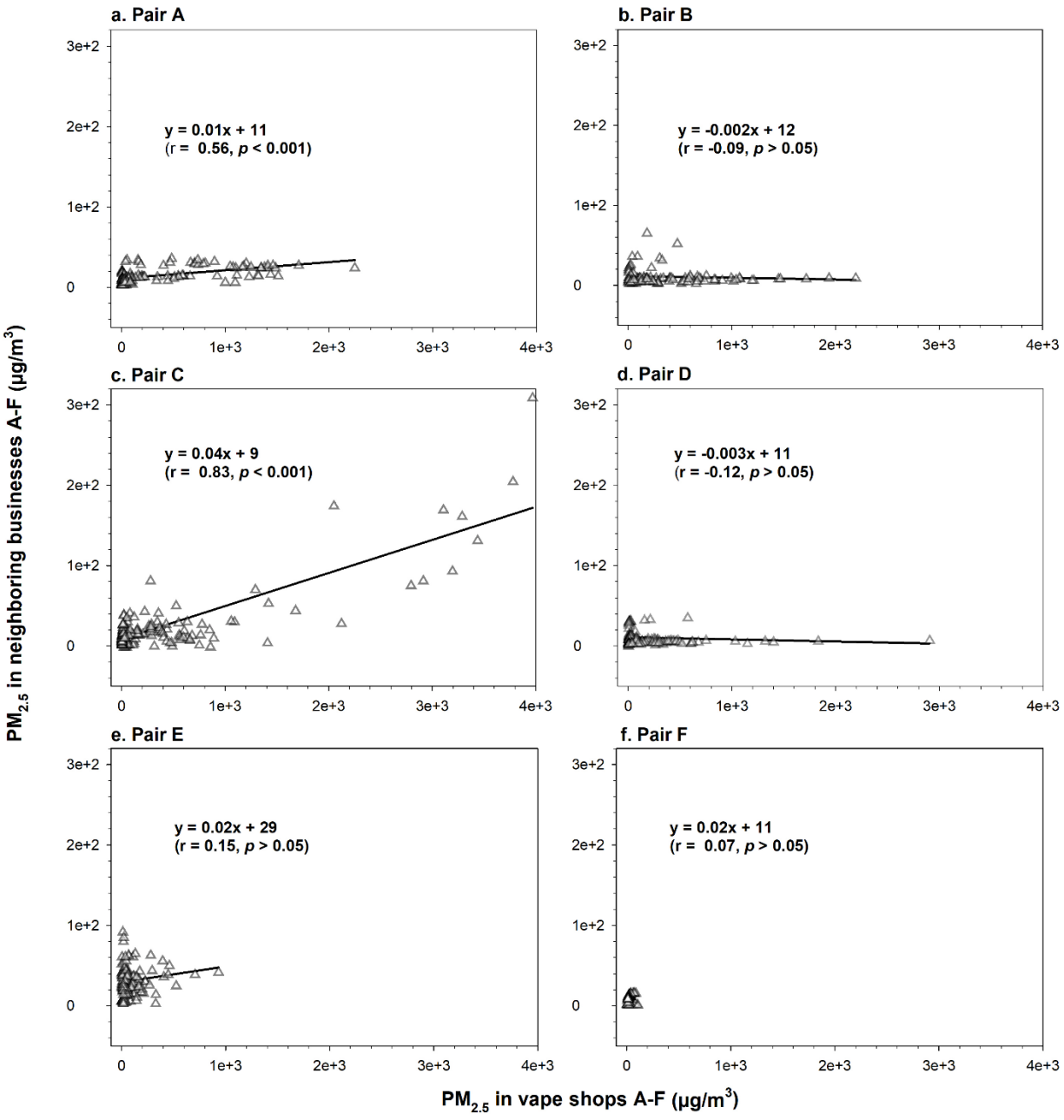


Figure A-2. Correlations between 10-min averaged $PM_{2.5}$ in vape shops and neighboring businesses A-F. Linear regression equations and lines are provided.

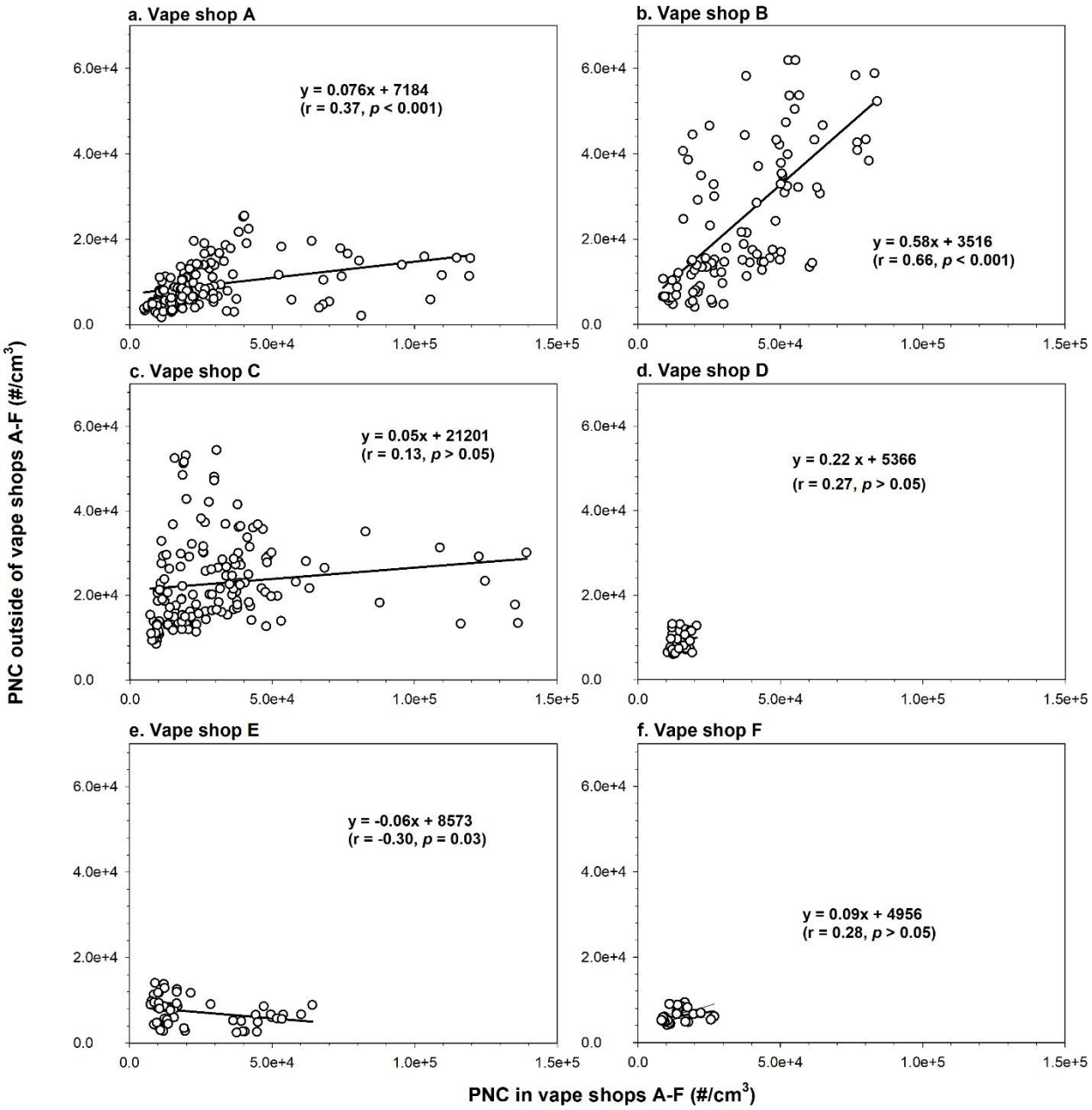


Figure A-3. Correlations between 10-min averaged PNC inside and outside vape shops A-F.

Linear regression equations and lines are provided.

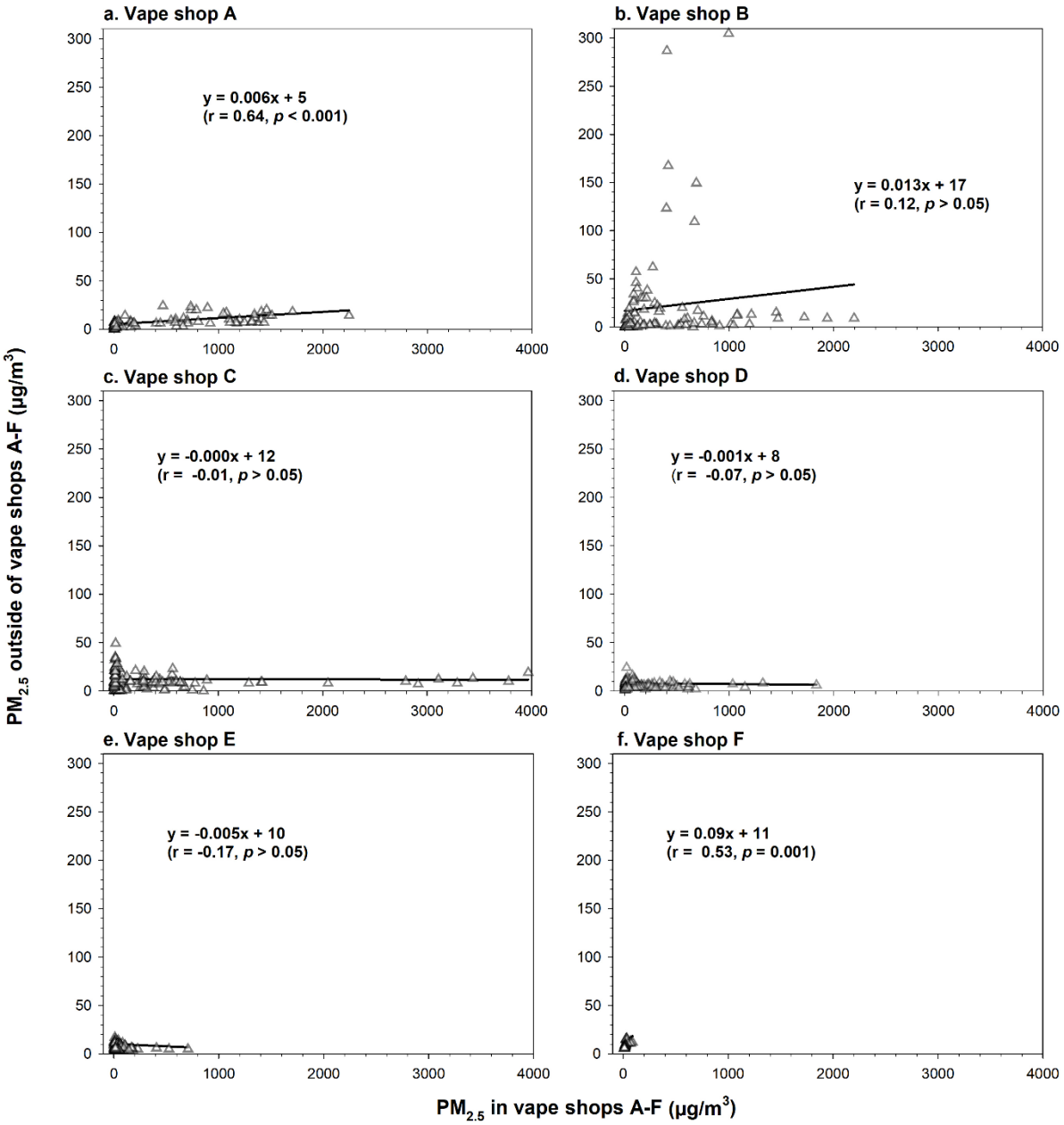


Figure A-4. Correlations between 10-min averaged $PM_{2.5}$ inside and outside vape shops A-F. Linear regression equations and lines are provided.

7. REFERENCES

Abramovitz A, McQueen A, Martinez RE et al. (2015) Electronic cigarettes: The nicotyrine hypothesis. Medical Hypotheses 85 (3):305-310. doi:10.1016/j.mehy.2015.06.002

Adroit Market Research (2018) Global E-Cigarette Market Size 2017 by Type (Disposable, Rechargeable, Modular), By Region and Forecast 2018 to 2025.

Agbenyikey W, Wellington E, Gyapong J et al. (2011) Secondhand tobacco smoke exposure in selected public places (PM2.5 and air nicotine) and non-smoking employees (hair nicotine) in Ghana. Tobacco Control 20 (2):107-111. doi:10.1136/tc.2010.036012

Ali FRM, Diaz MC, Vallone D et al. (2020) E-cigarette Unit Sales, by Product and Flavor Type - United States, 2014-2020. MMWR Morb Mortal Wkly Rep 69 (37):1313-1318. doi:10.15585/mmwr.mm6937e2

Allen JG, Flanigan SS, LeBlanc M et al. (2016) Flavoring Chemicals in E-Cigarettes: Diacetyl, 2,3-Pentanedione, and Acetoin in a Sample of 51 Products, Including Fruit-, Candy-, and Cocktail-Flavored E-Cigarettes. Environmental Health Perspectives 124 (6):733-739. doi:10.1289/ehp.1510185

Alzahrani T, Pena I, Temesgen N et al. (2018) Association Between Electronic Cigarette Use and Myocardial Infarction. American Journal of Preventive Medicine 55 (4):455-461. doi:10.1016/j.amepre.2018.05.004

Amalia B, Liu X, Lugo A et al. (2020) Exposure to secondhand aerosol of electronic cigarettes in indoor settings in 12 European countries: data from the TackSHS survey. Tobacco Control:tobaccocontrol-2019-055376. doi:10.1136/tobaccocontrol-2019-055376

American Nonsmokers' Rights Foundation (2019) Electronic smoking devices and secondhand aerosol. American Nonsmokers' Rights Foundation, Berkeley, CA

Anderson JO, Thundiyil JG, Stolbach A (2012) Clearing the Air: A Review of the Effects of Particulate Matter Air Pollution on Human Health. Journal of Medical Toxicology 8 (2):166-175. doi:10.1007/s13181-011-0203-1

Antoniewicz L, Bosson JA, Kuhl J et al. (2016) Electronic cigarettes increase endothelial progenitor cells in the blood of healthy volunteers. Atherosclerosis 255:179-185. doi:10.1016/j.atherosclerosis.2016.09.064

Asgharian B, Price OT, Rostami AA et al. (2018) Deposition of inhaled electronic cigarette aerosol in the human oral cavity. Journal of Aerosol Science 116:34-47. doi:https://doi.org/10.1016/j.jaerosci.2017.11.014

Baassiri M, Talih S, Salman R et al. (2017) Clouds and "throat hit": Effects of liquid composition on nicotine emissions and physical characteristics of electronic cigarette aerosols. Aerosol Science and Technology 51 (11):1231-1239. doi:10.1080/02786826.2017.1341040

Ballbè M, Martínez-Sánchez JM, Sureda X et al. (2014) Cigarettes vs. e-cigarettes: Passive exposure at home measured by means of airborne marker and biomarkers. Environmental Research 135:76-80. doi:10.1016/j.envres.2014.09.005

Batterman S (2017) Review and Extension of CO2-Based Methods to Determine Ventilation Rates with Application to School Classrooms. International Journal of Environmental Research and Public Health 14 (2). doi:10.3390/ijerph14020145

Bauld L, MacKintosh AM, Eastwood B et al. (2017) Young People's Use of E-Cigarettes across the United Kingdom: Findings from Five Surveys 2015-2017. International Journal of Environmental Research and Public Health 14 (9). doi:10.3390/ijerph14090973

Baweja R, Curci KM, Yingst J et al. (2016) Views of experienced electronic cigarette users. Addiction Research & Theory 24 (1):80-88. doi:10.3109/16066359.2015.1077947

Bayly JE, Bernat D, Porter L et al. (2018) Secondhand exposure to aerosols from electronic nicotine delivery systems and asthma exacerbations among youth with asthma. Chest (November):1-6. doi:10.1016/j.chest.2018.10.005

Behar RZ, Hua M, Talbot P (2015) Puffing Topography and Nicotine Intake of Electronic Cigarette Users. Plos One 10 (2). doi:10.1371/journal.pone.0117222

Benowitz NL, Burbank AD (2016) Cardiovascular toxicity of nicotine: Implications for electronic cigarette use. Trends in Cardiovascular Medicine 26 (6):515-523. doi:10.1016/j.tcm.2016.03.001

Berg CJ (2018) Vape shop location and marketing in the context of the Food and Drug Administration regulation. Public Health 165:142-145. doi:10.1016/j.puhe.2018.09.002

Bohac DL, Hewett MJ, Hammond SK et al. (2011) Secondhand smoke transfer and reductions by air sealing and ventilation in multiunit buildings: PFT and nicotine verification. Indoor Air 21 (1):36-44. doi:10.1111/j.1600-0668.2010.00680.x

Bolte G, Heitmann D, Kiranoglu M et al. (2008) Exposure to environmental tobacco smoke in German restaurants, pubs and discotheques. Journal of Exposure Science and Environmental Epidemiology 18 (3):262-271. doi:10.1038/sj.jes.7500590

Breland A, Soule E, Lopez A et al. (2017) Electronic cigarettes: what are they and what do they do? Annals of the New York Academy of Sciences 1394 (1):5-30. doi:10.1111/nyas.12977

Burnett RT, Pope CA, Ezzati M et al. (2014) An Integrated Risk Function for Estimating the Global Burden of Disease Attributable to Ambient Fine Particulate Matter Exposure. Environmental Health Perspectives 122 (4):397-403. doi:10.1289/ehp.1307049

Carlos WG, Alexander LEC, Gross JE et al. (2019) Vaping-associated Pulmonary Illness (VAPI). American Journal of Respiratory and Critical Care Medicine 200 (7):P13-P14. doi:10.1164/rccm.2007P13

Carnevale R, Sciarretta S, Violi F et al. (2016) Acute Impact of Tobacco vs Electronic Cigarette Smoking on Oxidative Stress and Vascular Function. Chest 150 (3):606-612. doi:10.1016/j.chest.2016.04.012

CDC (2020a) CDC, States Update Number of Hospitalized EVALI Cases and EVALI Deaths.

CDC (2020b) Youth Tobacco Use: Results from the National Youth Tobacco Survey. Centers for Disease Control and Prevention https://www.fda.gov/tobacco-products/youth-and-tobacco/youth-tobacco-use-results-national-youth-tobacco-survey. Accessed December 22 2020

Cervellati F, Muresan XM, Sticozzi C et al. (2014) Comparative effects between electronic and cigarette smoke in human keratinocytes and epithelial lung cells. Toxicology in Vitro 28 (5):999-1005. doi:10.1016/j.tiv.2014.04.012

Chatterjee S, Tao J-Q, Johncola A et al. (2019) Acute exposure to e-cigarettes causes inflammation and endothelial oxidative stress in non-smoking healthy young subjects. American Journal of Physiology-Lung Cellular and Molecular Physiology. doi:10.1152/ajplung.00110.2019

Chen-Sankey JC, Kong G, Choi K (2019) Perceived ease of flavored e-cigarette use and e-cigarette use progression among youth never tobacco users. Plos One 14 (2). doi:10.1371/journal.pone.0212353

Chen C, Zhao B (2011) Review of relationship between indoor and outdoor particles: I/O ratio, infiltration factor and penetration factor. Atmospheric Environment 45 (2):275-288. doi:https://doi.org/10.1016/j.atmosenv.2010.09.048

Chen R, Aherrera A, Isichei C et al. (2017) Assessment of indoor air quality at an electronic cigarette (Vaping) convention. Journal of Exposure Science & Environmental Epidemiology. doi:10.1038/s41370-017-0005-x

Chen WH, Wang P, Ito K et al. (2018) Measurement of heating coil temperature for e-cigarettes with a "top-coil" clearomizer. Plos One 13 (4). doi:10.1371/journal.pone.0195925

Cheng TR (2014) Chemical evaluation of electronic cigarettes. Tobacco Control 23:11-17. doi:10.1136/tobaccocontrol-2013-051482

Chun LF, Moazed F, Calfee CS et al. (2017) Pulmonary toxicity of e-cigarettes. American Journal of Physiology-Lung Cellular and Molecular Physiology 313 (2):L193-L206. doi:10.1152/ajplung.00071.2017

Crotty Alexander LE, Drummond CA, Hepokoski M et al. (2018) Chronic inhalation of e-cigarette vapor containing nicotine disrupts airway barrier function and induces systemic inflammation and multiorgan fibrosis in mice. American Journal of Physiology-Regulatory, Integrative and Comparative Physiology 314 (6):R834-R847. doi:10.1152/ajpregu.00270.2017

Cullen KA, Ambrose BK, Gentzke AS et al. (2018) Use of Electronic Cigarettes and Any Tobacco Product Among Middle and High School Students - United States, 2011-2018. Mmwr-Morbidity and Mortality Weekly Report 67 (45):1276-1277. doi:10.15585/mmwr.mm6745a5

Czogala J, Goniewicz ML, Fidelus B et al. (2014) Secondhand Exposure to Vapors From Electronic Cigarettes. Nicotine & Tobacco Research 16 (6):655-662. doi:10.1093/ntr/ntt203

Dang H, Mascenik T, Graves LM et al. (2018) Chronic E-Cigarette Exposure Alters the Human Bronchial Epithelial Proteome. American Journal of Respiratory and Critical Care Medicine 198 (1):36-36. doi:10.1164/rccm.201710-2033oc

Dicpinigaitis PV, Chang AL, Dicpinigaitis AJ et al. (2016) Effect of e-cigarette use on cough reflex sensitivity. Chest 149 (1):161-165. doi:10.1378/chest.15-0817

Dinakar C, O'Connor GT (2016) The Health Effects of Electronic Cigarettes. New England Journal of Medicine 375 (14):1372-1381. doi:10.1056/NEJMra1502466

Dockery DW, Spengler JD (1981) INDOOR-OUTDOOR RELATIONSHIPS OF RESPIRABLE SULFATES AND PARTICLES. Atmospheric Environment 15 (3):335-343. doi:10.1016/0004-6981(81)90036-6

Drehmer JE, Nabi-Burza E, Walters BH et al. (2019) Parental Smoking and E-cigarette Use in Homes and Cars. Pediatrics 143 (4). doi:10.1542/peds.2018-3249

El-Hellani A, El-Hage R, Baalbaki R et al. (2015) Free-base and protonated nicotine in electronic cigarette liquids and aerosols. Chemical Research in Toxicology 28 (8):1532-1537. doi:10.1021/acs.chemrestox.5b00107

El-Hellani A, Salman R, El-Hage R et al. (2018) Nicotine and Carbonyl Emissions From Popular Electronic Cigarette Products: Correlation to Liquid Composition and Design Characteristics. Nicotine & Tobacco Research 20 (2):215-223. doi:10.1093/ntr/ntw280

England LJ, Aagaard K, Bloch M et al. (2017) Developmental toxicity of nicotine: A transdisciplinary synthesis and implications for emerging tobacco products. Neuroscience and Biobehavioral Reviews 72:176-189. doi:10.1016/j.neubiorev.2016.11.013

Etter JF, Zather E, Svensson S (2013) Analysis of refill liquids for electronic cigarettes. Addiction 108 (9):1671-1679. doi:10.1111/add.12235

Farsalinos KE, Gillman G, Poulas K et al. (2015) Tobacco-Specific Nitrosamines in Electronic Cigarettes: Comparison between Liquid and Aerosol Levels. International Journal of Environmental Research and Public Health 12 (8):9046-9053. doi:10.3390/ijerph120809046

Farsalinos KE, Romagna G, Tsiapras D et al. (2013) Evaluation of Electronic Cigarette Use (Vaping) Topography and Estimation of Liquid Consumption: Implications for Research Protocol Standards Definition and for Public Health Authorities' Regulation. International Journal of Environmental Research and Public Health 10 (6):2500-2514. doi:10.3390/ijerph10062500

Feng Y, Kleinstreuer C, Rostami A (2015) Evaporation and condensation of multicomponent electronic cigarette droplets and conventional cigarette smoke particles in an idealized G3-G6 triple bifurcating unit. Journal of Aerosol Science 80:58-74. doi:10.1016/j.jaerosci.2014.11.002

Ferrari M, Zanasi A, Nardi E et al. (2015) Short-term effects of a nicotine-free e-cigarette compared to a traditional cigarette in smokers and non-smokers. BMC Pulmonary Medicine 15 (1):1-9. doi:10.1186/s12890-015-0106-z

Flora JW, Meruva N, Huang CB et al. (2016) Characterization of potential impurities and degradation products in electronic cigarette formulations and aerosols. Regulatory Toxicology and Pharmacology 74:1-11. doi:10.1016/j.yrtph.2015.11.009

Flouris AD, Chorti MS, Poulianiti KP et al. (2013) Acute impact of active and passive electronic cigarette smoking on serum cotinine and lung function. Inhalation Toxicology 25 (2):91-101. doi:10.3109/08958378.2012.758197

Flouris AD, Poulianiti KP, Chorti MS et al. (2012) Acute effects of electronic and tobacco cigarette smoking on complete blood count. Food and Chemical Toxicology 50 (10):3600-3603. doi:10.1016/j.fct.2012.07.025

Floyd EL, Queimado L, Wang J et al. (2018) Electronic cigarette power affects count concentration and particle size distribution of vaping aerosol. Plos One 13 (12). doi:10.1371/journal.pone.0210147

Forster M, McAughey J, Prasad K et al. (2018) Assessment of tobacco heating product THP1.0. Part 4: Characterisation of indoor air quality and odour. Regulatory Toxicology and Pharmacology 93:34-51. doi:10.1016/j.yrtph.2017.09.017

Franchini M, Mannucci PM (2009) Particulate Air Pollution and Cardiovascular Risk: Short-term and Long-term Effects. Seminars in Thrombosis and Hemostasis 35 (7):665-670. doi:10.1055/s-0029-1242720

Fromme H, Dietrich S, Heitmann D et al. (2009) Indoor air contamination during a waterpipe (narghile) smoking session. Food and Chemical Toxicology 47 (7):1636-1641. doi:10.1016/j.fct.2009.04.017

Fung CCD, Shu S, Zhu Y (2014) Ultrafine particles generated from coloring with scented markers in the presence of ozone. Indoor Air 24 (5):503-510. doi:10.1111/ina.12103

Fuoco FC, Buonanno G, Stabile L et al. (2014) Influential parameters on particle concentration and size distribution in the mainstream of e-cigarettes. Environmental Pollution 184:523-529. doi:10.1016/j.envpol.2013.10.010

Galstyan E, Galimov A, Sussman S (2019) Commentary: The Emergence of Pod Mods at Vape Shops. Evaluation & the Health Professions 42 (1):118-124. doi:10.1177/0163278718812976

Geiss O, Bianchi I, Barahona F et al. (2015) Characterisation of mainstream and passive vapours emitted by selected electronic cigarettes. International Journal of Hygiene and Environmental Health 218 (1):169-180. doi:10.1016/j.ijheh.2014.10.001

Geiss O, Bianchi I, Barrero-Moreno J (2016) Correlation of volatile carbonyl yields emitted by e-cigarettes with the temperature of the heating coil and the perceived sensorial quality of the generated vapours. International Journal of Hygiene and Environmental Health 219 (3):268-277. doi:10.1016/j.ijheh.2016.01.004

Gentzke AS, Wang TW, Marynak KL et al. (2019) Exposure to Secondhand Smoke and Secondhand E-Cigarette Aerosol Among Middle and High School Students. Preventing chronic disease 16:E42-E42. doi:10.5888/pcd16.180531

Gillman IG, Kistler KA, Stewart EW et al. (2016) Effect of variable power levels on the yield of total aerosol mass and formation of aldehydes in e-cigarette aerosols. Regulatory Toxicology and Pharmacology 75:58-65. doi:10.1016/j.yrtph.2015.12.019

Giovenco DP, Lewis MJ, Delnevo CD (2014) Factors Associated with E-cigarette Use A National Population Survey of Current and Former Smokers. American Journal of Preventive Medicine 47 (4):476-480. doi:10.1016/j.amepre.2014.04.009

Glantz SA, Bareham DW (2018) E-Cigarettes: Use, Effects on Smoking, Risks, and Policy Implications. In: Fielding JE, Brownson RC, Green LW (eds) Annual Review of Public Health, Vol 39, vol 39. Annual Review of Public Health. pp 215-235. doi:10.1146/annurev-publhealth040617-013757

Gong LW, Xu B, Zhu YF (2009) Ultrafine Particles Deposition Inside Passenger Vehicles. Aerosol Science and Technology 43 (6):544-553. doi:10.1080/02786820902791901

Goniewicz ML, Boykan R, Messina CR et al. (2018) High exposure to nicotine among adolescents who use Juul and other vape pod systems ('pods'). Tobacco Control. doi:10.1136/tobaccocontrol-2018-054565

Goniewicz ML, Knysak J, Gawron M et al. (2014) Levels of selected carcinogens and toxicants in vapour from electronic cigarettes. Tobacco Control 23 (2):133-139. doi:10.1136/tobaccocontrol-2012-050859

Goniewicz ML, Lee L (2015) Electronic Cigarettes Are a Source of Thirdhand Exposure to Nicotine. Nicotine & Tobacco Research 17 (2):256-258. doi:10.1093/ntr/ntu152

Grand View Research (2021) E-cigarette And Vape Market Size, Share & Trends Analysis Report By Distribution Channel (Online, Retail), By Product (Disposable, Rechargeable), By Component, By Region, And Segment Forecasts, 2021 - 2028.

Guo H, Morawska L, He CR et al. (2010) Characterization of particle number concentrations and PM2.5 in a school: influence of outdoor air pollution on indoor air. Environmental Science and Pollution Research 17 (6):1268-1278. doi:10.1007/s11356-010-0306-2

Hammond D, Rynard VL, Reid JL (2020) Changes in Prevalence of Vaping Among Youths in the United States, Canada, and England from 2017 to 2019. JAMA Pediatr. doi:10.1001/jamapediatrics.2020.0901

Hammond SK, Leaderer BP (1987) A diffusion monitor to measure exposure to passive smoking Environmental Science & Technology 21 (5):494-497. doi:10.1021/es00159a012

Hartmann-Boyce J, Begh R, Aveyard P (2018) Electronic cigarettes for smoking cessation. BMJ 360:j5543. doi:10.1136/bmj.j5543

He CR, Morawska LD, Hitchins J et al. (2004) Contribution from indoor sources to particle number and mass concentrations in residential houses. Atmospheric Environment 38 (21):3405-3415. doi:10.1016/j.atmosenv.2004.03.027

Hecht SS, Carmella SG, Kotandeniya D et al. (2015) Evaluation of Toxicant and Carcinogen Metabolites in the Urine of E-Cigarette Users Versus Cigarette Smokers. Nicotine Tob Res 17 (6):704-709. doi:10.1093/ntr/ntu218

Hecht SS, Stepanov I, Carmella SG (2016) Exposure and Metabolic Activation Biomarkers of Carcinogenic Tobacco-Specific Nitrosamines. Accounts of Chemical Research 49 (1):106-114. doi:10.1021/acs.accounts.5b00472

Hinds WC (1999) Aerosol technology: properties, behavior, and measurement of airborne particles. 2nd edn. John Wiley & Sons,

Holcomb LC (1993) Indoor air quality and environmental tobacco smoke: concentration and exposure. Environment International 19 (1):9-40. doi:10.1016/0160-4120(93)90004-2

Hood NE, Ferketich AK, Klein EG et al. (2014) Associations between self-reported in-home smoking behaviours and surface nicotine concentrations in multiunit subsidised housing. Tobacco Control 23 (1):27-32. doi:10.1136/tobaccocontrol-2012-050666

Hua M, Yip H, Talbot P (2013) Mining data on usage of electronic nicotine delivery systems (ENDS) from YouTube videos. Tobacco Control 22:103-106. doi:10.1136/tobaccocontrol-2011-050226

Huang J, Duan Z, Kwok J et al. (2019) Vaping versus JUULing: how the extraordinary growth and marketing of JUUL transformed the US retail e-cigarette market. Tobacco Control 28 (2):146-151. doi:10.1136/tobaccocontrol-2018-054382

Huang SJ, Xu YM, Lau ATY (2018) Electronic cigarette: A recent update of its toxic effects on humans. Journal of Cellular Physiology 233 (6):4466-4478. doi:10.1002/jcp.26352

IARC (2019) Agents Classified by the IARC Monographs, Volumes 1–123, vol 1-123. International Agency for Research on Cancer, International Agency for Research on Cancer

Ingebrethsen BJ, Cole SK, Alderman SL (2012) Electronic cigarette aerosol particle size distribution measurements. Inhalation Toxicology 24 (14):976-984. doi:10.3109/08958378.2012.744781

Jenkins PL, Phillips TJ, Mulberg EJ et al. (1992) ACTIVITY PATTERNS OF CALIFORNIANS - USE OF AND PROXIMITY TO INDOOR POLLUTANT SOURCES. Atmospheric

Environment Part a-General Topics 26 (12):2141-2148. doi:10.1016/0960-1686(92)90402-7

Jenkins RA, Ilgner RH, Tomkins BA et al. (2004) Development and application of protocols for the determination of response of real-time particle monitors to common indoor aerosols. J Air Waste Manage Assoc 54 (2):229-241. doi:10.1080/10473289.2004.10470892

Jensen RP, Strongin RM, Peyton DH (2017) Solvent Chemistry in the Electronic Cigarette Reaction Vessel. Scientific Reports 7. doi:10.1038/srep42549

Jiang H, Ahmed CMS, Martin TJ et al. (2020) Chemical and Toxicological Characterization of Vaping Emission Products from Commonly Used Vape Juice Diluents. Chemical Research in Toxicology 33 (8):2157-2163. doi:10.1021/acs.chemrestox.0c00174

Johnson JM, Naeher LP, Yu XZ et al. (2018) Air monitoring at large public electronic cigarette events. International Journal of Hygiene and Environmental Health 221 (3):541-547. doi:10.1016/j.ijheh.2018.02.003

Kennedy RD, Awopegba A, De Leon E et al. (2017) Global approaches to regulating electronic cigarettes. Tobacco Control 26 (4):440-445. doi:10.1136/tobaccocontrol-2016-053179

Khachatoorian C, Jacob P, Benowitz NL et al. (2019) Electronic cigarette chemicals transfer from a vape shop to a nearby business in a multiple-tenant retail building. Tobacco Control 28 (5):519-525. doi:10.1136/tobaccocontrol-2018-054316

Khlystov A, Samburova V (2016) Flavoring Compounds Dominate Toxic Aldehyde Production during E-Cigarette Vaping. Environmental Science & Technology 50 (23):13080-13085. doi:10.1021/acs.est.6b05145

Kienhuis AS, Soeteman-Hernandez LG, Bos PMJ et al. (2015) Potential harmful health effects of inhaling nicotine-free shisha-pen vapor: a chemical risk assessment of the main components propylene glycol and glycerol. Tobacco Induced Diseases 13. doi:10.1186/s12971-015-0038-7

Kim HJ, Shin HS (2013) Determination of tobacco-specific nitrosamines in replacement liquids of electronic cigarettes by liquid chromatography-tandem mass spectrometry. Journal of Chromatography A 1291:48-55. doi:10.1016/j.chroma.2013.03.035

Kim SY, Sim S, Choi HG (2017) Active, passive, and electronic cigarette smoking is associated with asthma in adolescents. Scientific Reports 7 (1):1-8. doi:10.1038/s41598-017-17958-y

King BA, Travers MJ, Cummings KM et al. (2010) Secondhand Smoke Transfer in Multiunit Housing. Nicotine & Tobacco Research 12 (11):1133-1141. doi:10.1093/ntr/ntq162

Klager S, Vallarino J, MacNaughton P et al. (2017) Flavoring Chemicals and Aldehydes in E-Cigarette Emissions. Environmental Science & Technology 51 (18):10806-10813. doi:10.1021/acs.est.7b02205

Konstantopoulou SS, Behrakis PK, Lazaris AC et al. (2014) Indoor air quality in a bar/restaurant before and after the smoking ban in Athens, Greece. Science of the Total Environment 476:136-143. doi:10.1016/j.scitotenv.2013.11.129

Kosmider L, Kimber CF, Kurek J et al. (2018) Compensatory Puffing With Lower Nicotine Concentration E-liquids Increases Carbonyl Exposure in E-cigarette Aerosols. Nicotine & Tobacco Research 20 (8):998-1003. doi:10.1093/ntr/ntx162

Kosmider L, Sobczak A, Fik M et al. (2014) Carbonyl Compounds in Electronic Cigarette Vapors: Effects of Nicotine Solvent and Battery Output Voltage. Nicotine & Tobacco Research 16 (10):1319-1326. doi:10.1093/ntr/ntu078

Layden JE, Ghinai I, Pray I et al. (2019a) Pulmonary Illness Related to E-Cigarette Use in Illinois and Wisconsin — Preliminary Report. New England Journal of Medicine. doi:10.1056/NEJMoa1911614

Layden JE, Ghinai I, Pray I et al. (2019b) Pulmonary Illness Related to E-Cigarette Use in Illinois and Wisconsin — Final Report. New England Journal of Medicine 382 (10):903-916. doi:10.1056/NEJMoa1911614

Lee H-W, Park S-H, Weng M-w et al. (2018a) E-cigarette smoke damages DNA and reduces repair activity in mouse lung, heart, and bladder as well as in human lung and bladder cells. Proceedings of the National Academy of Sciences 115 (7):E1560-E1569. doi:10.1073/pnas.1718185115

Lee JGL, Orlan EN, Sewell KB et al. (2018b) A new form of nicotine retailers: a systematic review of the sales and marketing practices of vape shops. Tobacco Control 27 (E1):E70-E75. doi:10.1136/tobaccocontrol-2017-054015

Lee KW, Chen H (1984) Coagulation rate of polydisperse particles. Aerosol Science and Technology 3 (3):327-334. doi:10.1080/02786828408959020

Lee MS, LeBouf RF, Son YS et al. (2017) Nicotine, aerosol particles, carbonyls and volatile organic compounds in tobacco- and menthol-flavored e-cigarettes. Environmental Health 16. doi:10.1186/s12940-017-0249-x

Lee SC, Li WM, Chan LY (2001) Indoor air quality at restaurants with different styles of cooking in metropolitan Hong Kong. Science of the Total Environment 279 (1-3):181-193. doi:10.1016/s0048-9697(01)00765-3

Leventhal AM, Dai H (2020) Prevalence of Flavored e-Cigarette Use Among Subpopulations of Adults in the United States. JNCI: Journal of the National Cancer Institute. doi:10.1093/jnci/djaa118

Li L, Lee ES, Nguyen C et al. (2020a) Effects of propylene glycol, vegetable glycerin, and nicotine on emissions and dynamics of electronic cigarette aerosols. Aerosol Science and Technology:1-12. doi:10.1080/02786826.2020.1771270

Li L, Lin Y, Xia T et al. (2020b) Effects of Electronic Cigarettes on Indoor Air Quality and Health. Annual Review of Public Health 41:363-380. doi:10.1146/annurev-publhealth-040119-094043

Li L, Lin Y, Xia T et al. (2020c) Effects of Electronic Cigarettes on Indoor Air Quality and Health. Annual Review of Public Health 41

Li L, Nguyen C, Lin Y et al. (2020d) Impacts of electronic cigarettes usage on air quality of vape shops and their nearby areas. Science of The Total Environment:143423. doi:https://doi.org/10.1016/j.scitotenv.2020.143423

Li L, Zhu Y (2021) Vaping and Secondhand Exposure (in press). In: Zhang Y, Hopke PK, Mandin C (eds) Handbook of Indoor Air Quality. Springer Nature.,

Li Y, Chen Z (2003) A balance-point method for assessing the effect of natural ventilation on indoor particle concentrations. Atmospheric Environment 37 (30):4277-4285. doi:https://doi.org/10.1016/S1352-2310(03)00527-2

Liang CK, Pankow JF (1996) Gas/particle partitioning of organic compounds to environmental tobacco smoke: Partition coefficient measurements by desorption and comparison to urban particulate material. Environmental Science & Technology 30 (9):2800-2805. doi:10.1021/es960050x

Liu J, Fung D, Jiang J et al. (2014) Ultrafine particle emissions from essential-oil-based mosquito repellent products. Indoor Air 24 (3):327-335. doi:10.1111/ina.12080

Liu JM, Liang QW, Oldham MJ et al. (2017) Determination of Selected Chemical Levels in Room Air and on Surfaces after the Use of Cartridge- and Tank-Based E-Vapor Products or Conventional Cigarettes. International Journal of Environmental Research and Public Health 14 (9). doi:10.3390/ijerph14090969

Lopez MJ, Fernandez E, Perez-Rios M et al. (2013) Impact of the 2011 Spanish Smoking Ban in Hospitality Venues: Indoor Secondhand Smoke Exposure and Influence of Outdoor Smoking. Nicotine & Tobacco Research 15 (5):992-996. doi:10.1093/ntr/nts218

Luo Y, Wu Y, Li L et al. (2021) Dynamic Imaging and Characterization of Volatile Aerosols in E-Cigarette Emissions Using Deep Learning-Based Holographic Microscopy. ACS Sensors 6 (6):2403-2410. doi:10.1021/acssensors.1c00628

Malas M, van der Tempel J, Schwartz R et al. (2016) Electronic Cigarettes for Smoking Cessation: A Systematic Review. Nicotine & Tobacco Research 18 (10):1926-1936. doi:10.1093/ntr/ntw119

Manigrasso M, Buonanno G, Fuoco FC et al. (2015) Aerosol deposition doses in the human respiratory tree of electronic cigarette smokers. Environmental Pollution 196:257-267. doi:10.1016/j.envpol.2014.10.013

Margham J, McAdam K, Forster M et al. (2016) Chemical Composition of Aerosol from an E-Cigarette: A Quantitative Comparison with Cigarette Smoke. Chemical Research in Toxicology 29 (10):1662-1678. doi:10.1021/acs.chemrestox.6b00188

Marini S, Buonanno G, Stabile L et al. (2014) Short-term effects of electronic and tobacco cigarettes on exhaled nitric oxide. Toxicology and Applied Pharmacology 278 (1):9-15. doi:10.1016/j.taap.2014.04.004

Martuzevicius D, Prasauskas T, Setyan A et al. (2018) Characterization of the Spatial and Temporal Dispersion Differences Between Exhaled E-Cigarette Mist and Cigarette Smoke. Nicotine & Tobacco Research:1-7. doi:10.1093/ntr/nty121

McAuley TR, Hopke PK, Zhao J et al. (2012) Comparison of the effects of e-cigarette vapor and cigarette smoke on indoor air quality. Inhalation Toxicology 24 (12):850-857. doi:10.3109/08958378.2012.724728

McConnell R, Barrington-Trimis JL, Wang K et al. (2017) Electronic cigarette use and respiratory symptoms in adolescents. American Journal of Respiratory and Critical Care Medicine 195 (8):1043-1049. doi:10.1164/rccm.201604-0804OC

McKelvey K, Baiocchi M, Halpern-Felsher B (2018) Adolescents' and Young Adults' Use and Perceptions of Pod-Based Electronic Cigarettes. Jama Network Open 1 (6). doi:10.1001/jamanetworkopen.2018.3535

McMillen R, Klein JD, Wilson K et al. (2019) E-Cigarette Use and Future Cigarette Initiation Among Never Smokers and Relapse Among Former Smokers in the PATH Study. Public Health Reports 134 (5):528-536. doi:10.1177/0033354919864369

McMillen RC, Gottlieb MA, Shaefer RMW et al. (2015) Trends in Electronic Cigarette Use Among US Adults: Use is Increasing in Both Smokers and Nonsmokers. Nicotine & Tobacco Research 17 (10):1195-1202. doi:10.1093/ntr/ntu213

Melstrom P, Koszowski B, Thanner MH et al. (2017) Measuring PM2.5, Ultrafine Particles, Nicotine Air and Wipe Samples Following the Use of Electronic Cigarettes. Nicotine & Tobacco Research 19 (9):1055-1061. doi:10.1093/ntr/ntx058

Meng Q, Son Y, Kipen H et al. (2017) Particles Released From Primary E-Cigarette Vaping: Particle Size Distribution And Particle Deposition In The Human Respiratory Tract. American Journal of Respiratory and Critical Care Medicine 195

Mikheev VB, Brinkman MC, Granville CA et al. (2016) Real-Time Measurement of Electronic Cigarette Aerosol Size Distribution and Metals Content Analysis. Nicotine & Tobacco Research 18 (9):1895-1902. doi:10.1093/ntr/ntw128

Mikheev VB, Ivanov A, Lucas EA et al. (2018) Aerosol size distribution measurement of electronic cigarette emissions using combined differential mobility and inertial impaction methods: Smoking machine and puff topography influence. Aerosol Science and Technology 52 (11):1233-1248. doi:10.1080/02786826.2018.1513636

Mishra A, Chaturvedi P, Datta S et al. (2015) Harmful effects of nicotine. Indian Journal of Medical and Paediatric Oncology 36 (1):24-31. doi:10.4103/0971-5851.151771

Moheimani RS, Bhetraratana M, Peters KM et al. (2017a) Sympathomimetic effects of acute e-cigarette use: Role of nicotine and non-nicotine constituents. vol 6. doi:10.1161/JAHA.117.006579

Moheimani RS, Bhetraratana M, Yin F et al. (2017b) Increased cardiac sympathetic activity and oxidative stress in habitual electronic cigarette users: Implications for cardiovascular risk. JAMA Cardiology 2 (3):278-285. doi:10.1001/jamacardio.2016.5303

Moosmuller H, Arnott WP, Rogers CF et al. (2001) Time resolved characterization of diesel particulate emissions. 1. Instruments for particle mass measurements. Environmental Science & Technology 35 (4):781-787. doi:10.1021/es0013935

Morawska L, Ayoko GA, Bae GN et al. (2017) Airborne particles in indoor environment of homes, schools, offices and aged care facilities: The main routes of exposure. Environment International 108:75-83. doi:10.1016/j.envint.2017.07.025

Morean ME, Butler ER, Bold KW et al. (2018) Preferring more e-cigarette flavors is associated with e-cigarette use frequency among adolescents but not adults. Plos One 13 (1). doi:10.1371/journal.pone.0189015

Nguyen C, Li L, Sen CA et al. (2019) Fine and ultrafine particles concentrations in vape shops. Atmospheric Environment 211:159-169. doi:10.1016/j.atmosenv.2019.05.015

Nguyen T, Li GE, Chen H et al. (2018) Maternal E-Cigarette Exposure Results in Cognitive and Epigenetic Alterations in Offspring in a Mouse Model. Chemical Research in Toxicology 31 (7):601-611. doi:10.1021/acs.chemrestox.8b00084

Ogunwale MA, Li MX, Raju MVR et al. (2017) Aldehyde Detection in Electronic Cigarette Aerosols. Acs Omega 2 (3):1207-1214. doi:10.1021/acsomega.6b00489

Oh AY, Kacker A (2014) Do Electronic Cigarettes Impart a Lower Potential Disease Burden Than Conventional Tobacco Cigarettes?: Review on E-Cigarette Vapor Versus Tobacco Smoke. Laryngoscope 124 (12):2702-2706. doi:10.1002/lary.24750

Olfert IM, DeVallance E, Hoskinson H et al. (2018) Chronic exposure to electronic cigarettes results in impaired cardiovascular function in mice. Journal of Applied Physiology 124 (3):573-582. doi:10.1152/japplphysiol.00713.2017

Omaiye EE, McWhirter KJ, Luo W et al. (2019) High-Nicotine Electronic Cigarette Products: Toxicity of JUUL Fluids and Aerosols Correlates Strongly with Nicotine and Some Flavor Chemical Concentrations. Chemical Research in Toxicology. doi:10.1021/acs.chemrestox.8b00381

Overbeek DL, Kass AP, Chiel LE et al. (2020) A review of toxic effects of electronic cigarettes/vaping in adolescents and young adults. Critical Reviews in Toxicology 50 (6):531-538. doi:10.1080/10408444.2020.1794443

Pankow JF, Kim K, McWhirter KJ et al. (2017) Benzene formation in electronic cigarettes. Plos One 12 (3). doi:10.1371/journal.pone.0173055

Peters A, Wichmann HE, Tuch T et al. (1997) Respiratory effects are associated with the number of ultrafine particles. American Journal of Respiratory and Critical Care Medicine 155 (4):1376-1383. doi:10.1164/ajrccm.155.4.9105082

Pichelstorfer L, Hofmann W, Winkler-Heil R et al. (2016) Simulation of aerosol dynamics and deposition of combustible and electronic cigarette aerosols in the human respiratory tract. Journal of Aerosol Science 99:125-132. doi:10.1016/j.jaerosci.2016.01.017

Pichelstorfer L, Winkler-Heil R, Boy M et al. (2020) Aerosol dynamics simulations of the anatomical variability of e-cigarette particle and vapor deposition in a stochastic lung. Journal of Aerosol Science:105706. doi:https://doi.org/10.1016/j.jaerosci.2020.105706

Polosa R, Caponnetto P (2016) The Health Effects of Electronic Cigarettes. New England Journal of Medicine 375 (26):2608-2608. doi:10.1056/NEJMc1613869

Poulianiti K, Karatzaferi C, Flouris AD et al. (2016) Antioxidant responses following active and passive smoking of tobacco and electronic cigarettes. Toxicology Mechanisms and Methods 26 (6):455-461. doi:10.1080/15376516.2016.1196281

Prescient & Strategic Intelligence (2018) E-Cigarette Market by Product (Cig-a-like [Disposable, Rechargeable], Vaporizer [Open Tank, Closed System], Vape Mod), by Distribution Channel (Vape Shops, Supermarkets, Online, Tobacconists), Aftermarket Products (Refill, Battery & Charger), by Geography (U.S., Canada, U.K., France, Russia, Germany, Italy, China, Japan, South Korea, South Africa) – Global Size, Share, Development, Growth, and Demand Forecast, 2013–2023.

Protano C, Avino P, Manigrasso M et al. (2018) Environmental Electronic Vape Exposure from Four Different Generations of Electronic Cigarettes: Airborne Particulate Matter Levels. International Journal of Environmental Research and Public Health 15 (10). doi:10.3390/ijerph15102172

Protano C, Manigrasso M, Cammalleri V et al. (2020) Impact of Electronic Alternatives to Tobacco Cigarettes on Indoor Air Particular Matter Levels. International Journal of Environmental Research and Public Health 17 (8). doi:10.3390/ijerph17082947

Qasim H, Karim ZA, Silva-Espinoza JC et al. (2018) Short-Term E-Cigarette Exposure Increases the Risk of Thrombogenesis and Enhances Platelet Function in Mice. Journal of the American Heart Association 7 (15). doi:10.1161/jaha.118.009264

Qu Y, Szulejko JE, Kim KH et al. (2019) The effect of varying battery voltage output on the emission rate of carbonyls released from e-cigarette smoke. Microchemical Journal 145:47-54. doi:10.1016/j.microc.2018.10.019

Ratjen F, Jensen R, Klingel M et al. (2019) Effect of changes in tidal volume on multiple breath washout outcomes. PloS one 14 (7):e0219309-e0219309. doi:10.1371/journal.pone.0219309

Robinson RJ, Hensel EC, Morabito PN et al. (2015) Electronic Cigarette Topography in the Natural Environment. PloS One 10 (6). doi:e0129296
10.1371/journal.pone.0129296

Romagna G, Allifranchini E, Bocchietto E et al. (2013) Cytotoxicity evaluation of electronic cigarette vapor extract on cultured mammalian fibroblasts (ClearStream-LIFE): comparison with tobacco cigarette smoke extract. Inhalation Toxicology 25 (6):354-361. doi:10.3109/08958378.2013.793439

Rossiter WJ, Godette M, Brown PW et al. (1985) An investigation of the degradation of aqueous ethylene-glycol and propylene-glycol solutions using ion chromatography. Solar Energy Materials 11 (5-6):455-467. doi:10.1016/0165-1633(85)90016-4

Ruprecht AA, De Marco C, Saffari A et al. (2017) Environmental pollution and emission factors of electronic cigarettes, heat-not-burn tobacco products, and conventional cigarettes. Aerosol Science and Technology 51 (6):674-684. doi:10.1080/02786826.2017.1300231

Russo ET, Hulse TE, Adamkiewicz G et al. (2015) Comparison of Indoor Air Quality in Smoke-Permitted and Smoke-Free Multiunit Housing: Findings From the Boston Housing Authority. Nicotine & Tobacco Research 17 (3):316-322. doi:10.1093/ntr/ntu146

Saffari A, Daher N, Ruprecht A et al. (2014) Particulate metals and organic compounds from electronic and tobacco-containing cigarettes: comparison of emission rates and secondhand exposure. Environmental Science-Processes & Impacts 16 (10):2259-2267. doi:10.1039/c4em00415a

Scheitel M, Stanic M, Neuberger M (2016) PM10, PM2.5, PM1, number and surface of particles at the child's seat when smoking a cigarette in a car. Aims Environmental Science 3 (4):582-591. doi:10.3934/environsci.2016.4.582

Schober W, Szendrei K, Matzen W et al. (2014a) Use of electronic cigarettes (e-cigarettes) impairs indoor air quality and increases FeNO levels of e-cigarette consumers. International Journal of Hygiene and Environmental Health 217 (6):628-637. doi:10.1016/j.ijheh.2013.11.003

Schober W, Szendrei K, Matzen W et al. (2014b) Use of electronic cigarettes (e-cigarettes) impairs indoor air quality and increases FeNO levels of e-cigarette consumers. International Journal of Hygiene and Environmental Health 217 (6):628-637. doi:10.1016/j.ijheh.2013.11.003

Schripp T, Markewitz D, Uhde E et al. (2013) Does e-cigarette consumption cause passive vaping? Indoor Air 23 (1):25-31. doi:10.1111/j.1600-0668.2012.00792.x

Schripp T, Wensing M, Uhde E et al. (2008) Evaluation of ultrafine particle emissions from laser printers using emission test chambers. Environmental Science & Technology 42 (12):4338-4343. doi:10.1021/es702426m

Scungio M, Stabile L, Buonanno G (2018) Measurements of electronic cigarette-generated particles for the evaluation of lung cancer risk of active and passive users. Journal of Aerosol Science 115:1-11. doi:10.1016/j.jaerosci.2017.10.006

Shi SS, Zhu SH, Lee ES et al. (2016) Performance of wearable ionization air cleaners: Ozone emission and particle removal. Aerosol Science and Technology 50 (3):211-221. doi:10.1080/02786826.2016.1139045

Sleiman M, Logue JM, Montesinos VN et al. (2016) Emissions from Electronic Cigarettes: Key Parameters Affecting the Release of Harmful Chemicals. Environmental Science & Technology 50 (17):9644-9651. doi:10.1021/acs.est.6b01741

Son Y, Giovenco DP, Delnevo C et al. (2020) Indoor Air Quality and Passive E-cigarette Aerosol Exposures in Vape-Shops. Nicotine & Tobacco Research. doi:10.1093/ntr/ntaa094

Son Y, Wackowski O, Weisel C et al. (2018) Evaluation of E-Vapor Nicotine and Nicotyrine Concentrations under Various E-Liquid Compositions, Device Settings, and Vaping Topographies. Chemical Research in Toxicology 31 (9):861-868. doi:10.1021/acs.chemrestox.8b00063

Sosnowski TR, Kramek-Romanowska K (2016) Predicted Deposition of E-Cigarette Aerosol in the Human Lungs. Journal of Aerosol Medicine and Pulmonary Drug Delivery 29 (3):299-309. doi:10.1089/jamp.2015.1268

Sosnowski TR, Odziomek M (2018) Particle Size Dynamics: Toward a Better Understanding of Electronic Cigarette Aerosol Interactions With the Respiratory System. Frontiers in Physiology 9. doi:10.3389/fphys.2018.00853

Soule EK, Maloney SF, Spindle TR et al. (2017) Electronic cigarette use and indoor air quality in a natural setting. Tobacco Control 26 (1):109-112. doi:10.1136/tobaccocontrol-2015-052772

Sturm R (2016) Total deposition of ultrafine particles in the lungs of healthy men and women: experimental and theoretical results. Annals of Translational Medicine 4 (12). doi:10.21037/atm.2016.06.05

Sundahl M, Berg E, Svensson M (2017) Aerodynamic particle size distribution and dynamic properties in aerosols from electronic cigarettes. Journal of Aerosol Science 103:141-150. doi:https://doi.org/10.1016/j.jaerosci.2016.10.009

Sussman S, Baezconde-Garbanati L, Garcia R et al. (2016) Commentary: Forces That Drive the Vape Shop Industry and Implications for the Health Professions. Evaluation & the health professions 39 (3):379-388. doi:10.1177/0163278715586295

Talih S, Balhas Z, Salman R et al. (2017) Transport phenomena governing nicotine emissions from electronic cigarettes: Model formulation and experimental investigation. Aerosol Science and Technology 51 (1):1-11. doi:10.1080/02786826.2016.1257853

Taylor DR, Pijnenburg MW, Smith AD et al. (2006) Exhaled nitric oxide measurements: clinical application and interpretation. Thorax 61 (9):817-827. doi:10.1136/thx.2005.056093

Taylor M, Jaunky T, Hewitt K et al. (2017) A comparative assessment of e-cigarette aerosols and cigarette smoke on in vitro endothelial cell migration. Toxicology Letters 280:S235-S236. doi:10.1016/j.toxlet.2017.07.651

Terzano C, Di Stefano F, Conti V et al. (2010) Air pollution ultrafine particles: toxicity beyond the lung. European Review for Medical and Pharmacological Sciences 14 (10):809-821

Truth Initiative (2019) E-cigarettes: Facts, stats and regulations. Truth Initiative. https://truthinitiative.org/research-resources/emerging-tobacco-products/e-cigarettes-facts-stats-and-regulations. Accessed November 2019 2019

Tzortzi A, Teloniatis S, Matiampa G et al. (2018) Passive Exposure to E-cigarette Emissions: Minor Respiratory Effects. Tobacco Prevention & Cessation 4 (Supplement):1-8. doi:10.18332/tpc/90305

U.S. Department of Health and Human Services (2016) Deeming Tobacco Products To Be Subject to the Federal Food, Drug, and Cosmetic Act, as Amended by the Family Smoking Prevention and Tobacco Control Act; Restrictions on the Sale and Distribution of Tobacco Products and Required Warning Statements for Tobacco Products. Fed. Regist., Docket No. FDA-2014-N-0189

U.S. Environmental Protection Agency (2016) 40 CFR 50.18. National primary ambient air quality standards for PM2.5. U.S. Environmental Protection Agency, Washington, D.C.

U.S. Environmental Protection Agency (2020) Indoor Air Quality (IAQ): Indoor Particulate Matter. U.S. Environmental Protection Agency. https://www.epa.gov/indoor-air-quality-iaq/indoor-particulate-matter#main-content. Accessed September, 2020 2020

Vallone DM, Cuccia AF, Briggs J et al. (2020) Electronic Cigarette and JUUL Use Among Adolescents and Young Adults. JAMA Pediatr. doi:10.1001/jamapediatrics.2019.5436

Vardavas CI, Anagnostopoulos N, Kougias M et al. (2012) Short-term pulmonary effects of using an electronic cigarette: Impact on respiratory flow resistance, impedance, and exhaled nitric oxide. Chest 141 (6):1400-1406. doi:10.1378/chest.11-2443

Vo UUT, Morris MP (2014) Nonvolatile, semivolatile, or volatile: Redefining volatile for volatile organic compounds. J Air Waste Manage Assoc 64 (6):661-669. doi:10.1080/10962247.2013.873746

Volesky KD, Maki A, Scherf C et al. (2018) The influence of three e-cigarette models on indoor fine and ultrafine particulate matter concentrations under real-world conditions. Environmental Pollution 243:882-889. doi:10.1016/j.envpol.2018.08.069

Wang TW, Marynak KL, Agaku IT et al. (2017) Secondhand Exposure to Electronic Cigarette Aerosol Among US Youths. JAMA Pediatr 171 (5):490-492. doi:10.1001/jamapediatrics.2016.4973

Williams M, Villarreal A, Bozhilov K et al. (2013) Metal and Silicate Particles Including Nanoparticles Are Present in Electronic Cigarette Cartomizer Fluid and Aerosol. Plos One 8 (3):1-11. doi:10.1371/journal.pone.0057987

Williams R (2020) The rise of disposable JUUL-type e-cigarette devices. Tobacco Control 29 (e1):e134. doi:10.1136/tobaccocontrol-2019-055379

World Health Organization (2006.) Air Quality Guidelines: Global Update for 2005. WHO, Copenhagen

Wright TP, Song C, Sears S et al. (2016) Thermodynamic and kinetic behavior of glycerol aerosol. Aerosol Science and Technology 50 (12):1385-1396. doi:10.1080/02786826.2016.1245405

Yingst JM, Veldheer S, Hrabovsky S et al. (2015) Factors Associated With Electronic Cigarette Users' Device Preferences and Transition From First Generation to Advanced Generation Devices. Nicotine & Tobacco Research 17 (10):1242-1246. doi:10.1093/ntr/ntv052

Yoong SL, Stockings E, Chai LK et al. (2018) Prevalence of electronic nicotine delivery systems (ENDS) use among youth globally: a systematic review and meta-analysis of country level data. Australian and New Zealand Journal of Public Health 42 (3):303-308. doi:10.1111/1753-6405.12777

Zervas E, Litsiou E, Konstantopoulos K et al. (2018) Physical characterization of the aerosol of an electronic cigarette: impact of refill liquids. Inhalation Toxicology 30 (6):218-223. doi:10.1080/08958378.2018.1500662

Zhang L, Lin Y, Zhu Y (2020) Transport and mitigation of exhaled electronic cigarette aerosols in a multizone indoor environment, in press. Aerosol and Air Quality Research

Zhang QF, Zhu YF (2010) Measurements of ultrafine particles and other vehicular pollutants inside school buses in South Texas. Atmospheric Environment 44 (2):253-261. doi:10.1016/j.atmosenv.2009.09.044

Zhang YP, Sumner W, Chen DR (2013) In Vitro Particle Size Distributions in Electronic and Conventional Cigarette Aerosols Suggest Comparable Deposition Patterns. Nicotine & Tobacco Research 15 (2):501-508. doi:10.1093/ntr/nts165

Zhao J, Pyrgiotakis G, Demokritou P (2016a) Development and characterization of electronic-cigarette exposure generation system (Ecig-EGS) for the physico-chemical and toxicological assessment of electronic cigarette emissions. Inhalation Toxicology 28 (14):658-669. doi:10.1080/08958378.2016.1246628

Zhao T, Shu S, Guo Q et al. (2016b) Effects of design parameters and puff topography on heating coil temperature and mainstream aerosols in electronic cigarettes. Atmospheric Environment 134:61-69. doi:http://dx.doi.org/10.1016/j.atmosenv.2016.03.027

Zhao TK, Nguyen C, Lin CH et al. (2017) Characteristics of secondhand electronic cigarette aerosols from active human use. Aerosol Science and Technology 51 (12):1368-1376. doi:10.1080/02786826.2017.1355548

Zhao TK, Shu S, Guo QJ et al. (2016c) Effects of design parameters and puff topography on heating coil temperature and mainstream aerosols in electronic cigarettes. Atmospheric Environment 134:61-69. doi:10.1016/j.atmosenv.2016.03.027

Zhou S, Behrooz L, Weitzman M et al. (2017) Secondhand hookah smoke: an occupational hazard for hookah bar employees. Tobacco Control 26 (1):40-45. doi:10.1136/tobaccocontrol-2015-052505